VIBRATIONAL SPECTRA OF ORGANO~~METALLIC~~ Sn COMPOUNDS

by PÄRN TAIMSALU.

A thesis submitted for the
DEGREE OF DOCTOR OF PHILOSOPHY
in the University of London

Department of Chemistry,
Imperial College of Science and Technology,
London, S. W. 7.

July, 1963.

ABSTRACT

A brief historical survey of far infra-red spectroscopy is given, together with a review of the principles, instrumentation and methods. The design, construction and use of a far infra-red vacuum grating spectrometer are described. The handling of samples in different states of aggregation and the measurement and calculation of their far infra-red spectra are discussed.

The infra-red absorption spectra of $PbEt_4$, $SnEt_4$ and $Sn(nPr)_4$ have been observed over a frequency range down to 55 cm^{-1}. Nearly complete vibrational assignments are made by comparison with comparable compounds, which indicate that substantial proportions of both trans and gauche forms of the n-propyl group are present in liquid $Sn(nPr)_4$. Rotation about the metal-carbon bonds is nearly free or restricted by a barrier of less than 1 kcal $mole^{-1}$. Rotation about the C_1-C_2 bond of the propyl group is restricted by a barrier of 3-4 kcal $mole^{-1}$. No changes in simple valence force field constants derived from $SnMe_4$ and propane are needed to fit the skeletal frequencies of the SnEt chain in $SnEt_4$. Thermodynamic functions for $SnEt_4$ are calculated (at 273.16°K).

The vibrational spectra of a number of alkyl tin chlorides have been observed down to 55 cm^{-1}. Valence force field calculations were carried out for $SnMe_3Cl$, $SnMe_2Cl_2$ and $SnMeCl_3$ in order to facilitate the assignment of the low frequency fundamentals. The spectra of $SnEt_3Cl$ and $Sn(nPr)_3Cl$ are assigned by comparison with the tetraethyls. The assignment of $SnEt_3Cl$ assumes some coupling between the CH_2 wagging and rocking modes. The spectrum of $Sn(nPr)_3Cl$ indicates that again both forms of the n-propyl group are present.

Solvent studies show that the Sn-Cl stretching frequency is extremely sensitive to environment. Spectra of the solid, liquid and solutions of the methyl tin chlorides indicate that chlorine bridging between the molecules takes place. Spectra of $SnMe_3Cl$ dissolved in a wide variety of solvents exhibit fractional shifts of the Sn-Cl stretching frequency which are of the same order of magnitude as observed in the near infra-red for other highly polar bonds. In acetonitrile solution a distinct complex is formed between the nitrile and the lower alkyl tin chlorides. Solutions of $SnMe_3Cl$ in acetonitrile-benzene mixtures show two distinct Sn-Cl stretching bands.

ACKNOWLEDGEMENTS

I am deeply grateful to Dr.J.L.Wood for the guidance and encouragement which he has continously extended throughout the course of this research.

I wish to thank Mr.H.G.Cobley, Mr.D.Alger and the technical staff of the Chemistry Department for their assistance in the construction and maintenance of the far infra-red spectrometer, and also my fellow students for innumerable stimulating and helpful discussions.

Finally, I wish to thank Pure Chemicals Ltd. for supplying nearly all the compounds studied in this work, and their Chief Chemist, Mr. Jankowski, for his advice and help in the preparation of some of them.

I am greatly indebted to Pure Chemicals Ltd. for the award of a Research Studentship without which this work would not have been possible.

CONTENTS

ABSTRACT	i
ACKNOWLEDGEMENTS	iii
CONTENTS	iv
INTRODUCTION	0
1: HISTORICAL	2
1.1: Early history of infra-red	2
1.2: The discovery of reststrahlen and the far infra-red.	3
1.3: The method of focal isolation	4
1.4: Sources: introduction of the quartz mercury lamp	6
1.5: Early detectors	7
1.6: First grating spectrometers	8
1.7: The Michigan spectrometer	9
1.8: Early work in the far infra-red	10
1.9: Post-war developments	11
2: PRINCIPLES AND INSTRUMENTATION	13
2.1: Sources of far infra-red radiation	13
2.2: Detectors	14
2.21: General remarks	14
2.22: The Golay detector	15
2.23: The superconducting bolometer	17
2.3: Monochromators	18
2.31: The echelette grating	18
2.32: Filters	20
2.321: General considerations	20
2.322: The chopper	21
2.323: Reststrahlen filters	21
2.324: Other reflection filters	22
2.325: Transmission filters	23

2.4: Spectrometer optics 23
2.41: General considerations 23
2.42: Source optics 24
2.43: G rating monochromator optics 25
2.431: The Pfund-Hardy system 25
2.432: The Pfund autocollimator 26
2.433: The off-axis paraboloid 28
2.434: The Czerny-Turner mount 28
2.435: The Ebert-Fastie system 29
2.44: Detector optics 30
2.441: Condensing mirror 30
2.442: Image transformers or slicers 30
2.5: Interferometric spectroscopy 32

3: CONSTRUCTION AND OPERATION OF A FAR INFRA-RED VACUUM GRATING SPECTROMETER 33
3.1: Construction of the spectrometer 33
3.11: Introduction 33
3.12: Optical path of the spectrometer 36
3.13: The source area 36
3.131: The source and cooling jacket 36
3.132: The KBr chopper 40
3.14: The monochromator area 41
3.141: The slits 41
3.142: The Ebert mirror 41
3.143: The grating and mount 43
3.15: The condenser area 43
3.151: Description of the image slicer 44
3.152: Adjustment of the image slicer 46
3.16: The sample area 46
3.17: The detector area 47
3.171: The reststrahlen holders 50
3.172: The Greenler image reducer 50
3.173: The detector mounting 52

3.18: The grating drive and gearbox 54
3.19: Evacuation of the instrument 55
3.2: The calibration and use of the spectrometer 56
3.21: Filtering conditions 56
3.211: Filtering: the 200 lines cm^{-1} grating 56
3.212: Filtering: the 80 lines cm^{-1} grating 58
3.22: Calibration of the spectrometer 62
3.23: Sample handling 62
3.231: Gases 62
3.232: Liquids 63
3.233: Solids 66

4: THE VIBRATIONAL SPECTRA OF $PbEt_4$, $SnEt_4$ AND $Sn(nPr)_4$. 69
4.1: Introduction 69
4.2: Experimental 69
4.3: Results 70
4.4: Discussion 70
4.41: Vibrational assignment: $PbEt_4$ & $SnEt_4$ 70
4.42: Vibrational assignment: $Sn(nPr)_4$ 75
4.43: Force field calculations: $SnEt_4$ 79
4.44: Torsional frequencies 83
4.441: Calculation for $SnEt_4$ 83
4.442: Calculation for $Sn(nPr)_4$ 84
4.45: Thermodynamic calculations: $SnEt_4$ 85
4.5: Conclusions 88

5: VIBRATIONAL SPECTRA OF SOME ALKYL TIN CHLORIDES

5.1: The vibrational spectra of $SnMe_3Cl$, $SnMe_2Cl_2$ and $SnMeCl_3$ 89

5.11: Introduction 89

5.12: Experimental 89

5.121: Preparation of the compounds 89

5.122: Recording of spectra 90

5.13: Results 91

5.14: Discussion 91

5.141: $SnMe_3Cl$ 91

5.142: $SnMeCl_3$ 97

5.143: $SnMe_2Cl_2$ 101

5.15: Conclusions: Intercomparison of the methyl tin chlorides 106

5.2: The vibrational spectra of $SnEt_3Cl$ and $Sn(nPr)_3Cl$ 107

5.21: Introduction 107

5.22: Experimental 107

5.23: Results 107

5.24: Discussion 108

5.241: $SnEt_3Cl$ 108

5.242: $Sn(nPr)_3Cl$ 111

5.25: Conclusions 114

6: ENVIRONMENTAL EFFECTS ON THE FAR INFRA-RED SPECTRA OF ALKYL TIN CHLORIDES 122

6.1: Introduction 122

6.2: Experimental 123

6.3: Results 124

6.4: Discussion 124

6.41: $SnMe_3Cl$ 124

6.411: The dissociation of $SnMe_3Cl$ 124

6.412: General solvent effects in $SnMe_3Cl$ 126
6.413: F requency shifts in liquid and solid $SnMe_3Cl$ 128
6.414: The association of $SnMe_3Cl$ & MeCN 131
6.42: $SnEt_3Cl$ and $Sn(nPr)_3Cl$ 133
6.43: $SnMe_2Cl_2$ and $SnMeCl_3$ 135
6.5: Conclusions 137

APPENDIX: Tables of far infra-red spectra 138
a). $SnEt_4$ 139
b). $PbEt_4$ 140
c). $Sn(nPr)_4$ 142
d). $SnMe_3Cl$ 143
e). $SnMe_2Cl_2$ 149
f). $SnMeCl_3$ 151
g). $SnEt_3Cl$ 152
h). $Sn(nPr)_3Cl$ 155

REFERENCES 157

INTRODUCTION

The study of organometallic compounds has formed an exciting branch of chemistry ever since Mendeleeff's prediction of germanium, which was partly founded on a comparison of the properties of organometallic derivatives of silicon, tin and lead. Since the war however, an ever increasing amount of work has been devoted to this field, largely because of the growing industrial importance of th ese compounds. Organotin compounds in particular are now extensively used as stabilisers for plastics and as the active component of some agricultural fungicides. An 80 page review by Ingham et. al. (94) appeared in 1960 and gives some idea of the complexity and extent of organotin chemistry.

The use of infra-red spectroscopy as an aid to structural determination and analysis of organotin compounds is limited because only the hydrocarbon vibrational modes give rise to absorption bands within the range of ordinary near infra-red spectrometers. Nearly all the vibrations involving bonds at the tin atom lie below 600 cm^{-1}, and of these all the bending modes (except the Sn-H bending) below 300 cm^{-1}. Thus for example, the Sn-Cl stretching vibration in $SnMe_3Cl$ (trimethyl tin monochloride) lies at 345 cm^{-1} and the C-Sn-C bendings near 145 cm^{-1}.

Low frequency Raman spectroscopy of reasonable reliability and accuracy is difficult even in the best of instances where the sample is a clear, photolysis resistant liquid available in comparatively large amounts. This explains why in only a few of the simplest cases has anything

approaching a complete vibrational assignment of an organotin molecule been reported in the literature.

There remains the technique of far infra-red spectroscopy, which is here taken to mean the region from 400 cm^{-1} bownwards (below the limit of commercial instruments equipped with potassium bromide prisms). In the past this technique has been beset with experimental difficulties that have limited its application to a few specific problems of theoretical importance inaccessible by any other means. At present however, with the availability of commercially supplied echelette grating replicas for the region and an adequately sensitive and uncomplicated (Golay) detector, these difficulties are more apparent than real. In spite of the increasing interest now shown in this region, the work reported in this thesis constitutes the first known application of far infra-red techniques to the vibrational spectroscopy of organometallic compounds.

For reasons mentioned earlier, most of the 'skeletal' frequencies of organotin compounds absorb in the far infra-red. Accordingly the greater part of this work is concerned with the measurement of far infra-red spectra. These are supplemented by spectra in the region 3500-400 cm^{-1} measured with the commercial spectrometers in use in this department, The results are presented and discussed in sections 4,5 and 6 of the thesis. Parts 1 and 2 review the history, principles, instrumentation and methods of far infra-red spectroscopy and part 3 describes the construction and use of the far infra-red vacuum grating spectrometer designed by Dr. J.L.Wood and built in this laboratory by Dr. Wood, Mr. H.G.Silver and the author.

1: HISTORICAL.

1.1: Early History of Infra-red.

Sir William Herschel discovered infra-red radiation in 1800, during the course of experiments to find filters which would remove the excessive heat from his telescopic images of the sun (1). Using a glass prism to disperse the sun's radiation and liquid in glass thermometers, he found the maximum temperature rise to occur beyond the red end of the visible spectrum and not in the yellow-green region which was visually the brightest. Because these two maxima did not coincide, Herschel remained convinced that the invisible heat rays and light were fundamentally different. The insensitivity of his thermometer and the absorption of the glass prism limited his work to the small region of the infra-red between about 0.8 and 3.5 microns.

It was not until the introduction of the thermopile that infra-red spectroscopy could properly be said to have begun. Following Seebeck's discovery of the thermoelectric effect in 1822, Nobili (2) constructed a thermopile and used it successfully in conjunction with an astatic galvanometer to measure very small changes in temperature. It was used by his pupil Melloni, in his pioneering investigations which included the discovery of the transparency of rock-salt to infra-red radiation in 1835 (3), and the detection of heat from the moon's surface.

In 1840 Sir John Herschel (son of the dicoverer) allowed the sun's spectrum to fall on paper coated with soot and dampened with alcohol (4). Dry spots were formed where the alcohol evaporated, giving a crude "photograph" of the sun' spectrum in which the damp regions indicated

absorption.

Svanberg's invention of the bolometer in 1849 remained unused until Langley rediscovered it in 1881 (5). This was superior to existing thermopiles and enabled accurate measurements at considerable dispersion to be made (Langley, Rubens, Trowbridge, Paschen and others).

During the next thirty years the infra-red field widened rapidly. The sensitivity of the thermopile was improved considerably by Rubens and others, and the Crookes radiometer and the microradiometer of Boys and d'Arsonval were introduced. The classical pioneering work of Coblentz (6) in molecular absorption spectrometry provided conclusive experimental evidence of the correlation between molecular structure and characteristic absorption frequencies, and the introduction by Bjerrum in 1916 (7) of the concept of treating vibrating polyatomic molecules as mechanical systems of point masses connected by Hooke's law forces laid the foundations of vibrational spectroscopy.

1.2: The discovery of reststrahlen and the far infra-red.

The property of selective or reststrahlen reflection was first discovered by Nichols in 1896 (9) in the near infra-red for quartz (at 1124 cm^{-1}). It was realised that heavier crystals would exhibit similar properties at much lower frequencies and in 1897 Rubens and Nichols (9a) reported investigations on a whole range of crystals which enabled Rubens and his collaborators to extend their studies in the infra-red down to about 35 cm^{-1}. Previous work had been limited to the region above 500 cm^{-1} where rock-salt and sylvite were transparent enough to be used as prism material. Gratings

could not be used at longer wavelengths because the detectors then available were too insensitive.

In the neighbourhood of its lattice frequencies a crystal becomes a metallic reflector, with reflectivities as high as 0.9. The lattice frequencies of alkali halide crystals and others such as fluorite and calcite lie in the far infra-red region below 400 cm^{-1}. After several reflections from such a crystal, far infra-red radiation with a bandwidth of about 15-30μ can be isolated. An interferometer consisting of thin parallel plates of crystal quartz, which is transparent below about 200 cm^{-1}, was used by Rubens and Hollnagel (10) for wavelength measurements. The distance between the plates was increased in steps and the intensity of the transmitted radiation measured with a radiometer. Interference in the air space gave rise to periodic maxima and minima of intensity. From the separation and logarithmic decrement of these maxima the wavelength and the width of the reststrahlen band could be determined.

The method of reststrahlen was widely used in early far infra-red work and because of its simplicity has even been used as recently as 1931 by Strong (11) and 1933 by O'Loane (12) to locate some far infra-red absorption bands of organic compounds.

1.3: The method of focal isolation.

In 1899 Rubens and Aschkinass (13) showed that it is possible to separate very long heat waves by means of a quartz prism of small angle, but that too much radiation was lost for this method to be practicable. The method of focal isolation introduced in 1911 by

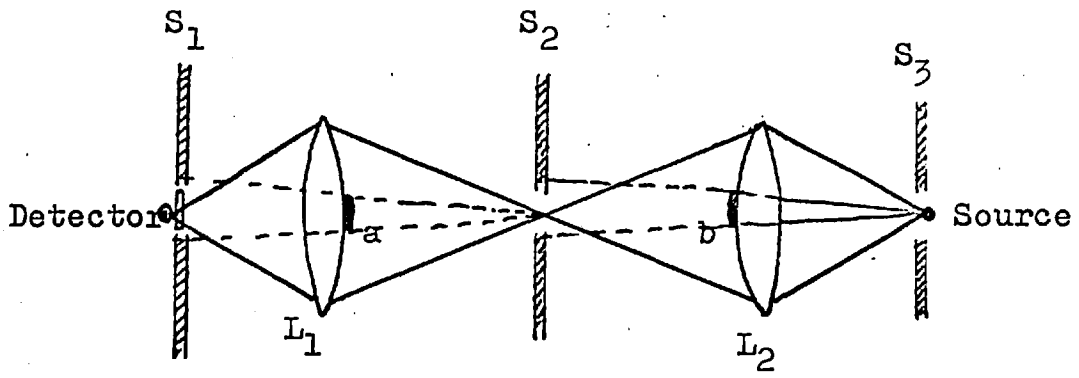


Fig.1: The Method of Focal Isolation
L_1 and L_2 are quartz lenses,
s_1, s_2, s_3 are screens
a and b are opaque stops.

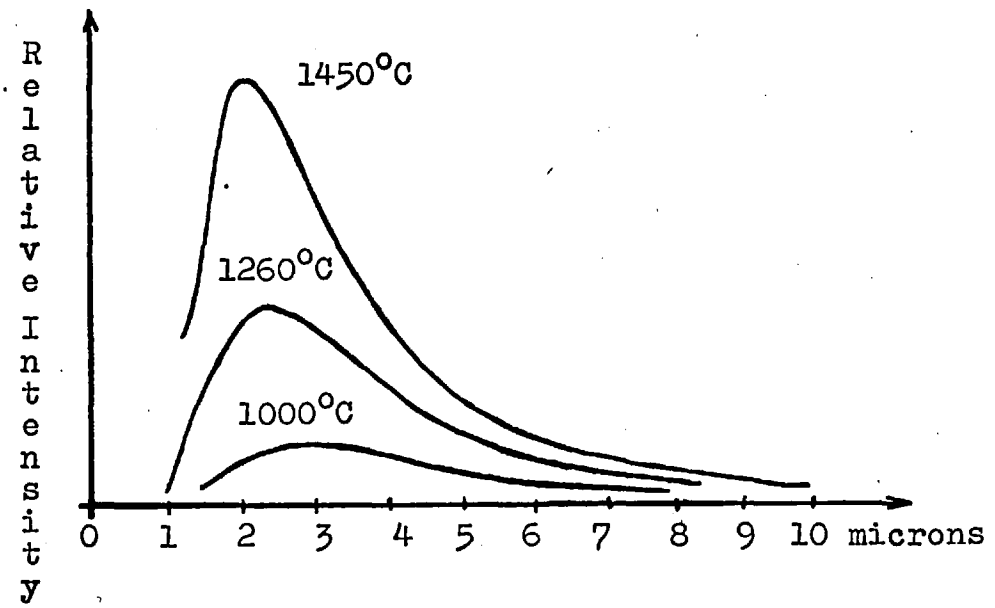


Fig.2: Spectral distribution of energy from a black body.

Rubens and Wood (14) however, gave results nearly as good as those obtained with the reststrahlen method. It is based on the fact that the focal length of suitable quartz lenses can vary by as much as 1 cm for wavelengths in the far infra-red.

Fig.1 is a diagram of one such arrangement. The small hole in an opaque screen is placed at the focal point for the chosen wavelength and a second quartz lens used to condense the emergent beam on to the detector. Small opaque stops are used to eliminate unrefracted axial radiation. Again an interferometer must be used for wavelength measurements.

1.4: Sources: Introduction of the quartz mercury lamp.

The source of far infra-red radiation commonly used in these early investigations was the Welsbach or Auer mantle which consists of a close mesh envelope of silk impregnated with thoria and a small percentage of ceria, heated to incandescence by a gas flame. It has the advantage of nearly zero emissivity in the near infra-red region around 10,000-1,700 cm^{-1} which simplifies the problem of filtering out these radiations.

In 1911 Rubens and von Bayer (15) introduced the quartz mercury lamp which has a greater emissivity in the far infra-red than any other source at present available. Later work by Koch (16) and Dahlke (17), who investigated the spectrum dependence on voltage, current density, vapour pressure, etc, showed that in the higher frequency far infra-red most of the emission is from the hot quartz envelope, while the lower frequencies originate mainly in the discharge itself.

During the course of experiments to close the

gap between heat waves and the radiation generated by electrical means, Nichols and Tear (18) detected radiation from the quartz mercury lamp out to 420μ, and radiation up to 220μ as harmonics from a Hertzian oscillator. In 1924 Glagolewa-Arkadiew (19) was able to generate radiation of wavelengths as short as 110 cm^{-1} by similar means.

1.5: Early detectors.

The first sensitive infra-red detector was Langley's bolometer (5), consisting of a Wheatstone bridge, one arm of which was a very thin blackened platinum strip exposed to the radiation. The resulting imbalance current was measured with a galvanometer.

Another early instrument was the microradiometer (20). This was essentially a pneumatic detector consisting of two gas-filled bulbs connected by a capillary in which were two electrodes dipped into a drop of conducting solution. One of the bulbs was exposed to the radiation, causing the gas to expand and move the drop. The resulting resistance change was used in the same manner as in the bolometer.

The sensitivities of these detectors were limited in the first instance by the susceptibility of the galvanometer to extraneous electrical and magnetic disturbances. In an effort to avoid these drawbacks the radiometer and radiomicrometer were introduced.

The radiometer (21) consisted of two vanes of very thin mica or platinum blackened on one side, balanced on a glass rod with a mirror attached, and suspended from a quartz fibre in an atmosphere of about 0.1mm Hg pressure. The higher momentum of molecules recoiling

from the vane exposed to radiation would rotate the assembly. This detector was used frequently by Rubens in his early investigations.

The radiomicrometer of Boys and d'Arsonval (22) consisted of a very small thermocouple in series with a single conducting wire loop suspended in vacuum between the poles of a strong fixed magnet. It is essentially a thermocouple and galvanometer combined, and was most frequently used in the early grating spectrometers until greatly improved compensated thermocouples came into use in the 1930's.

All these detectors were susceptible to zero drift caused largely by temperature and pressure changes in the atmosphere, and investigations were possible only during stable weather conditions.

1.6: First grating spectrometers.

The first grating spectrometers for the far infra-red were constructed in 1920 by Witt in Lund (23), and by Rubens in 1921 in Berlin (24). Witt used a 3 x 4 cm grating made by winding silver wire of diameter 0.17 mm on the threads of two precision screws, achieving a grating constant of 0.3mm. With a radiomicrometer as detector, he investigated the emission of Welsbach mantles coated with various mixtures of thoria and ceria. In the range 125-60 cm^{-1} he found five radiation minima as compared with two obtained earlier by Rubens with his reststrahlen method. It was realised quite early that these minima were caused by the absorbing properties of atmospheric water vapour.

In 1925 Czerny modified Rubens's instrument and with an improved radiomicrometer was able to measure the rotational bands of HCl gas between 250 and 100 cm^{-1}.

He also used wire gratings, of dimensions 8x8cm with constants of 0.4 and 0.8mm, and slit widths of about 2.5mm. His greatest difficulty was in finding suitable windows for the absorption cell which he overcame by making thin membranes of celluloid by spreading a solution of the latter over water and allowing the solvent to evaporate.

Until about 1930 the centre for far infra-red research was undoubtedly in Berlin, where Rubens and Czerny did most of their work. Thus Barnes (26) described work with a later instrument built by Czerny and with a wire grating spectrometer built by himself at Princeton in 1934 (27), which was capable of separating bands as close together as 1.3 cm^{-1}.

In 1929 Badger and Cartwright built an instrument with a laminar reflection grating made by etching out the grooves from a silverplated gold surface supported on plate glass.(28, 29). The instrument was evacuable to a vacuum better than 0.001mm Hg to eliminate water vapour absorption and to secure maximum thermocouple sensitivity.

1.7: The Michigan spectrometer.

The echelette grating was introduced as early as 1911 by R.W.Wood (30), but it was extremely difficult to rule the comparatively wide grooves required for the far infra-red region and the early workers had to make do with wire and laminar gratings. The Michigan spectrometer was designed by Randall to achieve a resolving power and precision comparable to the best near infra-red instruments of the day and he realised that this could be done only by using large echelette gratings.

Accordingly, the ruling engine constructed at the University of Michigan was designed to take 12"x12" blanks and be capable of ruling grooves up to 1mm in width. A great deal of work had to be carried out to find the best cutting tools and alloys for the blanks before they were able to rule satisfactory gratings.

The spectrometer was first described in 1932 (31) and used to record the rotational spectrum of water vapour (32) with a resolution and precision barely surpassed by the best far infra-red instruments in use today. This classic paper by Randall, Ginsberg, Dennison and Weber (32) which also contains a complete theoretical analysis of the observed spectrum, clearly showed that the then new quantum mechanics was also quite capable of solving a molecular problem as complex as the spectrum of an asymmetric rotator, and provided a great stimulus to far infra-red spectroscopy in general.

Fig. 8 is a diagram of the optical system of the spectrometer, which used a 10"x22" echelette grating, a thoria coated platinum strip as source, and a vacuum thermoelement as detector. The detector was later fitted with the Firestone resonance amplifier which gave a photographic record of the spectrum (33).

1.8: Early work in the far infra-red.

Mainly as a result of the insensitivity of available detecting methods, the early workers in the far infra-red region were limited to investigating the gross properties of materials: the resolution obtainable was insufficient to reveal absorption bands. Thus the work of Rubens and his collaborators was concerned with the measurement of reflection, transmission and broad absorp-

tion characteristics of a wide range of substances, from the alkali halide crystals to black paper. The first grating spectrometers too, were too crude to give any new results of importance and it was not until Czerny's work on HCl gas that far infra-red spectroscopy begun to yield results precise enough to contribute to the theoretical development of physics and chemistry.

Badger and Cartwright in 1929 (28) observed the rotational bands of ammonia gas and in 1933 Wright and Randall (34) were able to resolve the inversion splitting of these bands. Barnes in 1934 (35) investigated ND_3. The work of Randall et al. has already been mentioned, and in 1939 Fuson, Randall and Dennison (36) recorded and analysed the spectrum of heavy water vapour.

The war brought to a standstill what little work was being carried out in the far infra-red and only round about 1950 did there begin a revival of interest for this region of the spectrum.

1.9: Post-war developments.

During the war a large amount of work was devoted to the possible military applications of infra-red radiation, as a result of which great improvements were made in infra-red detectors and amplifiers. With highly sensitive and fast-responding detectors it became possible to modulate the radiation (i.e. chop, at frequencies around 10 c/s) and so amplify only the alternating component of the signal from the detector, thus avoiding the effects of zero drift. The a.c. signal also permitted the use of stable electronic amplification with output recorded automatically by electronic strip-chart recorders.

The Golay pneumatic detector (37), first described in 1947, is now commercially available as a compact,

simple to use unit. It is comparable in sensitivity and response to the improved bolometers and thermoelectric detectors and has the additional advantage of a comparatively large receiving area. The photoconductive detectors developed during the war are insensitive to far infra-red radiation as the energy of a quantum at these wavelengths is too small to lift electrons into the conduction band.

Much research was also devoted to finding new optical materials for the infrared. Of these, the most important was KRS-5, a mixture of thallium bromide and iodide which is fairly transparent down to about 200 cm^{-1}, but is used mainly as a reststrahlen reflection filter: it has a broad peak at about 80 cm^{-1}.

Improvements in the technique of growing large crystals made it possible to synthesise crystals of the caesium halides large enough to be used as prism material. CsI for example, is transparent down to about 200 cm^{-1} and has a useful reststrahlen peak at 70 cm^{-1}.

The transparency of 'teflon' and polyethylene to infra-red radiation has solved the problem of window materials, which had been one of the factors hindering the chemical applications of far infra-red spectroscopy (viz. the difficulties Czerny had in finding a suitable window material for his work on HCl gas).

Finally, high quality echelette gratings, which areindispensable for far infra-red work, became generally available for the region, and it is now possible to get even inexpensive but satisfactory replica gratings.

2:PRINCIPLES AND INSTRUMENTATION.

2.1: Sources of far infra-red radiation.

Almost all spectroscopic work in the far infra-red has to be done 'in absorption' since under normal conditions the emission is too weak to be detectable, and available methods of excitation usually destroy the system under investigation. Ideally what is required is a monochromatic source with continuously variable frequency such as is available to spectroscopists working in the microwave region. At present there are no such sources available: LASERs can be made to work in this region, but it is possible to 'tune' this output over only a very small range, and the so-called Varotron (38) is still in too early a stage of development for its full potentialities for far infra-red use to be assessed. Thus it is necessary to rely upon 'temperature' sources, whose energy spectrum is similar to that of a black body (fig.2).

The difficulties of using such sources in the far infra-red are the extremely small amount of radiation emitted in the region, and the presence of a very large amount of near infra-red radiation which create special problems of detection and filtering. For a black body at 2000°K for example, the energy emitted at 100 cm^{-1} is 10^{-6} of the energy emitted at 6950 cm^{-1} (the maximum of the black body curve). By increasing the temperature to 3000°K, an increase in the total emission of $(3/2)^4 =$ 5-fold is obtained, but it represents an energy increase of only 100 °/o at 2000 cm^{-1} and 60 °/o at 400 cm^{-1} (39). Thus no real advantage is obtained by increasing the source temperature above about 2000°K.

There are three sources which are generally used

in the far infra-red today. These are:

(a) The 'Globar', consisting of a silicon carbide or carborundum rod of about 1/4 " diameter and 3" long which is heated electrically to about 1200°K;

(b) A thoria coated platinum strip (dimensions about 4" x 0.3" x 0.005") heated to about 1300°K by a current of 100 amp.;

(c) the quartz mercury lamp of the type used in street lighting in which a discharge operates in a fused quartz envelope at a mercury vapour pressure of a few atmospheres.

The first two are the most effective in the region between about 4000 and 200 cm^{-1}, while the mercury lamp has to be used at longer wavelengths. Beyond about 100 cm^{-1} the bulk of the emission appears to originate in the mercury vapour discharge, but there seems to be no general agreement as to the nature of this radiation. On the one hand it is regarded as appearing from vibration-rotation transitions in excited quasi- molecules of mercury (18), or as being due to the deceleration of electrons in the field of positive ions. Rössler (40) favours the first hypothesis because he has observed similar effects from Zn and Cd discharges (elements belonging to the same group as Hg), but not with S or Tl.

2.2: Detectors.

2.21: General remarks.

In order to achieve a reasonable degree of resolution, the very small amount of energy has to be considerably dispersed. This necessitates the use of extremely sensitive detectors.

Of the detectors mentioned in section 1.5 only

the thermoelement and the bolometer have survived to the present day. Sophisticated developments of these are described in "Infra-red Methods" by Conn and Avery (41), and table I, after Yaroslavsky (42) gives an indication of how they compare with the Golay detector.

Table I.

	TYPE	SENSITIVITY*	TIME CONST.	RECEIVING AREA
(43)	Schwarz thermocouple	4.2×10^{-11} w	0.03sec	$0.4 mm^2$
(44)	Bird metallic bolometer	10^{-10} w	0.004sec	$0.02 mm^2$
(37)	Golay pneumatic	7.6×10^{-11} w	0.02sec	$4-7 mm^2$

* Minimum detectable power

2.22: The Golay detector (37,45).

This is a pneumatic thermal detector which responds uniformly throughout the spectrum and is equal to the very best room temperature bolometers and thermocouples. It has now been developed to the stage where it is only about ten times inferior to an idealised thermal detector operating at room temperature.

It consists of a small chamber A (fig. 3) containing a gas of low thermal conductivity (e.g. Xenon). Radiation reaches a thin absorbing membrane B in the chamber through a diamond window C. This membrane is a thin plastic film coated with aluminium such that its surface resistance matches the impedance of free space for electromagnetic radiation. This 'black' receiver warms the gas in the cell and the corresponding rise in pressure distorts a mirror membrane D at the other end

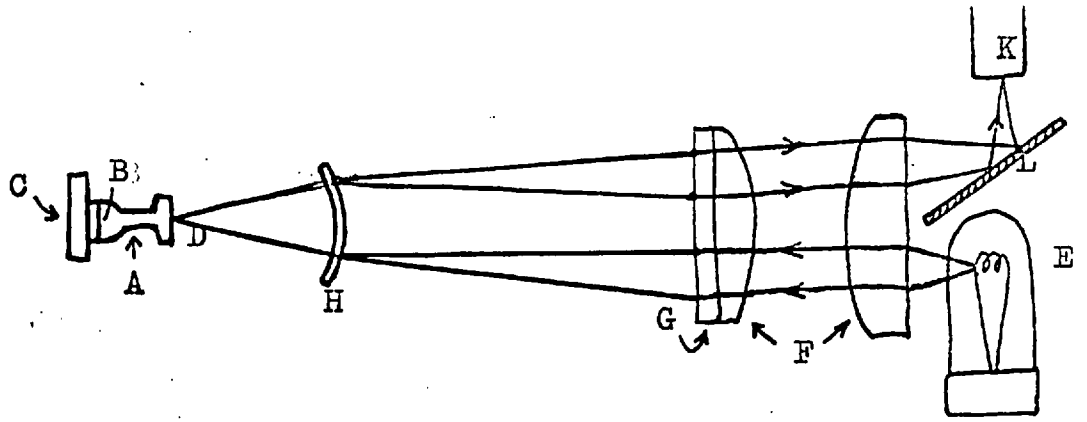


Fig.3: Schematic diagram of Golay Detector head. Key: p.15.

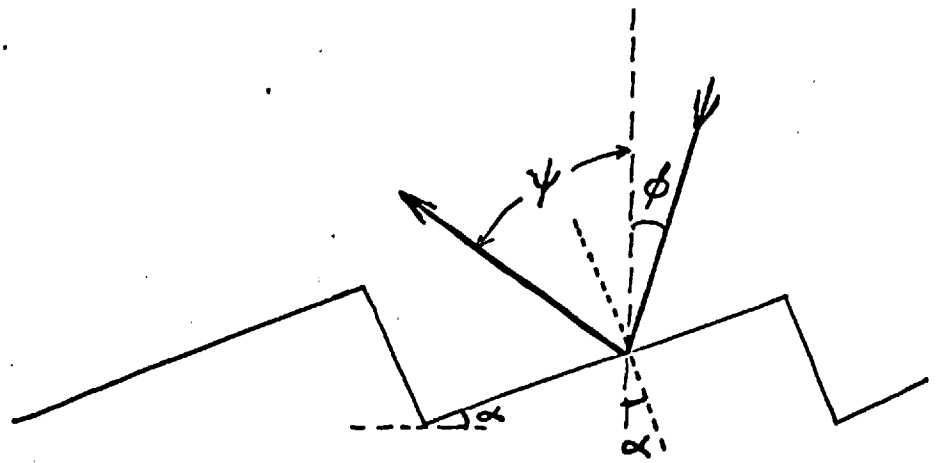


Fig.4: The Echelette Grating.
(see p.18).

of the cell. The cell is linked with a ballast chamber so that in the absence of a cha nging radiation signal pressures are the same on both sides of the membrane D which remains flat.

Light from the lamp E passes through condenser lenses F and a line grid G, and is concentrated on to the mirror membrane. A meniscus lens H forms an image of the grid superimposed on the grid itself and the returning beam is deflected into a photocell K by the mirror L.

Radiation striking the receiver causes deformation of the mirror membrane which produces a corresponding change in the relative positions of the line grid and its image, and hence a change in the intensity of light reaching the photocell. The radiation signal, which is modulated at 10 c/s, thus produces an alternating output from the photocell which is amplified, rectified and displayed on a potentiometric recorder.

The commercial model manufactured by Unicam Ltd. also works satisfactorily in a vacuum.

2.23: The superconducting bolometer.

Sensitivities much higher than those indicated in table I can only be attained with detectors operating at liquid helium temperatures. One such detector is the superconducting bolometer recently built by Bloor et al. (46) at Queen Mary's College, London. The temperature coefficient of resistance (dR/dT) of a superconducting metal near its transition temperature is several orders of magnitude greater than for normal metals at room temperature. The sensitive element used by these workers consisted of tin evaporated on to a very thin strip of mica, having a resistance of about 50 ohms and $\frac{dR}{dT}$ equal

to about 5×10^3 ohms deg.$^{-1}$ at 3.7°K. This detector has an approximately constant sensitivity throughout the range from 1-1500 μ, and a minimum detectable signal less than 10^{-12}w, falling on an area of 3 mm^2 when the overall time constant is 1.25 sec.

Several other detectors are mentioned briefly in a review of far infra-red spectroscopy by Wilkinson et al., (47), and in one by Martin (48).

2.3: Monochromators.

Since there are no transparent materials available which could be used as prisms in the far infra-red region, it is necessary to use grating monochromators consisting of a grating and suitable filters to separate the different orders.

2.31: The echelette grating.

The ratio of intensities in one of the first orders for the wire, laminar and echelette gratings is 1 : 4 : 10 respectively under favourable conditions (42). Thus the echelette grating is the most efficient means available at present for dispersing far infra-red radiation.

The grooves of an echelette grating are cut to give a saw tooth profile as shown in fig. 4. The angle α which the base of the groove makes with the plane of the grating is called the blaze angle. If ϕ is the angle of incidence of the beam, then the maximum intensity will be concentrated into those orders for which the angle of diffraction is $\phi + 2\alpha$, i.e. the angle for which the ordinary law of reflection from the groove surface is obeyed.

The diffraction formula for a grating is

$$n\lambda = d(\sin\phi \pm \sin\psi),$$

where ϕ and ψ are respectively the angles of incidence and diffraction, d the grating constant and n the order of the spectrum. If the spectra are brought into view by rotating the grating with fixed angles of incidence and diffraction, as is usual, then this becomes.

$$n = 2\,d\cos(\frac{\delta}{2})\sin\theta.$$

Here δ is the angle between the incident and diffracted beams, which is a constant determined by the geometrical arrangement of the slits and mirrors, and θ the angle of rotation of the grating from the specular position. In terms of wave numbers v, which is the more convenient unit for spectroscopic purposes,

$$v = \frac{n}{2d}\sec\frac{\delta}{2}\,\mathrm{cosec}\,\theta,$$

and the spectral slit width S_v cm^{-1} is given by

$$S_v = \frac{2D}{S}\,v(4d^2v^2 - 1)^{1/2}$$

where S is the mechanical slit width in cms and D the distance between the slit and the grating.

Most of the echelette gratings produced nowadays are blazed at about 30° ($\mathrm{cosec}\,\theta \doteqdot 2$), so that if it is used in the first order (as is usual), the frequency in wave numbers corresponding to the blaze angle is $\frac{1}{d}$ = to the number of lines cm^{-1}. The grating is then usable between the approximate limits $\frac{2}{3}\frac{1}{d}$ and $\frac{3}{2}\frac{1}{d}$; nearly all the energy being diffracted into this region. For a given order, the energy maximum is approximately symmetrical about the blaze angle, but there is a small secondary maximum on the high frequency side (49).

2.3.2: Filters

2.3.2.1: General considerations.

The grating is not a complete monochromator by itself, because if the diffraction angle for light of frequency v in the first order is θ, then light of frequencies 2v in the second order, 3v in the third etc. are also diffracted through the angle θ. Thus some means of filtering out these higher orders is required. The magnitude of this filtering problem in the far infrared can be seen by referring to table II, after Ötjen et al. (50). It is calculated for the blaze position of an ideal echelette grating ruled with 180 lines in.$^{-1}$ blazed to concentrate 100 cm^{-1} radiation into the first order. There are limitations on the conditions to which it applies (see ref.50), but the corrections would amount to no more than that due to the assumption of a black body source.(at 1300°K).

Table II.

Spectral region	Order of spectrum	Relative intensity
100 cm^{-1}	1	1
200	2	8
300	3	24
400	4	54
500	5	99
1000-770	8-10	1370
2500-1430	15-25	25100
10000-2500	26-100	145000

The table shows that in the 100 cm^{-1} region the ratio of unwanted to wanted radiation is about 10^5. But since the short wave radiation, which accounts for most of the unwanted light, is sharply concentrated into the blaze direction, the problem is much simpler if the grating is used just off the blaze angle.

2.3.2.2: The chopper.

All the detectors generally used for infra-red work today are designed to react only to chopped radiation so that zero drifts etc. can be eliminated. If the chopper segments are made from a substance which is opaque only in a certain region of the spectrum, then radiation in that region only is detected because the rest remains unchopped.

Rock salt and potassium bromide are transparent in the visible and near infra-red so that only radiation below about 600 and 400 $c\bar{m}^{1}$ respectively is modulated when these crystals are used as choppers. This method however is not completely efficient since the crystals reflect about 3-4°/o from each surface, and therefore about 6-8°/o of the unwanted radiation is also detected. This effect can be partially compensated for by by reducing the areas of the open portions of the chopper by appropriately arranged 'tooth-picks'. The unwanted light is then modulated at twice the chopping frequency which is not passed by the amplifier.

2.3.2.3: Reststrahlen filters.

These and their mode of action have already been mentioned in section 1.2. They a re invariably used in far infra-red spectrometers operating in the region above 50 cm^{-1}, but there are no crystals available with reststrahlen peaks below this limit. Table III gives the reststrahlen frequencies for some of the more frequently used substances.

There is one further property of reststrahlen crystals which is sometimes utilised to increase their effectiveness as filters. This is that at the reststrahlen

frequency the reflected beam is unpolarised whereas at all other frequencies the beam is polarised if the angle of reflection is near the Brewster angle. If a second crystal is placed with its plane of incidence perpendicular to that of the first crystal, then the two reflectors act like crossed Nicol prisms for radiation not of the reststrahlen frequency. This method was first reported by Czerny (51) and by Strong (52), and was used by Lord and McCubbin in their far infra-red spectrometer.

Table III

Reststrahlen frequencies.

substance	frequency cm^{-1}
CaF_2	435, 305
LiF	385
$CaCO_3$	1493, 340
NaF	279
NaCl	192
KCl	158
KBr	121
CsI	70
KRS-5	83

2.3.2.4: Other reflection filters.

The scatter plate has frequently been used in the far infra-red. It consists of a metallic plate (e.g. aluminium) ground to give a rough surface which reflects long wavelength radiation but scatters radiation of wavelength comparable to and less than the dimensions of the surface imperfections. By grinding with different grades of carborundum, scatter plates can be made with cut-offs (which, unfortunately are not particularly sharp) at any desired wavelength.

The echelette grating can also be used in much

the same way, with greater efficiency (54). High frequency radiation is diffracted normally and lost to the beam, but frequencies below about 0.6/(grating constant) are specularly reflected as the zeroth order.

2.3.2.5: Transmission filters.

Very few substances are transparent in the far infra-red. Crystalline quartz has the rather unusual property of having a region of high absorption extending from about 2400-240 cm^{-1} but is comparatively transparent at frequencies below this range. Thus about 35-40 mm of crystal quartz absorbs totally between 2500 and 100 cm^{-1} but transmits 75°/o at 20 cm^{-1}. Fused quartz is much less effective.

Black polythene is invaluable for the removal of near infra-red radiation. It consists of carbon black embedded in polyethylene and has good transmission beyond about 400 cm^{-1}. Since polythene itself is fairly transparent, most of the filtering action is due to the carbon black, which had earlier been used in a crude form as soot deposited on quartz or paraffin wax.

2.4: Spectrometer optics.

2.4.1: General considerations.

Strong (55) has shown that for the far infra-red, where the Rayleigh-Jeans emission law is applicable to the source, the minimum wave number range dv embraced by the slits is given by:

$$dv = \left(\frac{wF}{BTAlt(d\theta/d\lambda)} \right)^{1/2}$$

where w is the minimum detectable power, T the source temperature, B the emissivity constant of the source, t the transmission factor of the spectrometer, $d\theta/d\lambda$ the angular dispersion, A the area of the collimator, F the focal length of the collimator and l the slit height. For high resolution, dv must be made as small as possible.

The quantities w, T, B, t are independent of the optical design. Ideally very large mirrors and gratings are required (large A), but the cost is prohibitive. Failing this, the focal length F should be small and the slits long, but these imply severely curved mirrors which introduce an intolerable degree of aberration.

As there are no suitable lens materials available for the far infra-red, it is necessary to use mirrors throughout. This complicates the design of an aberration free optical system because mirrors return the radiation to the object area unless used off-axis, in which case the aberrations accumulate rapidly.

2.4.2: Source optics.

It is required to illuminate the entrance slit with radiation from the source. Fortunately this presents no especial problem even when very long slits are used, as most of the sources such as the mercury lamp or the globar are already elongated. Usually the source is placed on the axis of a spherical mirror (e.g. in fig. 10) or alternatively off-axis on one side of the beam (e.g. fig.13). The effect of aberrations is comparatively unimportant here.

2.4.3: Grating monochromator optics.

In this section some of the principal types of far infra-red monochromator design are discussed with reference to actual spectrometers reported in the literature. What is required is a system which shall gather as much light as possible from the entrance slit, collimate it on to the grating and condense it on to the exit slit.

2.4.3.1: The Pfund-Hardy system.

This arrangement was originally introduced by Pfund in 1927 (56) as one in which the entrance and exit slits can be situated on the axes of concave mirrors in order to minimise aberrations.

In the original spectrograph two paraboloids were used as the collimating and condensing mirrors and two auxiliary plane mirrors to couple the grating into the light path. When paraboloids are used instead of spherical mirrors, the only aberration in the system is due to the finite length of the slits whose extremities lie off the axis. The slits must consequently be kept short - a drawback which can be off-set by using large mirrors.

This method was first used in the far infra-red by Maar (57), Hopf (58) and Meier (59) at Jena in Germany. The latter's arrangement is shown in fig.5; it differs from the original version in that the grating itself contains a central aperture and replaces one of the plane mirrors. The low resolution (3-20 cm^{-1}) achieved by these workers was due mainly to the insensitivity of the radiometer which they used as detector.

2.4.3.2: The Pfund autocollimator.

This system differs from the preceding one only in that the paraboloidal mirror used to illuminate the grating with parallel light is also used to condense the diffracted light on to the exit slit. The grating, containing a central aperture, is placed in front of the mirror, and the two slits close together on the axis behind the aperture. It was used by McCubbin and Sinton (60) in their second far infra-red spectrometer (fig.6). To leave enough room for both slits the aperture in the grating must be fairly large (10 in^2 in this case), so the grating itself must be fairly large. McCubbin and Sinton used a 12 x 12" grating, a 12", f/1 parabolic mirror and a Golay detector, and achieved a resolution of 1-2 cm^{-1} throughout their working range of 100-15cm^{-1}.

In 1956, Yaroslavsky, Zheludov and Stanevich(61) reported a high performance spectrometer (resolution of 0.3-0.5 cm^{-1} from 500-20 cm^{-1}) using a monochromator basically similar to the one described above. The grating, however, was fixed, and double passed for greater dispersion and elimination of stray radiation by means of an auxiliary plane mirror which was also rotated to scan the spectrum (fig.7).

A modification of the Pfund autocollimating system in which an unperforated grating can be used, is incorporated in the spectrometer of Bohn et al. (62) which was designed for chemical work not requiring very high resolution (fig.7). It differs from Yaroslavsky's arrangement in that the plane mirror and grating are interchanged, giving a single pass system.

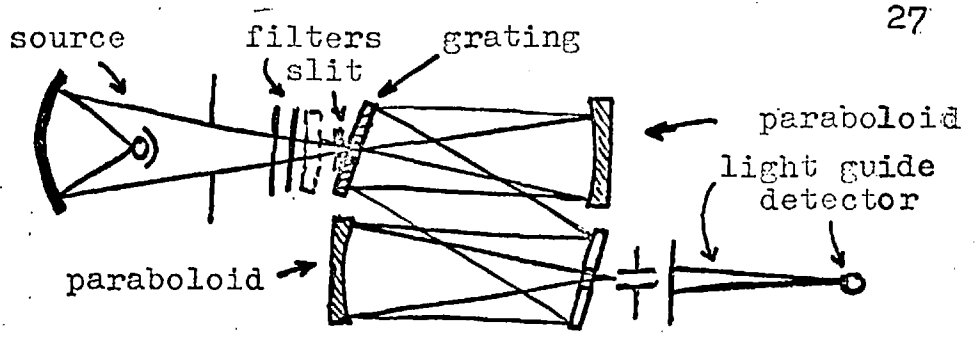


Fig. 5: MEIER'S SPECTROMETER

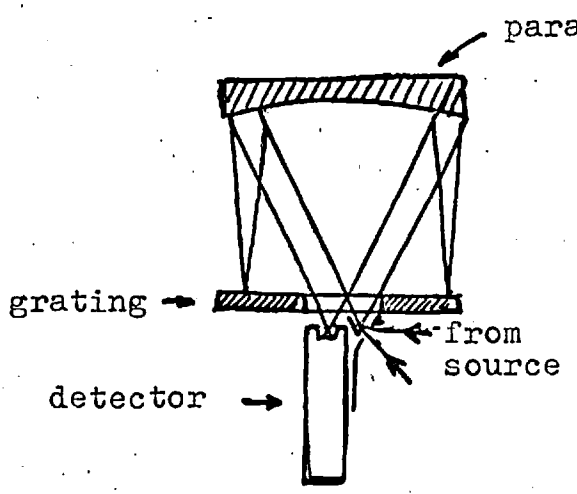


Fig.6: McCUBBIN&SINTON's SPECTROMETER

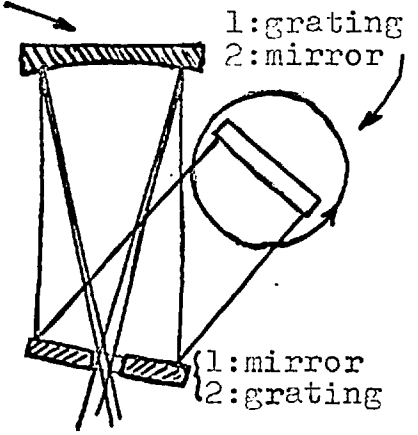


Fig.7: BOHN's (1) and YAROSLAWSKY's (2) MONOCHROMATOR

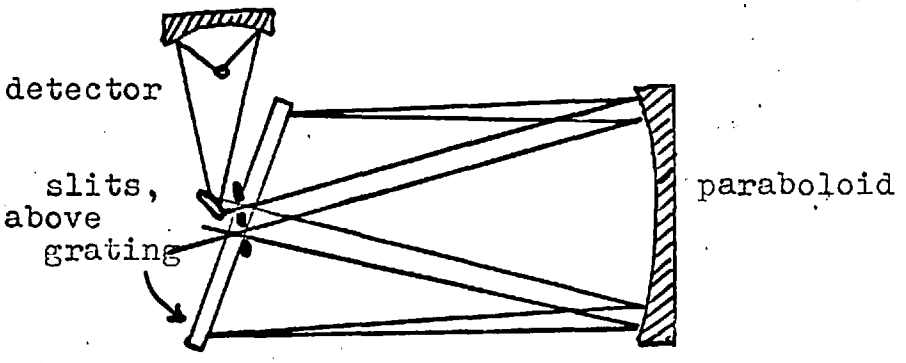


Fig. 8: RANDALL's SPECTROMETER

2.4.3.3: The off-axis paraboloid.

This system was first used in prism spectrometers and by Randall in the Michigan spectrometer (31). It is similar in principle to the Pfund auto-collimating system. The mirror is one half of a large paraboloid of aperture f/1.5 and the slits are mounted on the axis (see fig.8). The same type of monochromator was used by Ötjen et al. (50) in 1952. Both achieved a resolution between 0.5 and 1.0 cm^{-1} over the whole range (1000-50 cm^{-1} and 250-75 cm^{-1} respectively). Others who used this system were Lord and McCubbin (53).

2.4.3.4: The Czerny-Turner mount.

All the monochromator systems described above give their best results when a large parabolic mirror is used. The Czerny-Turner system however, only uses spherical mirrors, thereby considerably reducing the cost of the instrument. The principle was used by Czerny in his transmission grating instrument (25), and later discussed by Czerny and Turner (63). The mirrors and slits are arranged symmetrically so that the curvature of wavefront introduced by the first mirror is compensated by reflection at the second mirror (e.g. fig.9). Coma is completely eliminated and astigmatism considerably reduced.

The Czerny-Turner mounting has been used by several workers including Genzel and Eckhardt (64), Yoshinaga et al. (65) and Murzin and Demshina (66). Genzel & Eckhardt used a bolometer detector, an aperture of f/3 and achieved a resolution of 0.3-0.5 cm^{-1} in the range from 100-6.25 cm^{-1}. The spectrometer of Yoshinaga et al. is shown in fig.9 It employs a Golay detector and

and is capable of separating lines 0.25-0.5 cm^{-1} apart throughout the region from 500-10 cm^{-1}. All three used large echelette gratings of about 20 x 20 cms.

2.4.3.5: The Ebert-Fastie system.

This is a special case of the Czerny-Turner system in which the mirrors are part of the same spherical surface - usually one large single mirror. It was first described by Ebert in 1889 (67) but its full potentialities were not fully realised until 1952 when Fastie (68) showed that the system is capable of near theoretical resolution at f/6 in the infra-red even when very long slits are used. If the slits are curved and mounted with a common centre of curvature, the effect of astigmatism is eliminated as well as wavelength errors at the exit slit introduced by the curvature of the spectrum obtained from a plane grating. But the real advantages of the Ebert-Fastie system which make it especially suitable for the far infra-red are a). that more radiation can be pa ssed by the use of very long slits, b). the simple and easily mountable spherical optics and c). the fact that as a result of its symmetry it can be readily enclosed in a simple cylindrical vacuum tank.

Fig.10 shows the small and extremely compact instrument built by Robinson (69) which is capable of resolution slightly better than 0.5 cm^{-1} from 500-30cm^{-1}. Other Ebert spectrometers include two at King's College, London (47) and one at Queen Mary College, London (46) which employs a Golay detector normally, but for high resolution in the extreme infra-red a superconducting bolometer is used as detector.

2.4.4: Detector optics.

The receiving area of far infra-red radiation detectors is very small, being usually of the order of a few mm^2 at most and the resulting problem of condensing the radiation from the exit slit of the monochromator on to this small area has been solved in a number of ways which are described below.

2.4.4.1: Condensing mirror.

The beam from the exit slit is collected by a mirror and simply focussed on to the detector. If the detector is small enough not to obstruct much of the light falling on the mirror, it is placed on the axis at the focus. For long slits an elliptical mirror is sometimes used to give greater reduction in the length of the slit image (e.g. as used by Genzel and Eckhardt).

A Golay detector however, is rather bulky and must be placed off axis, in which case it is essential to use an ellipsoid. For example, Yoshinaga et al. (fig.(9) use an auxiliary plane mirror containing an aperture, and an ellipsoid whose two focal lengths are 165 and 838mm. The fabrication of ellipsoids having the necessary degree of eccentricity is difficult and costly. To avoid this difficulty, the Greenler image reducer using spherical mirrors can be used instead if the slits are short, or in conjunction with an image transformer if the slits are very long. (See section 3.1.7.2).

2.4.4.2: Image transformers or slicers.

Spherical mirrors do not, except for the aberrations they introduce, change the shape of an image. Rather than using highly eccentric ellipsoids it is often more advan-

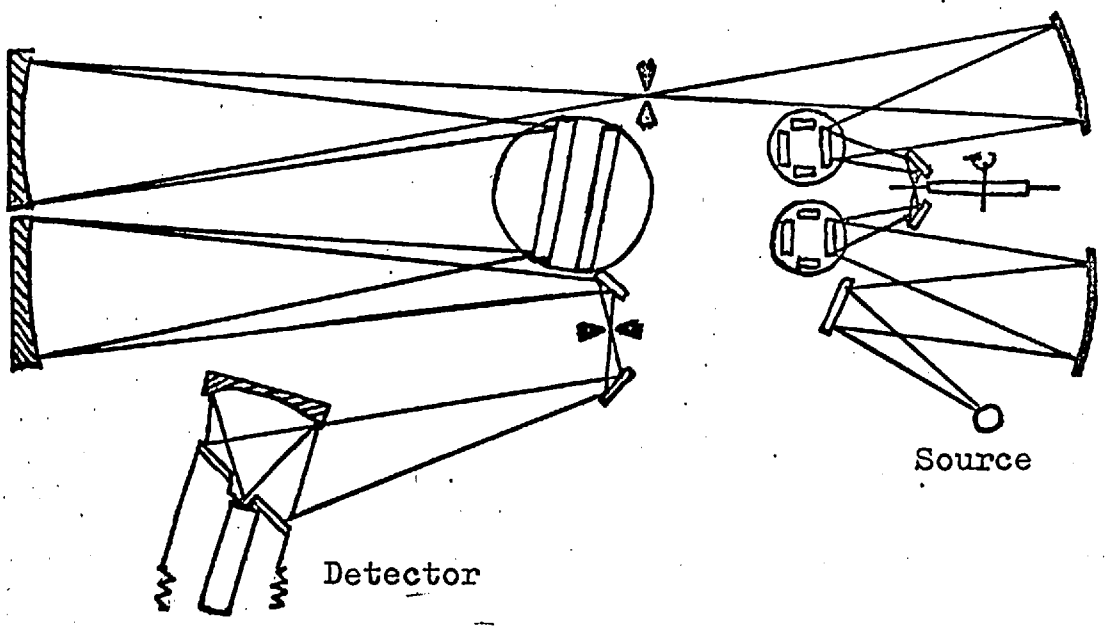


Fig.9: The Spectrometer of Yoshinaga et.al.

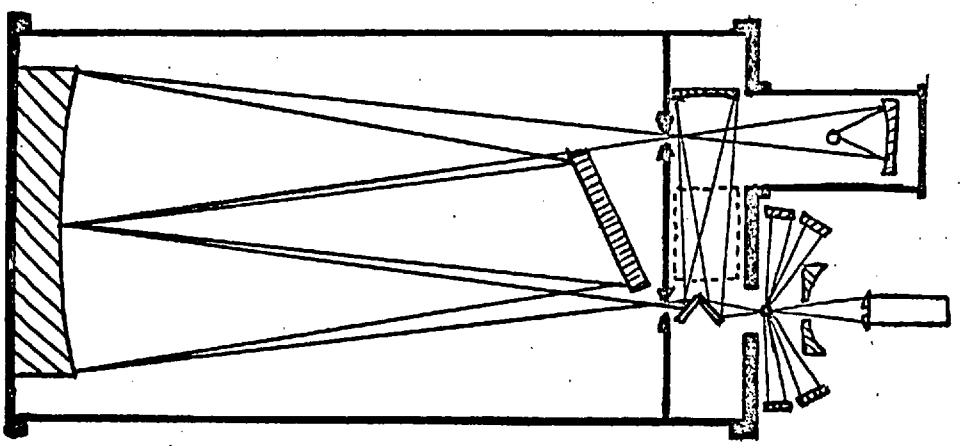


Fig.10: Robinson's Ebert Spectrometer

tageous as well as cheaper to use some simple form of arrangement image transformer. These usually consist of an arrangement whereby the image is "sliced" into several parts and each part sent via a different optical path to join the others in a new relative arrangement.

One such system, after Benesch and Strong was used by Robinson in his Ebert spectrometer (70), and another is described in detail in section 3.1.5.1.

2.5: Interferometric spectroscopy.

The quartz plate interferometer used by the early workers to estimate the widths of reststrahlen reflection peaks was a forerunner of the modern interferometric spectrometers. These are generally based on the Michelson arrangement in which a parallel beam of radiation is divided by a beam splitter (e.g. a thin film of 'Mylar') into two beams travelling at right angles. The beams are returned along their paths by plane mirrors, recombined and condensed onto a detector. As one of the mirrors is moved along the direction of the beam, the path difference between the two changes and the intensity at the detector would, if monochromatic radiation were used, vary sinusoidally with time. If "white" radiation is used, and an absorbing sample placed in the beam, the output at the detector is a complex function whose fourier transform over zero to infinite path difference gives the transmission spectrum of the sample. In practice, the mirror need only be moved through 1-2" to give adequate resolution (the theoretical resolving power depends on this distance).

The advantages which this type of spectrometer possesses over conventional ones is that the resolution is

not limited by the available energy: this is because the effective exposure time can be made long. In this way spectra have actually been obtained in emission. The major disadvantages are the necessity of having a constantly available automatic computer to perform the transforms, and the uncertainty as to how much radiation at a given wavelength is actually present at any stage.

One such spectrometer, built by Gebbie at the National Physical Laboratories, is described in ref.71a.

3:CONSTRUCTION AND OPERATION OF A FAR INFRA-RED VACUUM GRATING SPECTROMETER.

3.1: Construction of the spectrometer.

3.11: Introduction.

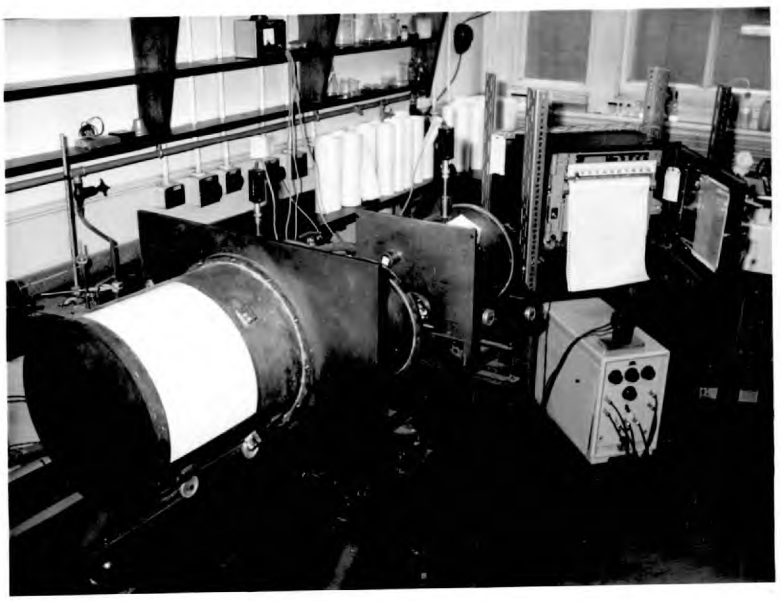
The design of the far infra-red vacuum grating spectrometer described in this section was dictated mainly by the following requirements: the spectrometer should be suitable for the measurement of the absorption bands of a wide range of compounds from room temperature down to liquid helium temperatures; it should be relatively inexpensive and mechanically simple to construct; it should employ spherical optics throughout; and it should have a resolving power not greatly inferior to those of more elaborate instruments. These requirements are met most readily by the Ebert optical arrangement: spherical optics only can be used; its symmetry simplifies the construction of a versatile evacuable enclosure and the permissible use of very long slits ensures that sufficient energy is available to maintain a reasonable resolving power even when small replica gratings are employed.

The spectrometer described below uses a 12" diameter Ebert mirror, 2.5 x 2.5" echelette gratings and a commercially supplied Golay pneumatic detector. This detector has the advantage that while being comparable in sensitivity to other room temperature thermal detectors, it has a large ($10mm^2$) receiving area which makes it insensitive to slight changes in the direction and focussing of the radiation. The model built by Unicam Instruments Limited can also be operated satisfactorily in a vacuum.

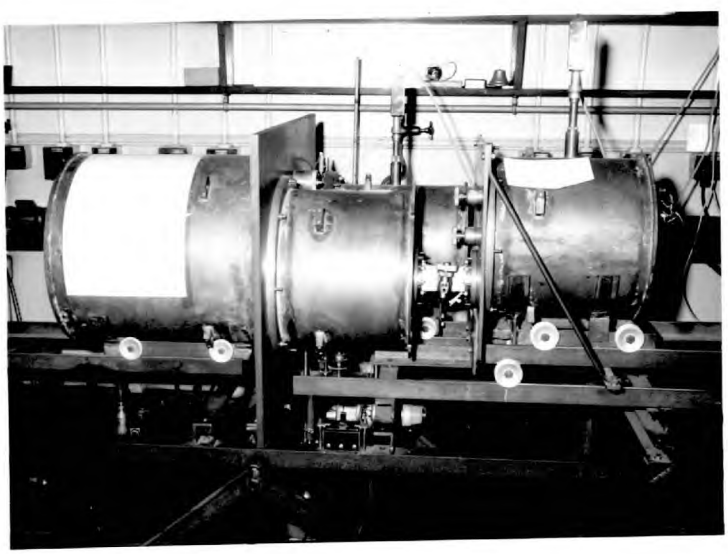
Figures 11 and 12 show the salient features of the instrument. It is built around a main vertical steel plate of dimensions 24x30x1/2" to which are secured all the components contained in the three sections labelled the source, monochromator and condenser areas. All three are enclosed by vacuum tight brass cylinders or drums bolted to the steel plate. These can be wheeled back to give easy access to the optical components, on carriages running along rails mounted on the large steel framework which supports the base-plate. Large rubber 'O' rings are placed in circular grooves in the drum flanges to ensure an airtight seal with the base-plate. This arrangement also avoids any distortions caused by evacuation of the system which might disturb the alignment of the optics.

The detector section is constructed around a second, smaller, brass base-plate and mounted on a trolley running along the same rails as the condenser drum. The sample area, which is sandwiched in between, is thus completely accessible, providing ample space for cryostats and large path length gas cells.

All the mirrors used in the spectrometer are either plane or spherical and are front aluminised. They were all glued with "Araldite" to brass backing plates which were



Figs.11&12: The Far Infra-red Spectrometer



kinematically mounted from the two base-plates of the instrument.

3.12: Optical path of the spectrometer.

Figure 13 is a diagram of the optical path of the spectrometer. Light from the source A is collected by the mirror B and brought to a focus on the entrance slit C which is placed in the focal plane of the Ebert mirror D. The beam emerging from C has an aperture of f/4 and is collimated by D onto the grating at E. The diffracted beam is then collected by D and condensed by it onto the exit slit C' through which it passes into the condenser drum. Here, the 3" high but narrow image of the exit slit is reduced in height by an image slicer, and is brought to a 3/4x3/4" focus in the middle of the sample area S by the concave mirror J. It then enters the detector area in which it is collected by a complementary mirror K and sent to its focus on a reststrahlen reflector at M. (See also fig.21). The light from M is collected by a spherical mirror N and reflected onto a second reststrahlen plate at P which directs it to a focus at the aperture of the secondary mirror of the Greenler image reducer Q. The latter finally condenses the beam onto the 3x3mm diamond window of the Golay detector R.

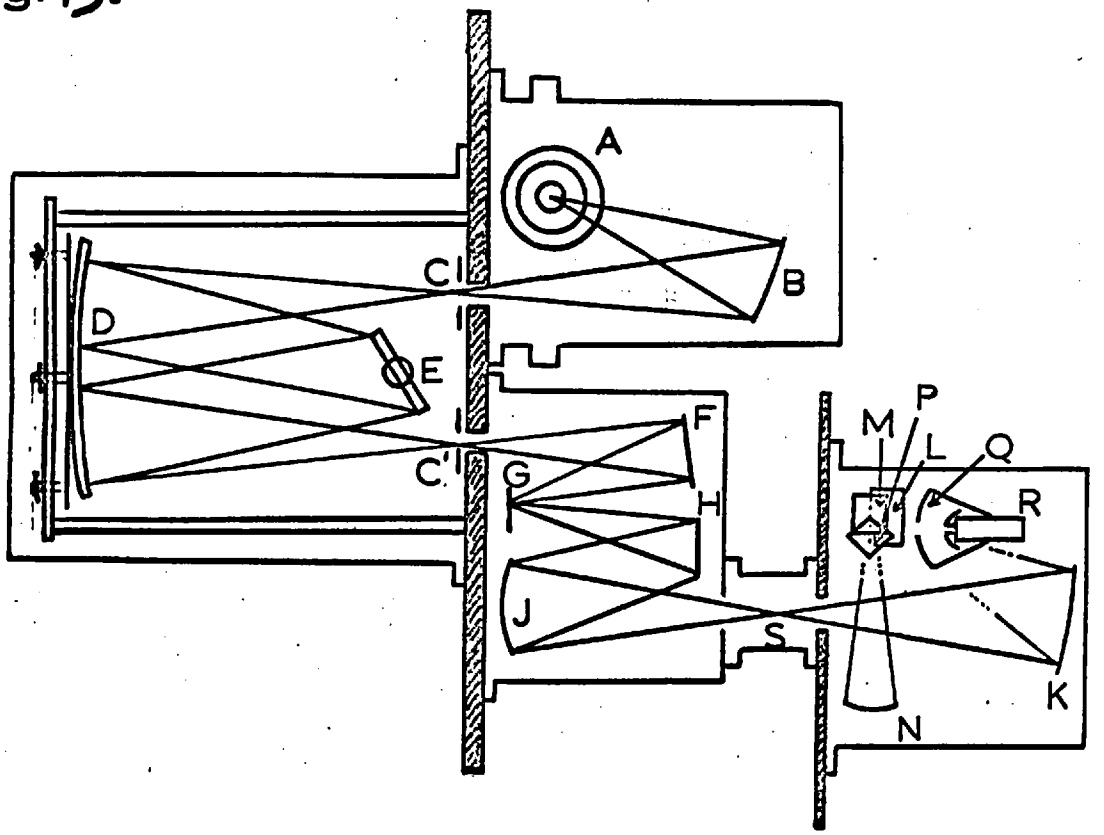
In the following sections the optics and construction of each part of the spectrometer are described in greater detail.

3.13: The source area.

3.131: The source and cooling jacket.

A Phillips 125w fused quartz mercury lamp is used as source throughout the operating frequency range of 400-55 cm^{-1}. Provision was also made for the installation

Fig. 13.



A	Hg source, Cu cooling jacket & KBr chopper blades.
B	Spherical mirror.
C	Entrance slit. C' Exit slit.
D	Spherical Ebert mirror.
E	Echelette grating.
F	"Sliced" spherical mirror.
G	Plane "matchstick" mirrors.
H	Plane mirror.
J	Spherical mirror.
S	Sample cell.
K	Spherical mirror.
L	Plane mirror.
M	1st reststrahlen "windmill".
N	Spherical mirror.
P	2nd reststrahlen "windmill.
Q	Greenler image reducer.
R	Golay pneumatic detector.

of a Globar source, but this has never been used since the mercury lamp proved to be comparatively satisfactory even for the higher frequency range.

The lamp fits a standard brass bayonet socket which is screwed into the upper end of the cooling jacket (see fig.14), consisting of two concentric cylinders of 1/8" brass, 4 1/2" long with diameters approximately 1 1/2" and 1 3/4", enclosing an annular space 1/4" wide through which water can be circulated. The jacket contains a rectangular aperture of dimensions 3 1/2 x 1/2" to allow light from the lamp to fill the condensing mirror, and is suspended vertically from a bracket screwed to the steel base-plate of the instrument.

To provide easy access to the source and mirror, all the electrical leads and water pipes are taken out through a circular brass collar 2 1/2" wide, which is bolted semi-permanently to the steel plate. Thus the source drum, which is bolted to this collar, can simply be wheeled back without disturbing the source unit and chopper. For the water circuit, two 1/4" copper tubes were soldered into the collar, and connected to the water jacket pipes by short lengths of thick rubber pressure tubing. This arrangement is perfectly satisfactory and airtight provided that the circulation of water is sufficient to prevent the jacket from overheating.

The electrical takeouts for the lamp and chopper motor are of the standard copper/porcelain type, and were soldered into holes drilled into the collar for the purpose. The inner, insulated cylindrical conductors of these, normally hollow, were plugged by solderding in copper rods to act as terminals on both sides of the collar.

The concave mirror B is rectangular in shape (6"x 3 1/2") and has a focal length of about 5 1/2". It is

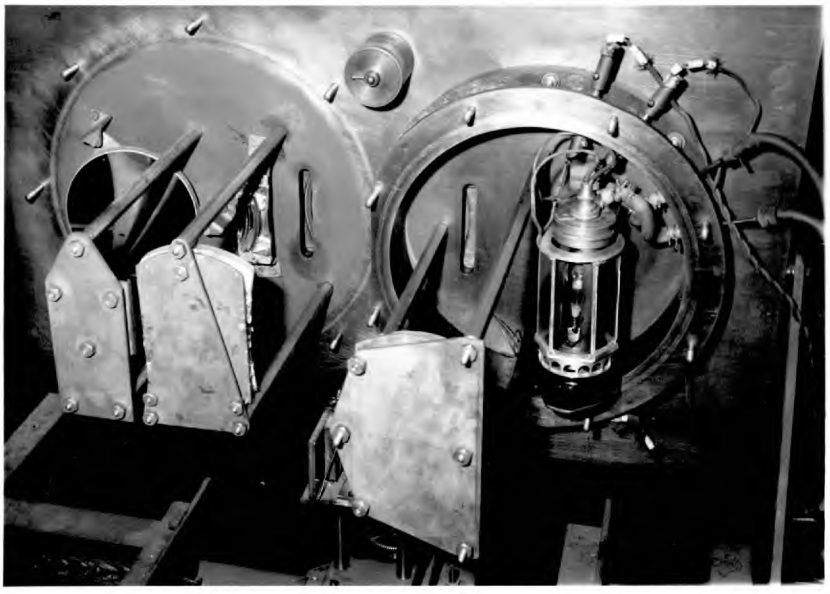


Fig.14: The Image slicer, (left) and the source and chopper

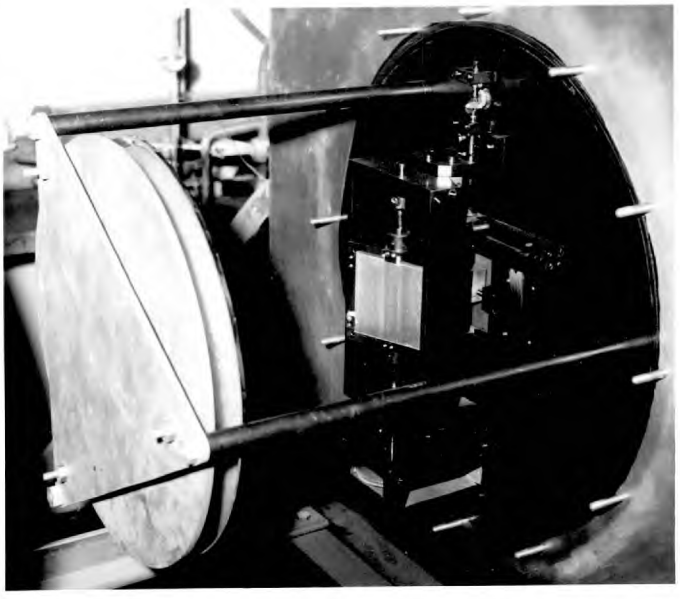


Fig.15: The Ebert mirror, grating and slits

placed about 12.5" from the entrance slit and 9.5" from the centre of the source to form a slightly magnified image of the latter at the slit. The aperture of the beam entering the monochromator is f/4. Unfortunately the off-axis use of the mirror gives an image whose curvature is opposed to the curvature of the slit, and there is not enough space available for the mirror to be placed on the inner side of the axis. Thus some of the light is inevitably lost, although this is not very serious because the "far infra-red image" of the source is much wider than the visible one.

3.132: The KBr chopper.

The filtering effect of selective chopping has been discussed in section 2.322. In this spectrometer, potassium bromide, which has a mean cut-off at about 350 cm^{-1} is used as the chopper material.

Three polished KBr plates of dimensions 3 1/2 x 1 1/4 x 1/8" are rotated vertically around the jacket of the source (fig.14). A 200 r.p.m. synchronous motor with its axis vertical is supported directly underneath the source by a brass bracket fixed to the steel plate. To the 1" diameter circular base of the spindle is fixed a large "dish" having a wide rim onto which are placed symmetrically three pairs of straight flanges to anchor the KBr plates. This dish is about 2 1/2" in diameter and 1" deep to accommodate the unilluminated base of the jacket, and is made of aluminium alloy in order to keep down the weight of the whole assembly. A ring of flanges, similar to the rim of the dish, is placed on top of the vertical KBr plates to stabilise them. As the assembly rotates, the KBr plates pass successively in front of the aperture in the jacket and modulate the radiation at a frequency of 10 c/s.

3.14: The monochromator area.

3.141: The slits.

The slits C,C' are 3" long and circularly curved about a point on the symmetry axis of the monochromator drum, and have a 3" radius of curvature. The slit mechanism is mounted on the steel base-plate of the spectrometer, behind two 3 1/2 x 1/2" slots cut into the plate with their centres 6" apart. Fig.16 is a full scale drawing of the mechanism showing the slits C,C' at their maximum opening (1/2"). A is a frame cut from sheet steel to form the inner jaw of one slit (C) and the outer jaw of the other(C'), and is connected to that end of the shaft K which has a left-handed thread. The other two jaws X and Y are coupled together and joined to the other, right-hand threaded end of the shaft. When this shaft is driven through a crown gear by rotating the shaft L, the jaws of the slits move bilaterally, i.e. the centres (dashed lines) of the slits always remain exactly 6" apart. Another set of crown gears at the other end of the shaft L connect the mechanism to a third shaft (not shown) which passes through the steel plate and out of the monochromator drum, and allows the slit width to be controlled from the outside. One complete rotation of the shaft changes the width of the slits by 1.5mm.

A simple arrangement of small rubber 'O' rings and collars renders the opening airtight and is also used for all other rotating shafts which pass into the evacuated area.

3.142: The Ebert mirror.

The mirror used has a diameter and focal length of 12"and is mounted 12" from the plane of the slits so

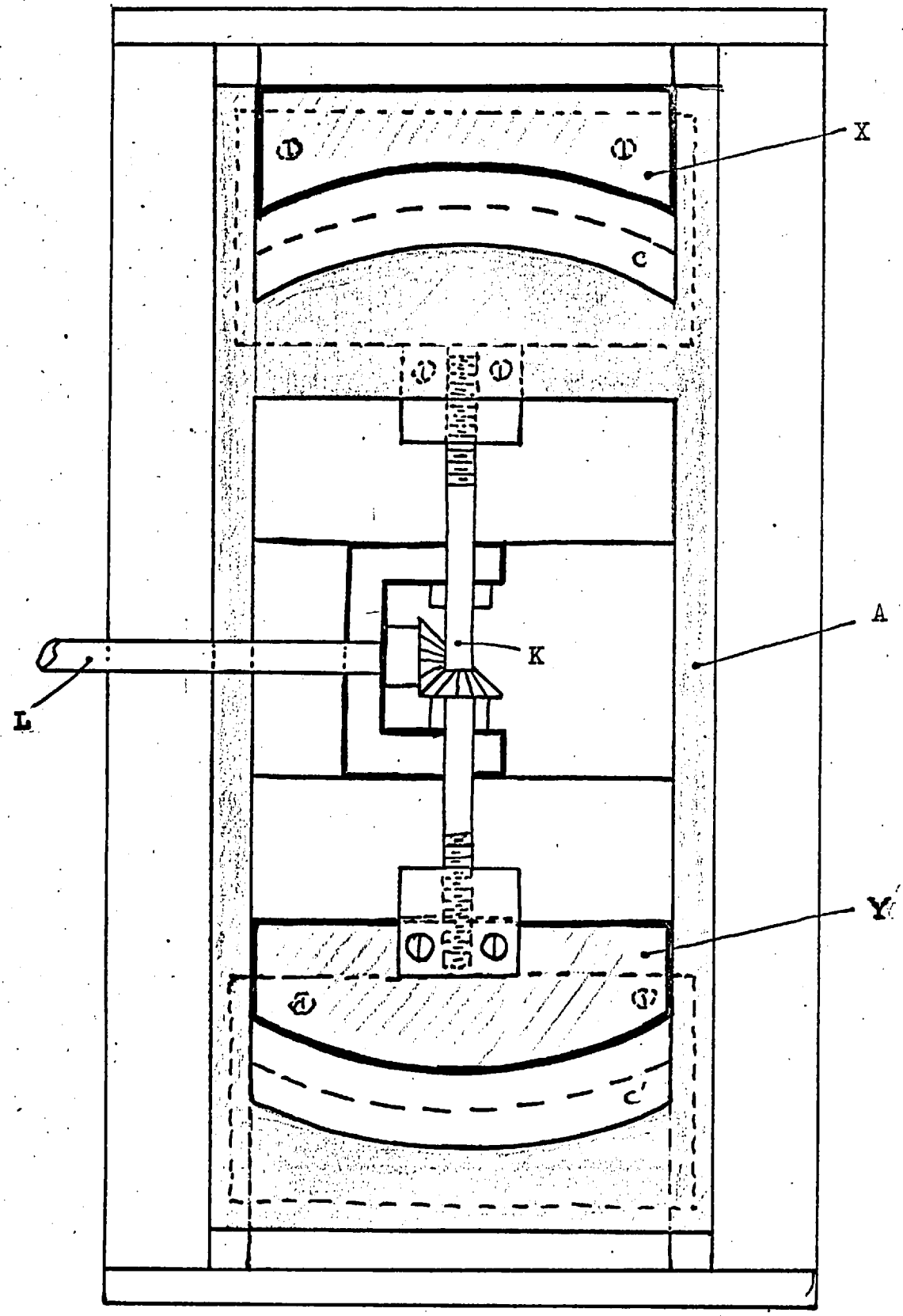


Fig.16: diagram of the slit mechanism.

that its axis passes through the centre of curvature of the slits (see fig.15). The mounting is similar to that described for the source mirror, and it is adjusted by observing the curved image of the entrance slit which should be in focus and exactly parallel to the exit slit.

3.143: The grating and mount.

Two gratings are available, one with 80 lines cm^{-1} and the other with 200 lines cm^{-1}. Both are Baush and Lomb replica gratings of dimensions 2.5 x 2.5 x 3/8", and are blazed at 27°, corresponding to 90 and 220 cm^{-1} respectively in the first order. They are mounted back to back in a special brass holder which is pivoted at the centre of a fixed brass frame so that the axis of rotation is vertical and located symmetrically between the slits (see fig.15). To allow enough space for the gratings to be reversed by rotation through 180°, the axis is set 3" forward from the base-plate. At the lower pivot there is the 2.5" diameter, 100 tooth cog of a worm gear to enable the grating to be driven by a horizontal shaft entering the monochromator area from the outside. One revolution of this shaft rotates the grating through 3.6° about its vertical axis. It is driven by an electric motor through a gearbox which is described in section 3.18.

3.15: The condenser area:

The focal dimensions of the f/4 beam emerging from the exit slit of the monochromator are about 3 x 1/8" (average slit width used). It is required to bring it to a smaller and more compact focus at the centre of the sample area without greatly increasing its speed. A sliced mirror image transformer is used for this purpose.

3.151: Description of the image slicer.

The image slicer described here is similar in principle to one with sliced lenses described by Carey (71). Its construction and mode of action can be seen by referring to fig.17, which is a perspective sketch of the optical components contained in the condenser drum.

The beam from the exit slit fills a rectangular (5 1/4 x 3") concave mirror of 4" focal length, placed about 9.5" from the plane of the slits. This mirror was sliced into horizontal sections F_{1-5} whose widths were chosen so that each receives light from about 2/3 of the length of the exit slit. The central strip F_3 is 3/4" wide and forms an image of the slit at I_3 (dotted line, fig.17) of which only the middle 2/3 is illuminated. Most of the light from F_3 however, is concentrated in the middle 1/3 of the image (shaded area). The strips F_2 and F_4 are both 1" wide and receive light from only the upper 2/3 and lower 2/3 of the slit respectively, so that again only 2/3 of the images at I_2 and I_4 are illuminated and most of the light is again concentrated into a single 1/3 of the image. In order that the outer strips F_1 and F_5 shall also receive light from about 2/3 of the slit, they were each made 1 1/4" wide. Like the other strips they form partially illuminated images, at I_1 and I_5. By appropriately tilting these mirror slices, the images can be separated laterally and their areas of maximum illumination can be brought adjacent to each other, as shown in the diagram. Fig. 18 is a photograph of the arrangement.

The five sections of the original beam arriving at I are travelling in different directions, although the aperture of each is still approximately f/4. In order to combine them into a single unidirectional f/4 beam, five

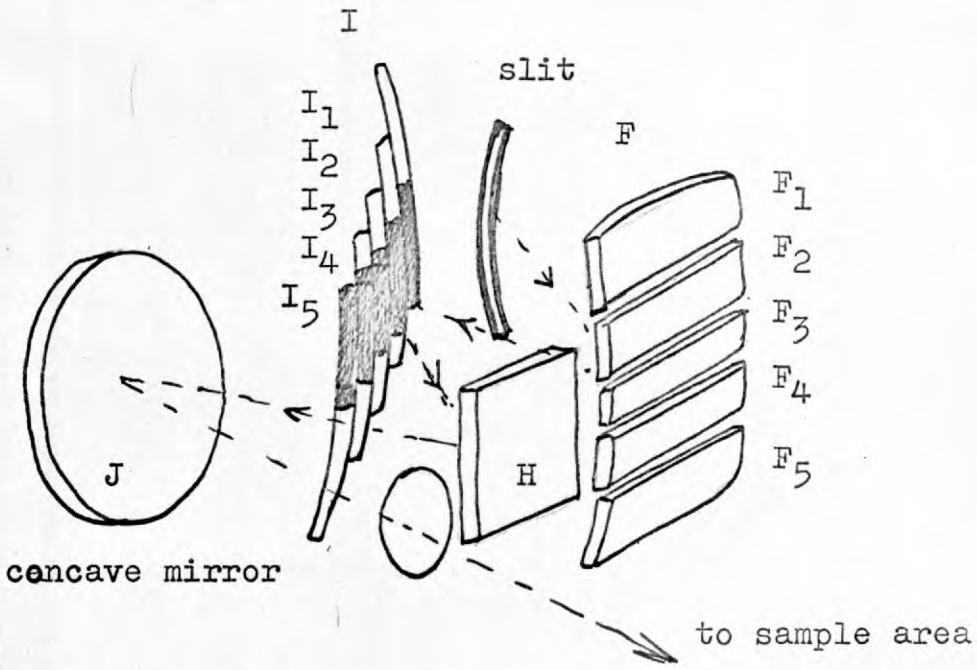


Fig. 17: Sketch of the Image Slicer.



Fig.18: Photo of image slicer section.

narrow, curved "matchstick" mirrors G are placed at I, one at each of the five images. These are adjusted individually to fill the plane mirror H (size 2.5 x 2.5") which then reflects the reconstituted beam onto a 5" diameter, 6 3/4" focal length concave mirror J. This is adjusted to bring the beam into focus at the centre of the sample area S which is 12.5" from the base plate and 2 1/4" from the end of the condenser drum. The beam leaves J with an aperture of about f/3 and has atS a cross-section of approximately 3/4 x 3/4".

The matchstick mirrors were made by slicing 1 1/2" long sections of an 1/8" thick watchglass of the appropriate curvature, and grinding and polishing the plane edges. They were cemented with Araldite onto a 1 1/4 x 3 1/2 x 1/8" brass plate which was mounted kinematically on three short brackets screwed to the base-plate.

3.152: Adjustment of the image slicer.

This was done as follows: the steel base plate with its optical components was supported horizontally with the image slicer section downwards. The sliced mirror was rested on strips of putty on the brass backing plate and each section was adjusted separately to give the five adjacent images separated sufficiently to accommodate the matchstick mirrors. The base and putty were then flooded with Araldite to cement the mirror sections into place. On reversing the base-plate, the matchstick mirrors could be positioned, adjusted and cemented in the same way.

3.16: The sample area.

The length of the sample area between the end of the condenser drum and the brass base-plate of the detector section is 5". For normal use this is sufficient, ~~but~~

but where it is required to use a large liquid helium cryostat, for example, this length can be increased by several inches simply by choosing mirrors of different focal lengths to replace J and K (fig.13).

Several sample cells are available, including a long path length gas cell. The cell used for the work reported in this thesis is shown diagrammatically in fig. 19. It can be used for limited cryoscopic work down to liquid nitrogen temperature if evacuated (via a tap, not shown). A is a simple stainless steel dewar container which fits into the main body of the cell (B) by a conical joint C. At the base of the dewar "finger" there is a copper sample holder with a 3/4" hole for the radiation to pass through. Brass flanges D,D' with 8 threaded studs symmetrically arranged on each are bolted to the cell with the polythene windows sandwiched in between (E,E'). These flanges in turn fit over studs fixed on the condenser drum at one end and the brass plate at the other. Rubber 'O' rings F,F' ensure airtight seals.

3.17: The detector area.

All the components in the detector drum are secured to a 1/4" thick vertical brass plate bolted at its base to one end of a long trolley which moves on the same rails as the condenser drum (fig. 20). This trolley enables the whole detector section to be moved away from the sample area. The framework of the trolley consists basically of a pair of rails to take the carriage supporting the detector drum so that this can be moved back and removed without disturbing the optics.

The radiation, which enters the detector area through a hole in the brass plate, is collected by the

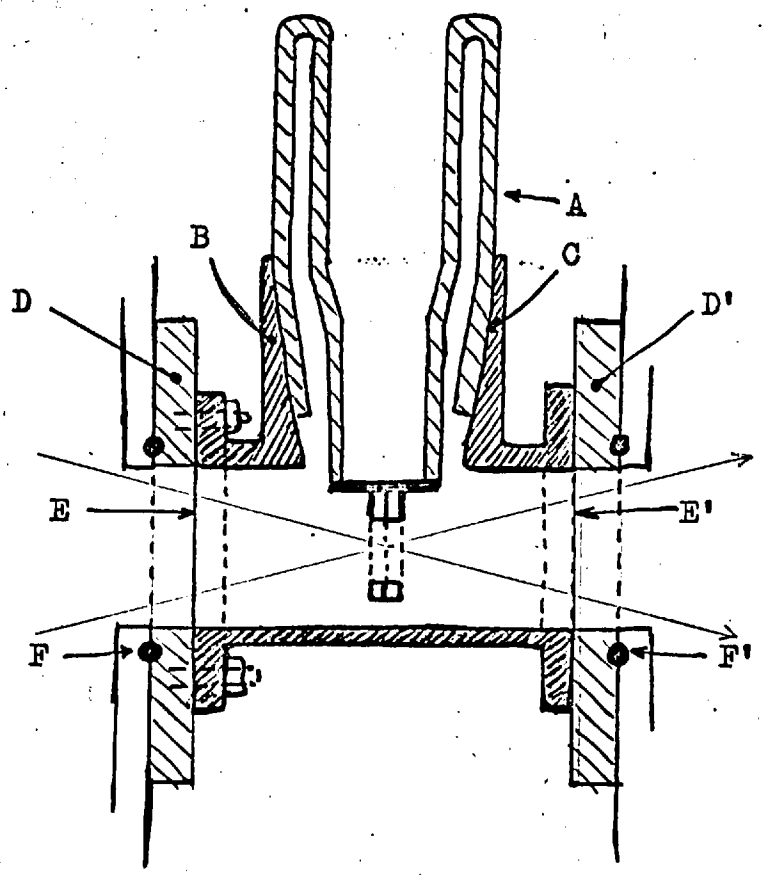
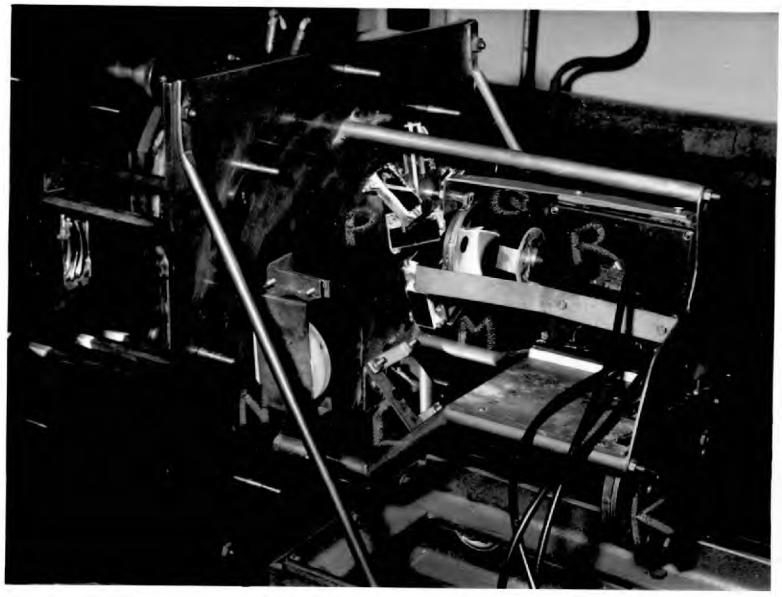
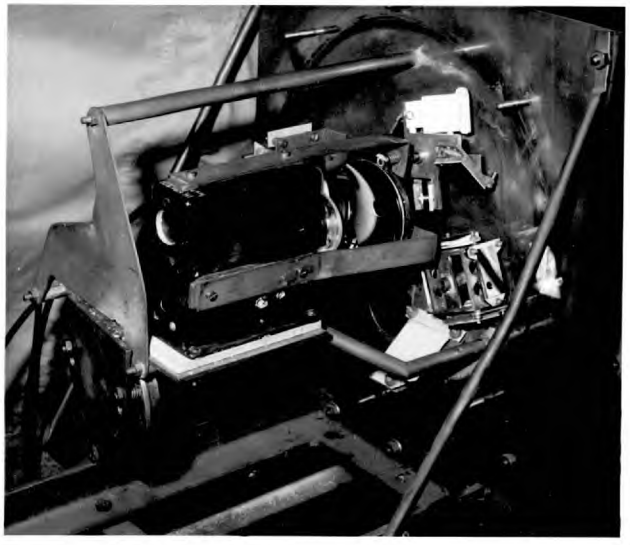


Fig.19: Diagram of dewar finger
Sample Cell.
Scale 1;2



Figs.20: The detector section



concave mirror K of diameter 4" and focal length 6" (fig. 19) and is directed onto the first reststrahlen crystal by the plane mirror L (2.5 x 1.5").

3.171: The reststrahlen holders.

To cover the entire spectral range of the instrument several different combinations of reststrahlen filters or mirrors are required. To enable this combination to be selected and adjusted from the outside, the reflectors are mounted on two "windmills" whose construction can be seen from fig. 20. Each has provision for 4 kinematically mounted reflectors which were cemented with Araldite to their brass backing plates. At the centre of the windmills are collars to take horizontal steel shafts entering the detector area through holes in the brass base-plate. The reststrahlen can then be changed by turning the shaft from the outside.

The rather widely spaced arrangement used here, in which the second reststrahlen plate P is illuminated by the concave mirror N (2 3/4" diameter, 3 5/8" focal length), allows for the reststrahlen to be "crossed" for greater filtering efficiency (see section 2.323).

3.172: The Greenler image reducer.

To condense the beam leaving the second reststrahlen P on to the Golay window, the Greenler image reducer (72) was chosen for its compactness and spherical optics. It consists of a large concave mirror M_1 of radius of curvature r_1 containing a central aperture, and a smaller, convex mirror M_2 of radius r_2 with a small central aperture. The arrangement and optical path is shown in fig.21. If the separation of the mirrors is d, then to obtain a de-

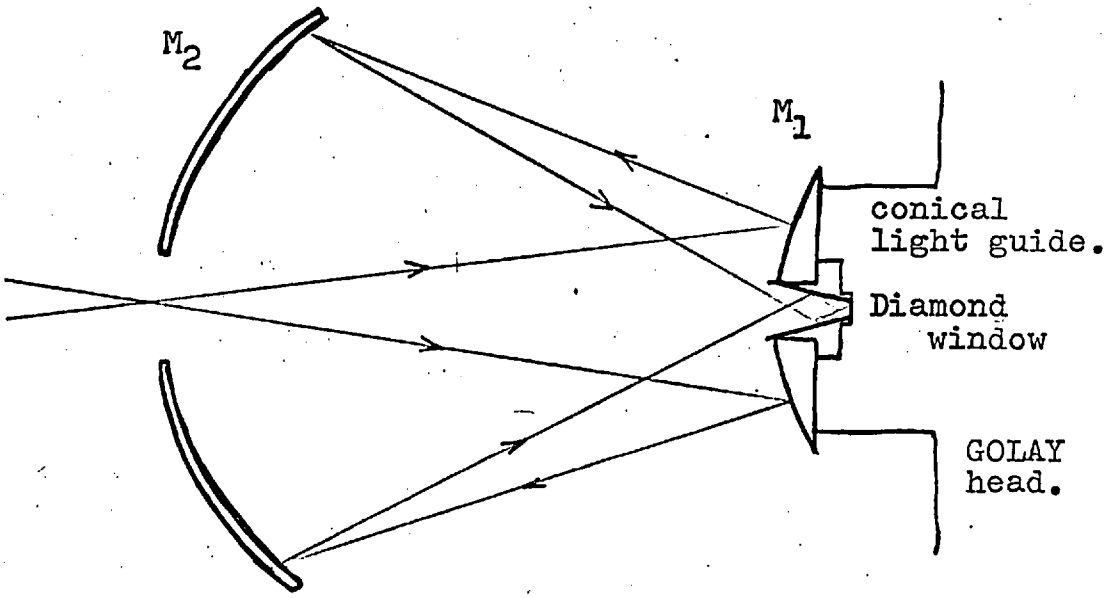


Fig.21: Diagram of the Greenler Image reducer.

magnification of -1/M, the radii required are given by

$$r_1 = \frac{-2Md}{1-2M} \quad \text{and} \quad r_2 = \frac{2d}{M-2}.$$

The dimensions of the mirrors used here are: $r_1 = 2.5"$ and $r_2 = 2.4"$; diameters 3 1/2" and 1 3/4"; diameters of central apertures 1/2" and 3/16" respectively. With a separation d = 2" the system gives approximately a 4-fold reduction in the size of the image brought to a focus at the aperture of the larger mirror.

The manner in which the mirrors were mounted in front of the Golay detector head can be seen from fig.19. The smaller mirror was cemented with Araldite directly onto the head. Three brass strips fastened to the casing of the head form supports for the kinematic mounting of the larger mirror.

It was found that a small light-cone made from aluminium foil and placed in the cavity leading to the Golay window gave almost a 50°/o increase in the signal.

3.173: The detector mounting.

The Golay detector head was bolted to a horizontal brass plate (fig.~~19~~ 20) which is supported by a framework of three brass rods screwed into the brass base-plate. The lower two rods were bent to keep clear of the optical path, but the framework is rigid enough to support the weight of the Golay.

The three electrical leads from the detector are taken out from the back of the drum through vacuum tight take-outs similar to those used for the source leads, except that in this case a thick copper wire was cemented with Araldite into the insulated hollow cylindrical conductor to form a coaxial arrangement. The leads inside the drum were provided with coaxial plugs and sockets so that they

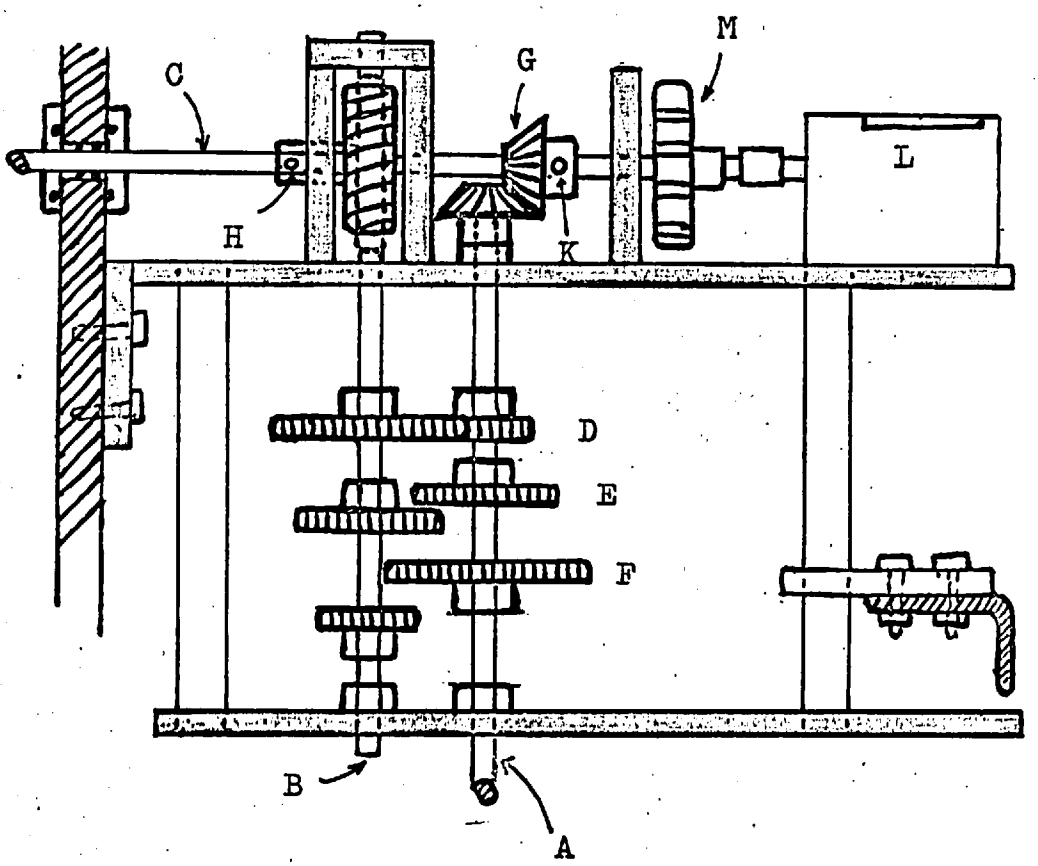


Fig.22: Diagram of the Gearbox for the grating drive.

may be disconnected when it is required to remove the drum completely.

The leads from the head are connected to the power supply and amplifier unit of the Golay, and the final output signal is recorded on a Honeywell Brown 'Elektronik' potentiometric strip-chart recorder driven at a speed of 1/2" per minute. The overall time constant is fairly fast (approximately 1-2 sec) but can be increased by damping the recorder and using a slower grating drive.

3.18: The grating drive and gearbox.

The grating is rotated by a motor and gearbox fixed to the lower end of the main base-plate and steel supporting frame of the instrument, directly below the source and condenser drums. Fig.22 is a drawing of the gearbox. The shaft A is driven at 2 r.p.m. by an electric motor. The second shaft B is connected by a 30 tooth worm gear to the grating shaft C which passes into the monochromator drum through the base-plate and drives the main vertical grating shaft through a 100 tooth worm gear. The two shafts A and B can be coupled by engaging one of the three sets of gear wheels D,E,F, which provide a choice of three gear ratios (2:1, 1:1, 1:2). For this purpose the set of wheels on shaft A can be moved bodily upwards or downwards along the shaft. A fast drive for running back or changing over to the other grating is provided through the 1:1 crown gears at G. To engage this drive the worm gear is disconnected by removing the pin at H and reinserting it at K.

For normal operation the combination F is used. This provides a total reduction of 150:1 from the motor to the grating so that the latter rotates at a speed of about 1/2 ^{o} per minute, corresponding to about 2cm^{-1}/min. at 100 cm^{-1}. The position of the grating at any stage is

indicated by a revolution counter at L which records the revolutions of the shaft C.

To provide a continuous series of reference marks on the spectra, a microswitch triggered by the spokes of the wheel M discharges an 8 mfd condenser (charged to 1.5v) through the recorder, giving a "pip" after every 0.3° rotation of the grating. This corresponds to about 1 cm^{-1} at 80 cm^{-1} and 10 cm^{-1} at 400 cm^{-1}. The wheel was made by removing the rim of the spoked wheel of a model locomotive. One of its 12 spokes was removed to give a double space between the pips after every eleventh pip to indicate one full revolution of the grating shaft C. Whatever the errors introduced by irregularities in the grating or recorder drives, the position of each of these pips corresponds accurately and consistently to a given angle of rotation of the grating--apart from errors in the final 100:1 worm gear and the grating mount itself.

3.19: Evacuation of the spectrometer.

Vacuum take-outs are provided in the sides of the monochromator and detector drums in the form of standard conical sockets. These are connected with thick pressure tubing via an oil trap to an Edwards "Speedivac" pump, which is capable of evacuating the instrument down to 0.1mm Hg in about half an hour. The pressure is monitored by Pirani gauges in the source and detector drums.

3.2: The calibration and use of the spectrometer.

3.21: Filtering conditions.

The use of the KBr chopper greatly simplifies the problem of filtering out unwanted radiation. The chopper used in the present instrument is uncompensated and consequently a considerable amount of near infra-red radiation is also chopped and detected. Nearly all of this, however, can be eliminated by placing in the beam (for convenience, near the sample area) a sheet of 500 gauge black polythene. This combination of KBr chopper and black polythene lets through very little radiation of frequencies higher than about 400 cm^{-1}, and is the basic filter combination employed in all the work with the spectrometer reported below.

It is still necessary to filter radiation below 400 cm^{-1} to isolate a single order and for this purpose reststrahlen reflection filters mounted on the "windmills" are used. The degree of filtering required at this stage depends strongly on the blaze characteristics of the grating used and on the working frequency. Hence it is convenient to discuss this for the two gratings separately.

3.211: Filtering: the 200 lines cm^{-1} grating.

This grating is blazed at 220 cm^{-1} in the first order and thus has as its approximate working limits 330 and 150 cm^{-1}. Crystals of $CaCO_3$, CaF_2 and NaF have their reflection peaks within this range. All three were tried, and of these, two reflections from NaF gave the strongest signal as well as a satisfactory degree of filtering. Fig.23 shows a water vapour spectrum taken with these filtering conditions. It was recorded with the spectrometer open to the atmosphere, and the stronger absorption

bands have cut the signal down completely, showing that there is very little unwanted radiation present. The spectrum also illustrates the order of resolution possible in this region, with a mechanical slit width of 1.25mm (corresponding to about 1 cm^{-1} at 300 cm^{-1}). The signal to noise ratio in this example is extremely high, and the resolution could probably be doubled if this were necessary. The frequency range over which 2 NaF can be usefully employed is 370 - 240 cm^{-1}.

NaCl (rock salt) has a reststrahlen peak at a frequency below that of NaF, and can be used satisfactorily from 280 - 180 cm^{-1}. In combination with the KBr chopper and black polythene, one reflection from NaCl gives a water vapour spectrum containing no spurious higher order bands. Similarly, compounds having strong bands at around 450 cm^{-1} show no trace of second order absorption in the NaCl region.

After about 180 cm^{-1} the intensity of the radiation begins to fall off when using 1 NaCl. It is possible to use one reflection from KCl, which has a peak at a slightly lower frequency, to give a little more signal in the region from 180 cm^{-1} to the 45° reflection peak of the grating at about 150 cm^{-1}. The entire usable range of 1 KCl overlaps that of NaCl and is from about 230-150 cm^{-1}.

Although the real high frequency limit of the spectrometer as used at present is about 370 cm^{-1}, it is possible to record bands up to 400 cm^{-1} or a little more by using one LiF crystal as reflector and observing in the second order. The amount of 400 cm^{-1} radiation is, however, too small for the same resolution to be obtainable as with NaF.

3.212: Filtering: the 80 lines cm^{-1} grating.

By rotating the grating holder through 180° the second grating can be brought into the beam. It is blazed at 90 cm^{-1} in the first order and has as its approximate working limits 60 and 135 cm^{-1}. The basic filters used are again the KBr chopper and the 500 g sheet of black polythene.

KCl can also be used with the 80 lines cm^{-1} grating but the first order maximum around 185 cm^{-1} lies outside the working range of the grating and the dispersion is very low. Two reflections from KCl however, give a nearly pure spectrum, and it is sometimes advantageous to use this as a means of confirming the presence of bands observed near the low frequency limit of the other grating.

KBr provides a very good reflection filter in the region from about 160 - 100 cm^{-1}. In this region and below it is possible to use the spectrum of gaseous HCl to determine the purity of the spectrum. The rotational spectrum of HCl consists of equally spaced bands separated by about 20 cm^{-1} which are fairly strong up to about 290 cm^{-1}(J=14) but begin to fall off in intensity at higher frequencies. If second order radiation were present, bands would appear on top of and midway in between the first order lines. The absence of these and any other unaccountable bands would show that the spectrum consists of fairly pure first order radiation. Thus when using one reflection from KBr and an HCl pressure of one atmosphere in the 10 cm gas cell, the bands are almost totally absorbing with no sign of weaker lines in between. This shows that the radiation down to about 120 cm^{-1} is nearly pure first order. At lower frequencies the amount of second order present begins to be appreciable, but provided this is borne in mind, the use of only one reflection

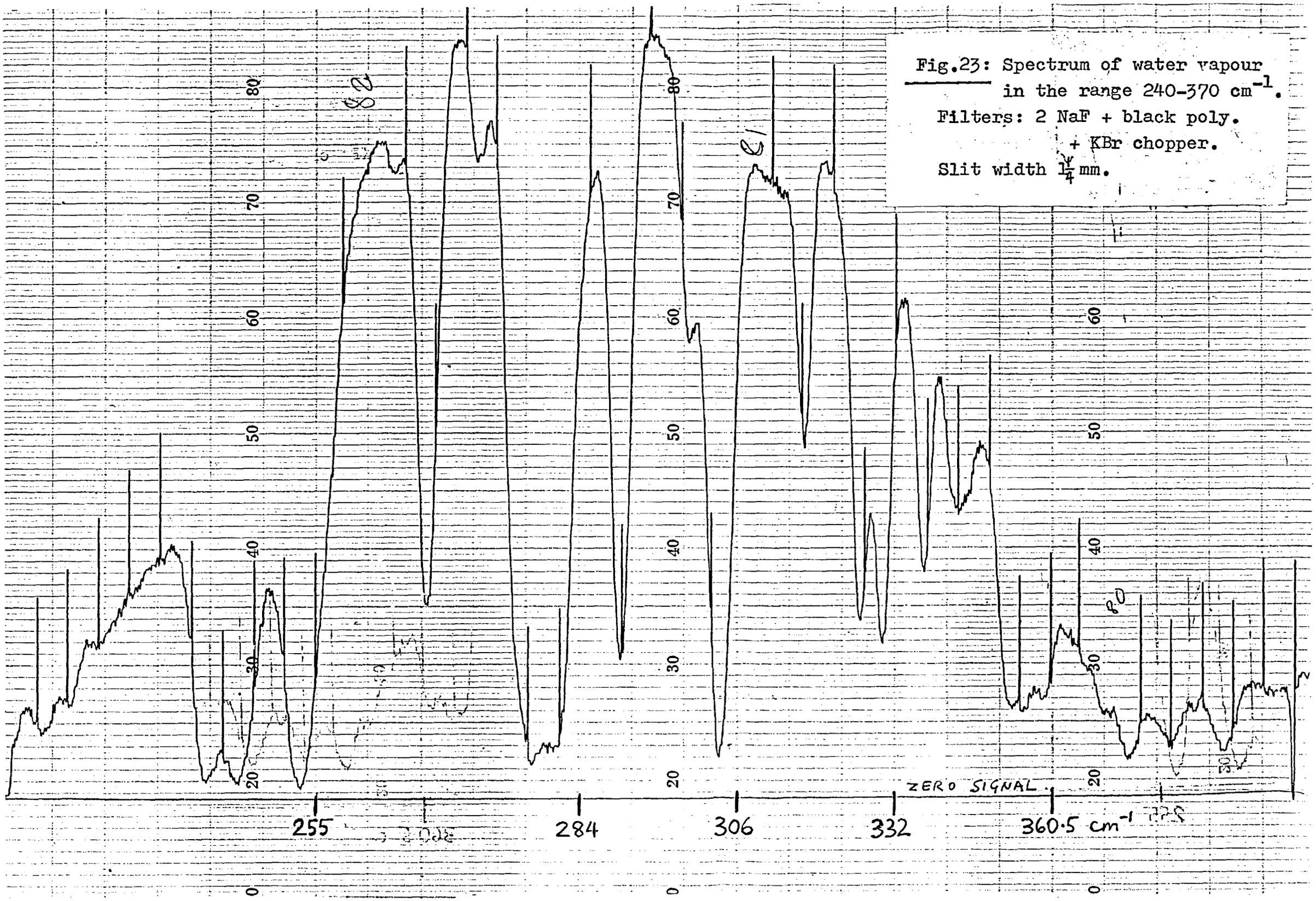


Fig.23: Spectrum of water vapour in the range 240-370 cm^{-1}.
Filters: 2 NaF + black poly. + KBr chopper.
Slit width $1\frac{1}{4}$ mm.

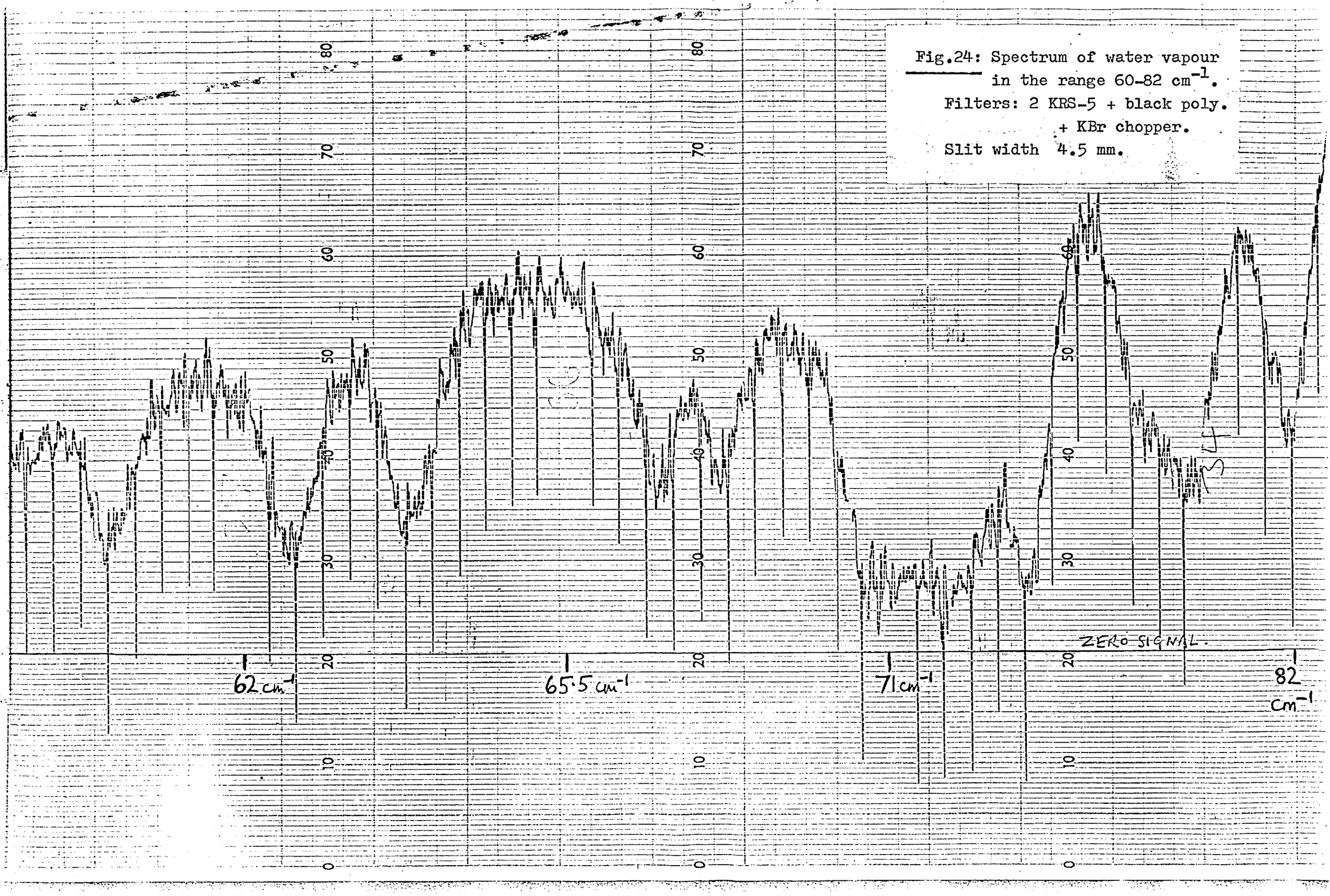


Fig.24: Spectrum of water vapour in the range 60-82 cm^{-1}.
Filters: 2 KRS-5 + black poly. + KBr chopper.
Slit width 4.5 mm.

is perfectly satisfactory. However, when two reflections are used this residual second order is eliminated, although with a reduction also in the first order intensity. Water vapour spectra confirm the above observations.

From about 110 cm^{-1} down to the low frequency limit of the spectrometer (55 cm^{-1}), two reflections from KRS-5 are required. CsI was also tried but proved to be less satisfactory. Fig.24 indicates the performance of the instrument in this range. All the water vapour bands appearing are genuine first order, and the purity of the radiation was confirmed further by an HCl spectrum. Only where this begins to overlap with the KBr reststrahlen region is there any indication of the presence of appreciable amounts of higher order radiation. In some of the earlier work with this spectrometer, a combination of one KRS-5 and one CsI reststrahlen was used, as this seemed to improve the spectral purity near 110cm^{-1}, but at lower frequencies the performance suffered as a consequence.

The table which follows summarises the filter combinations used to cover the entire useful range of the spectrometer, from about 400 - 55 cm^{-1}, and includes also the mechanical and spectral slit widths most frequently used in each range. The KBr chopper and black polythene were used throughout.

TABLE IV

Grating lines/cm	Optimum Usable Range	Reststrahlen	Mechanical Slit Width	Spectral Slit Width
200	370-240 cm^{-1}	2NaF	1.5 mm	1.2cm^{-1} at 300
200	290-180	1NaCl	2.25	1.2 at 250
200	230-150	1KCl	2.25	0.5 at 200
80	200-130	1KCl	2.25	2.1 at 200
80	160-110	1KBr	3.0	1.5 at 150
80	120-55	2KRS-5	5.25	1.1 at 100

3.22: Calibration of the spectrometer.

By starting each run from the central specular maximum (where the grating is parallel to the plane of the slits), it is possible to calculate the frequencies of the observed lines with a fair degree of accuracy. It is more convenient, however, to draw a large calibration graph and read off immediately the frequency corresponding to a given grating angle as defined by the reference or pip marks on the chart. The rotational lines of water vapour are known with great accuracy (32, 64) and there is an adequate number of them. The data of Randall et. al. (32) was used to draw the calibration curve which has to be checked periodically as there is a slight drift of the order of 1-2 cm^{-1} over several months, caused perhaps by wear in the 100 tooth worm gear or slight changes in the position of the grating in its holder. Often there are residual traces of water bands present in the spectra, and their position gives an indication of the reliability of the calibration.

The HCl spectrum was also used as a calibrant; it confirms the accuracy of the water vapour calibration but contains too few bands to furnish a complete curve by itself. Other gases such as CO and similar light rotators having a high dipole moment have been employed by other workers to calibrate their spectrometers, but for our purpose the water calibration is sufficiently accurate and reliable.

3.23: Sample handling.

3.231: Gases.

Two gas cells are available: a standard 10 cm path length cell and a 75 cm cell. The cells are fitted with windows of 1000 gauge polythene sheet which is thick

enough to withstand a pressure of one atmosphere. The cells are filled with the gas to be investigated in the normal manner, except that it is of greater importance to dry the gas. Nearly always the only way to eliminate water vapour bands is to introduce a little P_2O_5 into the cell. With gaseswhich might react with this compound, other drying agents such as anhydrous $CaSO_4$ or BaO have to be used. For the recording of background spectra the cell can be conveniently evacuated.

3.232: Liquids.

For the examination of liquid samples the dewar cell described in section 3.16 is used. Thick 1000 g polythene windows isolate the sample area from the evacuated spectrometer and the cell itself is not pumped out but kept free of water vapour by P_2O_5. The liquid sample, enclosed by very thin sheets of polythene is fixed to the base of the dewar finger. The polythene sheets can be separated by a thin spacer and clamped between the 'finger' and a copper ring, but the flexibility of the polythene and the crumpling action of some liquids upon it (e.g. benzene) render it impossible to obtain a film of uniform and controllable thickness. This being so, it is usually more convenient - especially with non-volatile liquids - to enclose the sample in a small polythene bag. This needs to be about 1" or 3/4" square and to have a narrow neck through which the sample can be introduced with a syringe. It is made by sealing the cut edges of the two adjacent sheets of polythene in a small, cold, gas flame. When this is done carefully and uniformly without allowing the polythene to catch fire, good leak-proof bags are obtained. The opening in the neck is then sealed in the same manner after the sample has been introduced: this is necessary

when using volatile liquids. With a little experience it is easy to judge the quantity of sample required, and the actual amount in the path of the radiation beam can also be varied simply by adjusting the position of the bag in the holder.

Theoretically, when this spectrum is compared with one taken without the sample in the beam (i.e. with a background) by plotting the ratios of the two signals at, say, each pip mark, the true fractional absorption spectrum of the sample is obtained. In practice the effect of interference in the polythene films used as window material is to give rise to spurious bands which could be confused with the actual absorption bands of the substance. Also the presence of small amounts of stray and higher order radiation hide the 'true' zero line which is normally taken as the reading when the slits are closed.

The interference effect arises from both the cell and sample windows. In the first case, the thick (polythene) cell windows superimpose a regular interference pattern onto the background which is most noticeable when working in the NaF region. As the apparatus is evacuated, the atmospheric pressure in the sample cell forces the windows outwards, slowly reducing their thickness. This causes changes in the interference pattern which show up when two runs are compared as described above. Fortunately after several hours this thinning out of the windows comes to an end, and the constant interference effect which remains does not greatly hinder the recording and analysis of the spectra.

In the case of the polythene sheets used to enclose the sample, however, the effect is more serious. That the interference occurs in the polythene film and not in the

liquid film is evidenced by the fact that it is present when only one sheet is used, and intensified when a second sheet is introduced. Differences between the refractive indices of air and the sample cause variations in the intensity of the superimposed interference pattern and it is this that confuses the interpretation of the 'ratio plot'. As the films are only a few wavelengths thick, it was not possible to eliminate this effect by making the film uneven in thickness, and the only way to reduce it to a tolerable minimum was to use a method of thick and thin sampling whereby the interference is kept constant by ensuring that the inner sides of the windows always remain in contact with the sample, so that there is no variation in the reflection coefficients governing the intensity of the interference pattern. Thus the background which is used in the comparison (ratio plot) is the spectrum of a very thin film of the sample. Of course this in itself can also cause an interference pattern, but in most cases does not seem to be very evident. The possibility must, however, always be kept in mind and affects to a certain extent the confidence with which a very weak absorption band may be regarded as being genuine. For the purpose of verifying such suspect bands, a third spectrum with a different thickness of sample is taken.

Since the ratio plot obtained from a comparison of the spectra gives in any case only a semi-quantitative indication of the relative intensities of the bands, the ordinate is taken as the "background" signal divided by the "sample" signal. This ratio is plotted rather than its reciprocal purely for convenience and in no way affects the determination of the frequency of a band or of its relative width.

3.233: Solids.

The easiest method of taking the spectra of solids is to grind the sample to a paste with 'Nujol' (the standard mull tecnique used in the near infra-red) and record its spectrum. 'Nujol', a high boiling paraffin, is completely transparent in the far infra-red, and being a non-volatile, viscous fluid, is very easy to handle. The spectrum of the mull is determined in the same way as described above. For the background either a very thin mull or a thin sample of 'Nujol' alone is satisfactory.

A number of solvents including benzene, cyclohexane and carbon disulphide are almost completely transparent in the far infra-red, and many others have only narrow regions of absorption. Solutions of solids are recorded im the same way as liquids, but especial care must be taken to ensure that the solvent does not evaporate and leave any solid in the bag.

Low melting solids (below, say 50°C) can be melted while in the sample bag to give a smooth crystalline or glassy film, or kept in the liquid state by hot water placed in the dewar.

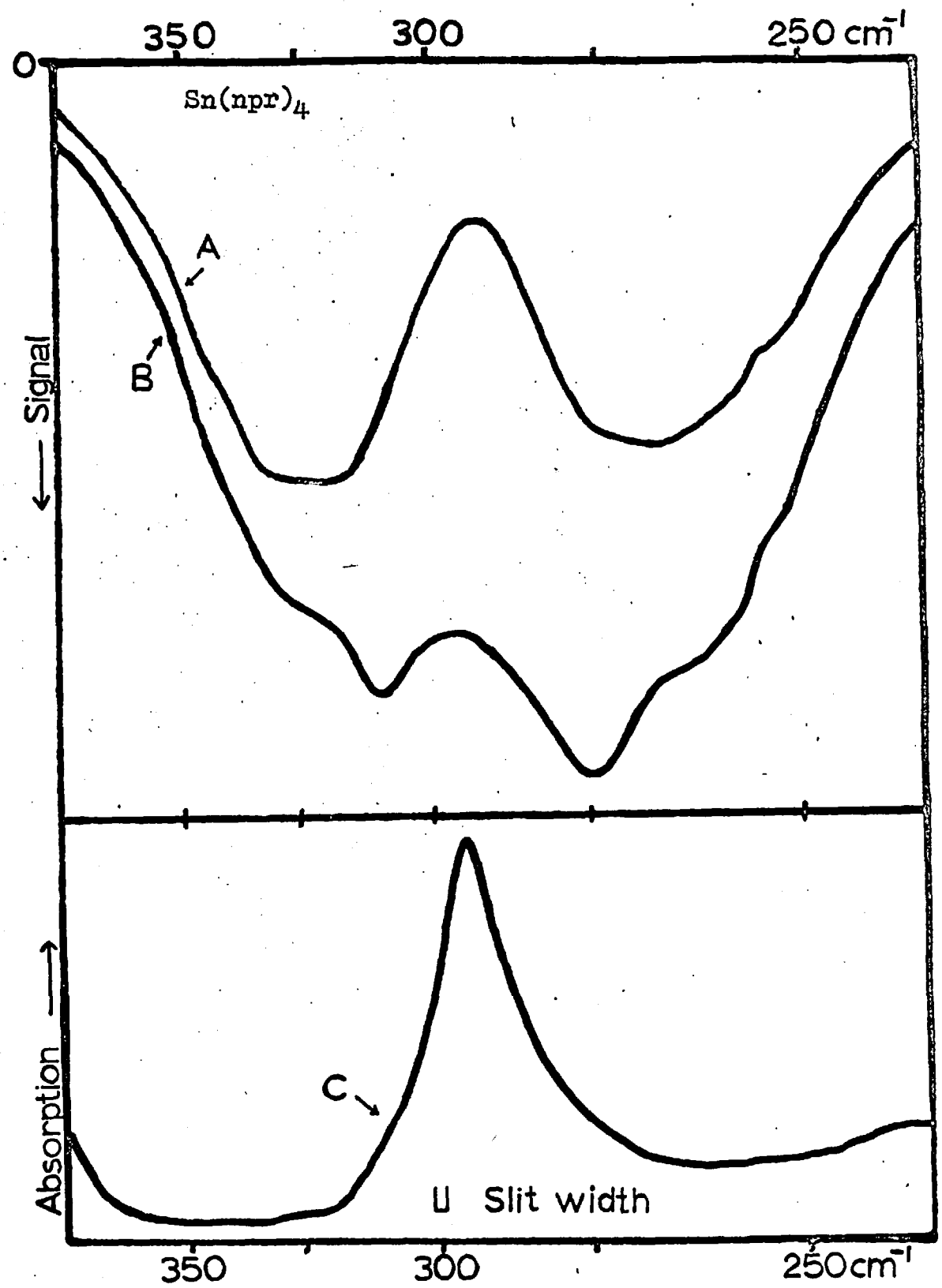


Fig.25: The 294 cm^{-1} band in $Sn(nPr)_4$; A, sample; B, background; C=signalB/ signalA.

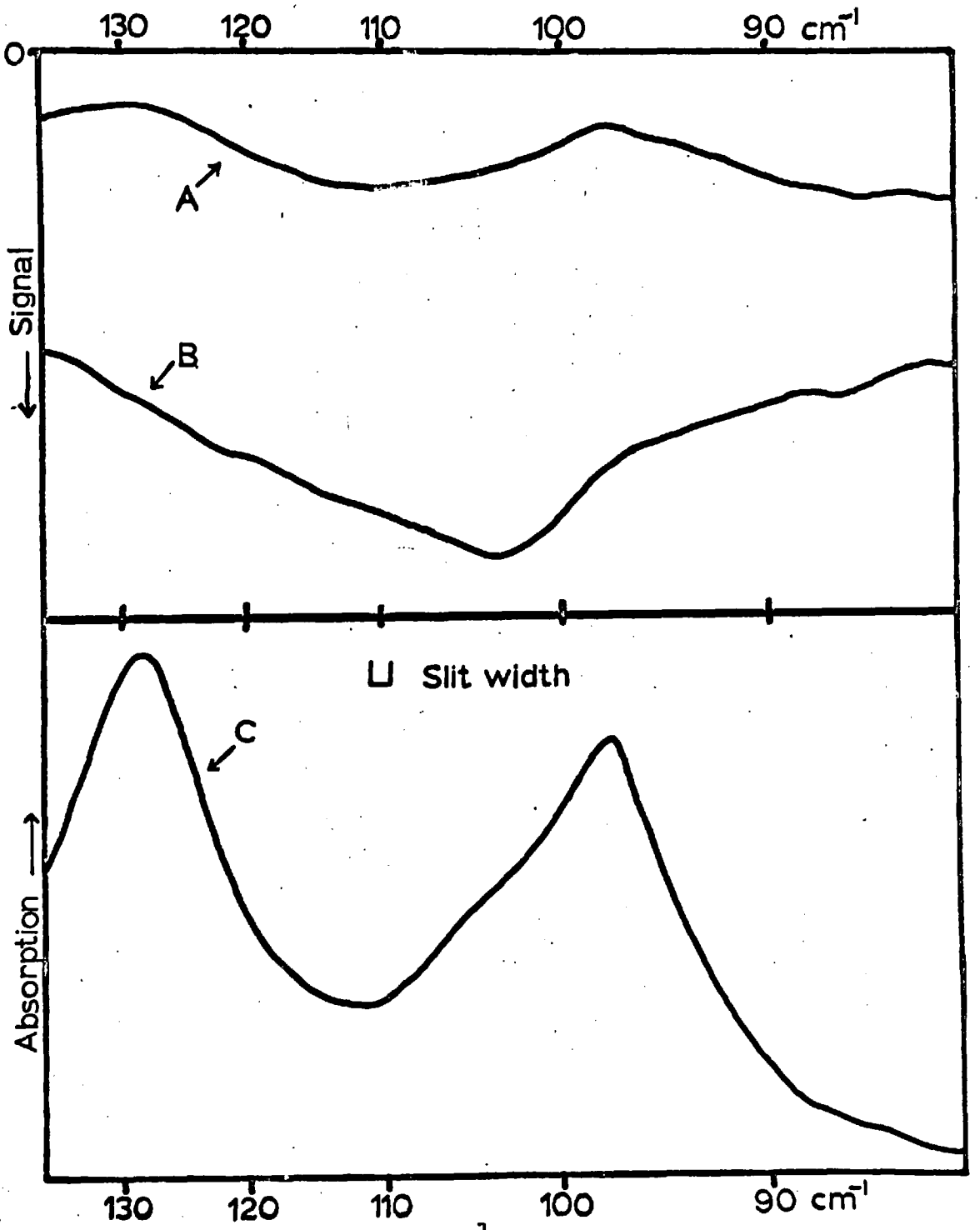


Fig.26: The 97 and 129 cm^{-1} bands in $Sn(nPr)_4$;
A, sample; B, background; C= sig.B/sig.A.

4: THE VIBRATIONAL SPECTRA OF $PbEt_4$, $SnEt_4$ AND $Sn(nPr)_4$.

4.1: Introduction.

The tetramethyls of group IVa metals have been extensively studied by Raman (73,74,75) and higher frequency infra-red spectroscopy (73), and as a consequence of the high symmetry of these compounds, it has been possible to make complete vibrational assignments of the fundamentals, and to evaluate force constants. The greater complexity and lower symmetry of the higher tetra-alkyls prevent the assignment of the skeletal modes without the addition of far infra-red data. The far infra-red spectra which are given below, account for the low frequency skeletal modes and also allow some inferences to be made about torsional barriers and isomerism in these compounds.

4.2: Experimental.

The spectra from 55-400 cm^{-1} were recorded with the vacuum grating spectrometer described in section 3.1. Resolving power and frequency calibration are to $\pm$ 1 cm^{-1} over the range but many of the absorption bands are broad, resulting in an uncertainty of $\pm$ 2 to 3 cm^{-1} in the position of the band centre. The samples were examined in the manner already described in section 3.232. Typical spectra showing the background (thin sample), the sample spectrum and the corresponding ratio plots are shown in figs. 25 and 26. Owing to the flexibility of the polythene, the sample thickness was not precisely controlled. Spectra at higher frequencies were recorded with a Perkin-Elmer model 21 spectrometer equipped with NaCl and KBr prisms.

The $PbEt_4$ was supplied by the Ethyl Corporation and the $SnEt_4$ and $Sn(nPr)_4$ by Pure Chemicals Limited.

A preparative scale gas chromatograph was built for the purification of samples having boiling points below about 200°C. It consisted of a 2 x 200 cm column of 60-80 mesh 'Celite' impregnated with 10°/o of silicone oil. Nitrogen was used as the carrier gas and a katharometer as detector. Gas chromatograms of the tin alkyls showed no indication of any other components (probably at least 98°/o pure). All samples were used without further purification.

4.3: Results.

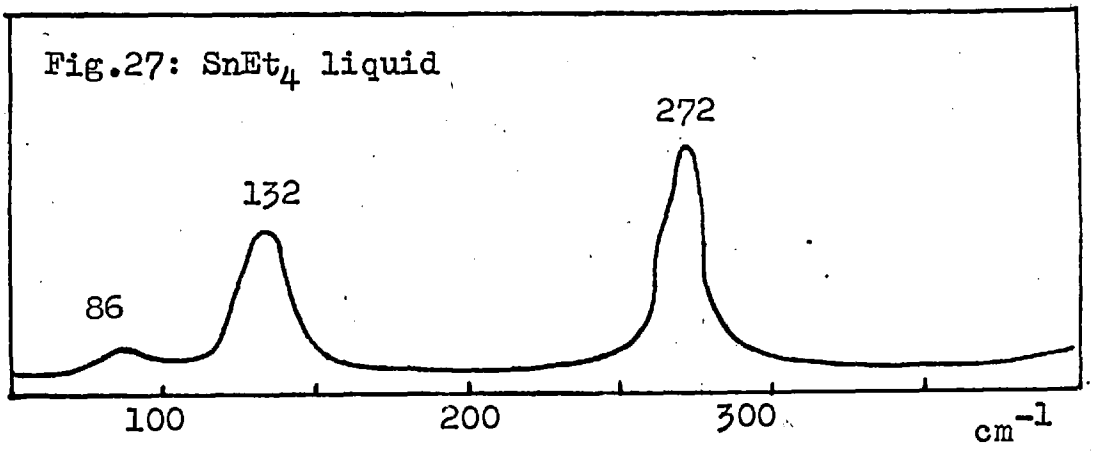
The spectra for the far infra-red region are shown in figs. 27,28,29 and the actual spectra taken are documented in the Appendix. The results for the tetraethyls are given in table V which also includes higher frequency and Raman data where available, and data for the corresponding tetramethyls taken from the literature.

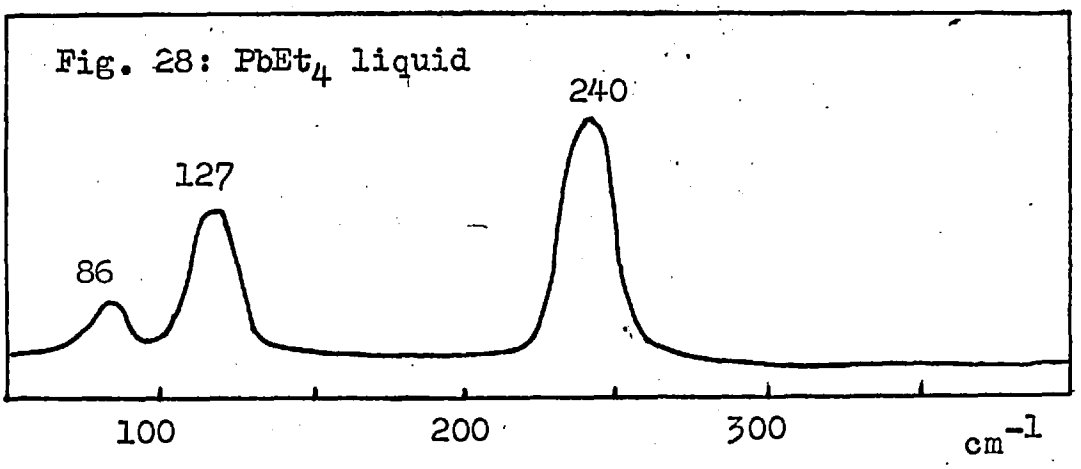
Table VI gives the results for $Sn(nPr)_4$ together with data for comparable compounds which are used as a basis for the assignments.

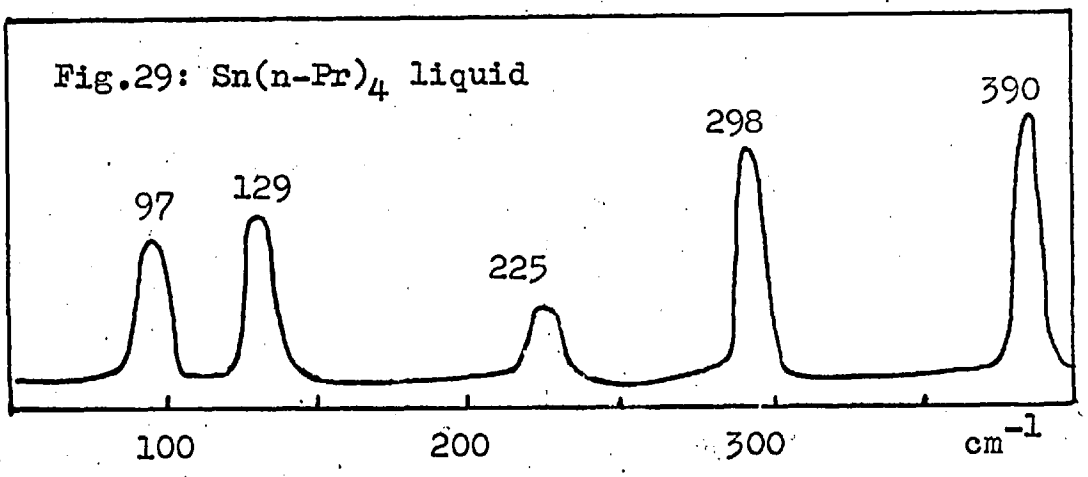
4.4: Discussion.

4.41: Vibrational assignment: $PbEt_4$ and $SnEt_4$.

The Raman spectra of both these compounds have been reported (75,76) and also the infra-red spectra at higher frequencies (75,77), but there has been no extensive discussion of the complete vibrational assignment. The situation is quite different in the tetramethyl compounds, for here, partly as a consequence of the high symmetry, a satisfactory account of all the vibrational fundamentals has been given by Lippincott (73) and independently by Edgell (74). This provides a good comparative


Fig.27: $SnEt_4$ liquid
272
132
86
100
200
300
cm-1


Fig. 28: $PbEt_4$ liquid
240
127
86
100
200
300
cm-1


Fig.29: $Sn(n\text{-}Pr)_4$ liquid
390
298
129
97
225
100
200
300
cm-1

basis for the interpretation of the spectra of the tetraethyls, and is therefore included in Table V. It was considered that an investigation of the far infra-red spectra of the tetramethyls would not substantially alter this account, and no work was undertaken on these compounds.

The replacement of methyl by ethyl reduces the symmetry and in principle could give rise to a complex spectrum dependent in detail on the configuration adopted by the ethyl groups. Fortunately the observed low frequency spectrum is remarkably simple. This suggests that as a result of the large mass of the metal atom, there is very little coupling between the vibrations of the ethyl groups, which can be considered as four independent groups attached to a heavy anchor, with their frequencies superimposed. A further consequence of the independence of the ethyl groups is that no effects of torsional isomerism appear in the spectrum.

The introduction of an ethyl group will give rise to three new skeletal frquencies. The C-C stretching is assigned to the band at 961 cm^{-1} in $SnEt_4$ and 957 cm^{-1} in $PbEt_4$ which have no counterpart in the tetramethyls. The X-C-C bending frequency would be expected to be at about 250 cm^{-1}, and the bands appearing in $SnEt_4$ at 272 cm^{-1} and in $PbEt_4$ at 240 cm^{-1} are assigned to this mode. The third new skeletal, the torsion about the X-C bond, would arise from restricted rotation. Butcher and Cahill (78) have calculated a potential barrier of 650 cal $mole^{-1}$ in $SnMeH_3$ from microwave data. Using a simplified model of $SnEt_4$ this barrier would correspond to a torsion frequency of 33 cm^{-1}, (see later), below the frequency range observable. From the trend of torsion barriers about Group IV X-C bonds, it is probable that the Pb-C barrier is very

small, and the torsion frequency would also be expected to be unobservable.

The only low frequency in the tetramethyls arises from the C-X-C bending motions, which give an E type fundamental, inactive in the infra-red, and an F_2 fundamental which is infra-red active. The replacement of methyl by ethyl groups can be viewed as a perturbation of the motion of the C atoms attached to the central atom. Accordingly the pronounced infra-red band at 132 cm^{-1} in $SnEt_4$ and at 122 cm^{-1} in $PbEt_4$ is identified as the counterpart of the F_2 fundamental. The complete symmetry designation of this fundamental depends on the configuration of the outer methyl groups, which is uncertain.

A weak infra-red band is found in $SnEt_4$ at 86 cm^{-1} and a rather stronger band in $PbEt_4$ also at 86 cm^{-1} (this is probably the same as the Raman band at 96.5 cm^{-1}). A suggested origin of these bands is the relaxation of the selection rule forbidding the E type C-X-C bending by the lower symmetry arising from the outer methyl groups.

There is one further molecular motion in the tetraethyls which could give rise to a low frequency band, viz. the torsion about the C-C bond. Although the anticipated barrier of about 3 Kcal $mole^{-1}$ would give a frequency well within the observed range, and allowed by the low symmetry of some configurations, the intensity of the band would probably be low as a result of the symmetry of the light methyl group and the large mass of the central metal atom. Accordingly, none of the observed bands is thought to arise from this motion. A similar observation concerning the absence of torsional bands arising from methyl groups in the n-propyl halides has been made by Brown and Sheppard (79).

	$SnMe_4$		$PbMe_4$		$SnEt_4$		$PbEt_4$	
Description and symm. design. in tetramethyls	I.R. (73)	R. (73,74)	I.R. (73)	R. (73)	I.R. (75)&this wk. bel.700	R. (75)	I.R. this work	R. (76)
C-H stretching	3000 s	2988 s	3000 vs	2996 vs	2842 vs		2950 vs	2927 s
	2920 s	2912 s	2920 vs	2924 vs	2813 vs		2895 vs	2869 w
CH_2 bending	-	-	-	-	1427 vs		1428 s	
CH_3 def. A	i.a.	1205 vs	i.a.	1170 vs	-	1146?vs	-	-
CH_3 def. E	i.a.	1400 w	i.a.	1400 w	-		-	
CH_3 def. F_1	i.a.	i.a.	i.a.	i.a.	-		-	-
CH_3 def. F_2	1443 s	1445 w	1448 vs	1450 w	1474 vs		1463 s	1460 w
CH_3 def. F_2	1198 s	1194 vs	1148 vs	1154 vs	1382 vs		1377 s	
CH_2 wagging	-	-	-	-	1191 vs	1201 m	1153 vs	1159 s
CH_3 rocking E	i.a.	768 w	i.a.	700 vw	1266	1089		
CH_3 rocking F_1	i.a.	i.a.	i.a.	i.a.	-			
CH_3 rocking F_2	770 vs	768 w	765 vs	767 m	946 vs		930 m	
CH_2 twisting	-	-	-	-	1012 vs		1013 s	
C-C stretching	-	-	-	-	961 vs		957 s	
CH_2 rocking	-	-	-	-	667vs,680vs		656s,674s	
C-X str. A	i.a.	508 vs	i.a.	459 vs	-	490 vs	n.i.	443 vs
C-X str. F_2	528 s	530 vs	478 vs	478 vs	508 s	508 s	n.i.	464 s
X-C-C bend.	-	-	-	-	272 s		240 s	241 w
C-X-C bend. E	i.a.	145 vs	i.a.	130 s	86 vw		86 m	96.5m
C-X-C bend. F_2	n.i.	160 vs	n.i.	145 vs	132 m		122 m	

TABLE V : Vibrational spectra and assignment of $SnEt_4$ and $PbEt_4$.

i.a. denotes inactive

n.i. denotes not investigated

An assignment of the higher frequency modes is also included in Table V. As the main interest of the present work was in the low frequency skeletal modes, the higher frequency modes have not been studied in detail, and their assignment should be regarded as tentative. A point that may be noted is that the marked change in the frequency of the methyl symmetrical deformation mode, and of the methyl rocking, in passing from $SnMe_4$ to $SnEt_4$ has a counterpart in MeI (80) and EtI (81). The assignment of the metal tetramethyls and of the alkyl halides are unchanged from those in references (73,74,80,81).

4.42: Vibrational assignment: $Sn(nPr)_4$.

Although it is to be anticipated that coupling between the attached groups via the central Sn atom continues to be small, a further new feature is introduced when one comes to n-propyl groups. This is that the group itself can take either of two internal torsional configurations - trans or gauche with respect to orientation about the C_1C_2 bond. Unlike the torsional configurations about the Sn-C bond, already discussed in the previous section, this isomerism does not depend upon the arrangement of one alkyl group with respect to other alkyl groups, and can occur in the absence of any interaction between the groups.

Even though our primary interest in the present work was in the low frequency skeletal modes, useful information concerning the molecular configuration can be obtained from the higher frequency spectrum of liquid $Sn(nPr)_4$ which has consequently been recorded up to 3500 cm^{-1}. The data is included in Table VI.

When comparison is made with the spectrum of liquid nPrI, there is notable similarity. In particular, there are 14 strong bands in the range between 500 and 1500 cm^{-1}, and the same number in this range in the spectrum of liquid nPrI. Sheppard has demonstrated that the complexity of the spectra of the liquid n-propyl halides arises from the occurrence of two torsional configurations of the n-propyl group (79). On crystallisation, the spectra become markedly simpler, and the bands then observed have been satisfactorily assigned to the trans form alone.

When the spectrum of liquid $Sn(nPr)_4$ is considered in more detail, a very satisfactory assignment of the bands between 500 and 1500 cm^{-1} can be made (Table VI) if it is assumed that both forms of the n-propyl group are present, but no satisfactory interpretation of the spectrum appears possible on the basis of only one form of the n-propyl group. Stuart models show that both forms of the groups can be accommodated about the Sn atom.

The high frequency spectrum has not been studied sufficiently to ensure that the tentative assignment proposed in Table VI is unambiguous, but the data is sufficient to substanciate that both forms of the n-propyl group contribute to the spectrum.

As it would seem probable that the two strong bands at 500 cm^{-1} and 590 cm^{-1} arise from the Sn-C stretching of the two forms (c.f. nPrI) these were observed during cooling of the liquid, but no change in the relative strengths of these bands was observed down to 80°K. The possibility of glass formation is small, as a sudden uniform change in the transmission occurred uniformly throughout the spectrum (which was repeatedly and rapidly scanned) after about 13 minutes cooling. The lack of sig-

nificant change in the relative band intensities before and after the break indicates rather that the crystallisation process has not required the n-propyl groups to assume a single form.

Turning now to the low frequency region, the band at 390 cm^{-1} has no counterpart in $SnEt_4$, but the C-C-C bending of the gauche form of nPrI was assigned to 390 cm^{-1} by Sheppard; for both these reasons this band is taken as the C-C-C bending frequency. The strong band at 129 cm^{-1} is similar in contour and intensity to the 132 cm^{-1} band in $SnEt_4$ and is similarly assigned to C-Sn-C bending. The strong, well defined band at 97 cm^{-1} bears no resemblance to the weak band at 86 cm^{-1} in $SnEt_4$. The 97 cm^{-1} and 129 cm^{-1} bands are of about equal strength, and so it would seem unlikely that the lower frequency band could arise from the relaxation of the symmetry prohibition of the E type C-Sn-C bending. A mode which would account for the introduction of a new low frequency band in $Sn(nPr)_4$ is the torsional vibration about the C_1-C_2 bond. The potential function for this torsion will not have triple cosine symmetry, and neither of the groups attached by this bond has local C_{3v} symmetry. The plausibility of assigning this band to torsion can be tested quite well by an approximate calculation of the barrier. This gave a value of 3.8 kcal $mole^{-1}$ (see later). The considerable strength of the torsion band would be anticipated from the asymmetry of the attached groups. The remaining torsional bands involving libration about the Sn-C_1 and C_2-C_3 bonds would not be observable for the same reasons as in $SnEt_4$.

Only one further band would be anticipated on the basis of four non-interacting n-propyl groups in a single configuration. In fact two bands are observed, one of

Description of vibration	$SnMe_4$ ref.(73)	MeI ref.(80)	$SnEt_4$ ref.(75) & this wk bel.700	EtI IR&R ref.(81)	$Sn(n\text{-}Pr)_4$ this work TRANS	$Sn(n\text{-}Pr)_4$ this work GAUCHE	n-PrI ref.(79). TRANS	n-PrI ref.(79). GAUCHE
C-H stretching	3000s 2920s		2842vs 2813vs		2880vs 2800vs 2690w			
CH_3 asymm. def.	1443s	1440	1474vs	1440	1455vs		1457	1457
CH_2 bending	d.n.a.	d.n.a.	1427vs	1440	1443vs		1429	1429
CH_2 wagging	d.n.a.	d.n.a.	1191vs	1210	1325vs 1190m	1318s 1270s	1324 1187vs	1340 1274vs
CH_3 symm. def.	1198s	1251	1382vs	1372	1405s	1365s	1378	1378
CH_3 rocking	i.a. in IR.	880	1089 (from R)	1049	1055vs		1093m	1077m
CH_2 twisting	d.n.a.	d.n.a.	1012vs	985	1150m	1170m	1130m	1195vs
C-C stretching	d.n.a.	d.n.a.	961vs	955	1018s		1019m	1011m
CH_3 rocking	770vs	880	946vs	960	985s		892s	875s
CH_2 rocking	d.n.a.	d.n.a.	667vs 680vs	740	655s 715m	685s 785s	827s 715m	816s 763s
C-X stretching	528s	533	508s	500	590s	500s	593s	503s
C-C-C bending	d.n.a.	d.n.a.	d.n.a.	d.n.a.	294?vs	390s	288	390
X-C-C bending	d.n.a.	d.n.a.	272s	262	225m	294vs	203	260
C-Sn-C bending	160vs (from R)	d.n.a.	132m	d.n.a.	129s		d.n.a.	
C-C torsion	d.n.a.	d.n.a.	d.n.a.	d.n.a.	97s		not observed	

d.n.a. denotes does not arise.

TABLE VI: Infra-red spectra of tetra n-alkyl tin compounds compared with n-alkyl iodides.

medium strength at 225 cm^{-1} and a strong band at 294 cm^{-1}. The assignment of 225 cm^{-1} as the combination band 97 + 127 cm^{-1} seems unlikely, as no other combination bands of this intensity have been invoked. A more probable assignment of these two bands is to the Sn-C-C bending vibrations of the two forms of the propyl group. If it is assumed that valence force field constants do not greatly change from one form to the other, the mass geometry would give rise to the higher frequency in the gauche form. In view of the uncertainty in the proportions of the two forms of the group, the relative strength of the two bands is of only slight significance. It may be mentioned, however, that in the far infra-red spectrum of liquid n-propyl chloride, which has recently been recorded in this laboratory at room temperature, the skeletal bending of the gauche form at 290 cm^{-1} is also much stronger than the bending of the trans form at 213 cm^{-1}.

The assignment of the vibrational frequencies of $Sn(nPr)_4$ is summarised in Table VI.

4.43: Force field calculations: $SnEt_4$.

One of the objects of the present investigation was to examine the information about the force field at the tin atom that could be gained from the low frequency vibrations. In order to make any headway it is necessary to introduce simplifying approximations.

First the applicability of a valence force field without interaction terms was tested on $SnMe_4$. Herzberg (83) gives the equations of the four fundamental frequencies of an XY_4 tetrahedral (T_d) molecule. Since there are only two force constants but four equations for the frequencies, there will be two checks on the applicability

of the force field used.

These are:

$$\frac{\nu_3\nu_4}{\nu_1\nu_2} = \frac{2}{3}\left(1 + \frac{4M_Y}{M_X}\right)^{1/2} \qquad \ldots\ldots\ (i)$$

$$\nu_3^2 + \nu_4^2 = \nu_1^2\left(1 + \frac{4M_Y}{3M_X}\right) + \frac{2}{3}\nu_2^2\left(1 + \frac{8M_Y}{3M_X}\right) \ldots\ldots\ (ii)$$

Using Edgell's assignment of the frequencies of $SnMe_4$ (74) and treating the methyl groups as point masses, as justified by Crawford (82), the following values were obtained upon substitution:

Eqn.(i): L.H.S.=1.04; R.H.S.=1.00

Eqn.(ii): L.H.S.=30.5x10^4cm^{-2}; R.H.S.=32.1x10^4cm^{-2}

One concludes that the vibrations of the SnC_4 framework can be represented quite well by using a valence force field, and we can proceed to $SnEt_4$.

The normal vibrations of $SnEt_4$ will depend on the configurations adopted by the ethyl groups. As it is probable that all configurations are present, and also that there is little direct interaction between the ethyl groups, the following simple model was used. An ethyl group was taken to be attached to an infinitely heavy mass which neither rotates nor moves linearly. The geometry is shown in fig.30 below:

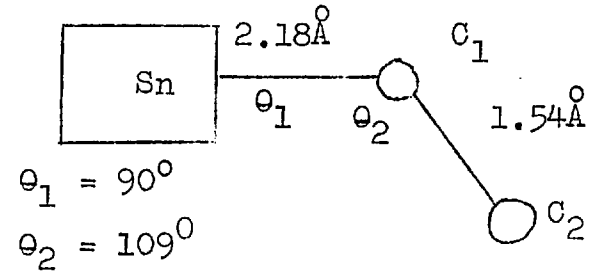


Fig. 30.

The CH_3 and CH_2 groups are represented by equivalent masses, as recommended by Crawford, taking the following values for the reciprocal masses:

$(1/m)_{C_2}$ along bond C_1C_2 = 0.0676 $(a.m.u.)^{-1}$

$(1/m)_{C_2}$ perp. bond C_1C_2 = 0.0727 $(a.m.u.)^{-1}$

$(1/m)_{C_1}$ both along and perp. bond SnC_1 = 0.0715 $(a.m.u.)^{-1}$.

The stretching and bending force constants $F_{r_1r_1}$ and $F_{\theta_1\theta_1}$ were transferred from $SnMe_4$, using two of the equations given by Herzberg (ref. 80, p.182), viz.:

$$4\pi^2\nu_1^2 = \frac{k_{rr}}{M_y}, \text{ giving } k_{rr} = 2.24 \times 10^5 \text{ dynes cm}^{-1}$$

$$4\pi^2\nu_2^2 = \frac{3k_{\theta\theta}}{M_y l^2}, \text{ giving } k_{\theta\theta} = 3.15 \times 10^{-12} \text{ dynes rad}^{-1}.$$

To calculate the tetrahedral bending frequency on the basis of the linear model shown in fig.30, we must take $F_{\theta_1\theta_1} = 3k_{\theta\theta}$ since the corresponding frequency equation for the linear case is $4\pi^2\nu^2 = \frac{k'_{\theta\theta}}{M l^2}$.

The other constants $F_{r_2r_2}$ and $F_{\theta_2\theta_2}$ were transferred from propane using an equivalent triatomic framework and the methods of Crawford an Herzberg (ref. 80, p.169).

All off-diagonal force constants were taken as zero, and the values of the four constants used in the calculations are given below:

$$F_{r_1 r_1} = 2.24 \times 10^5 \text{ dynes cm}^{-1}$$

$$F_{r_2 r_2} = 3.32 \times 10^5 \text{ dynes cm}^{-1}$$

$$F_{\theta_1 \theta_1} = 9.45 \times 10^{-12} \text{ dynes rad}^{-1}$$

$$F_{\theta_2 \theta_2} = 8.70 \times 10^{-12} \text{ dynes rad}^{-1}$$

For the in-plane bending of θ_1, the 4 x 4 G matrix was set up in the usual way, and from the eigenvalues of (GF) the following frequencies were obtained:

TABLE VII

Approx. description		$\nu_{obs.}$	$\nu_{calc.}$
ν_1	C-Sn-C bending	132 cm^{-1}	85 cm^{-1} (147)
ν_2	Sn-C-C bending	272	233
ν_3	Sn-C stretching	506	551
ν_4	C-C stretching	960	905

In view of the approximations involved, the agreement of the last three frequencies is as satisfactory as is usually found.

The frequency calculated from the model for the C-Sn-C bending mode is very dependent on the orientation of the ethyl group. If, referring again to fig.30 we now consider the motion in which the C_1 atom moves perpendicular to the plane of the diagram, there is no coupling with the in-plane motions, and 147 cm^{-1} is obtained for the bending frequency by a straightforward mechanical calculation. The two values 85 and 147 cm^{-1} are lower and upper bounds for this frequency, and could be refined by more detailed consideration of the particular relative orientations of the ethyl groups.

The inferences to be drawn from these calculations are that the assignment and the model are not obviously wrong, and secondly, that the valence force constants in $SnEt_4$ are not obviously altered from those in $SnMe_4$. Refinement of the force constants to give a closer fit with the observed frequencies was not attempted, for even when the number of known frequencies is sufficient to determine a set of force constants, many sets of solutions for the latter may arise, owing to the non-linear form of the equations (85,86). As examination of numerical examples indicates that there is in general no a-priori limit to the difference between two sets of solutions, a successive approximation method starting from transferred force constants may "home" onto an incorrect set. The question of the closeness of such sets of force constants has been raised by Freeman and Ross (86), but without reaching a conclusion about their proximity. It may be added that the ambiguity does not arise in Urey and Bradley's original paper (87).

These considerations indicate that the agreement of calculated and observed frequencies cannot necessarily be taken as sufficient proof of the correctness of the force constants used. For this reason a perturbation method based on the (GF) matrix, to fit force constants to the observed frequencies, was not pursued.

4.44: Torsional frequencies.

4.441: Calculation for $SnEt_4$.

The torsional frequency about the Sn-C bond was calculated for the framework shown in fig.31 overleaf. For simplicity the reduced moment was calculated for the SnC_3 top, by the method given in ref.(88).

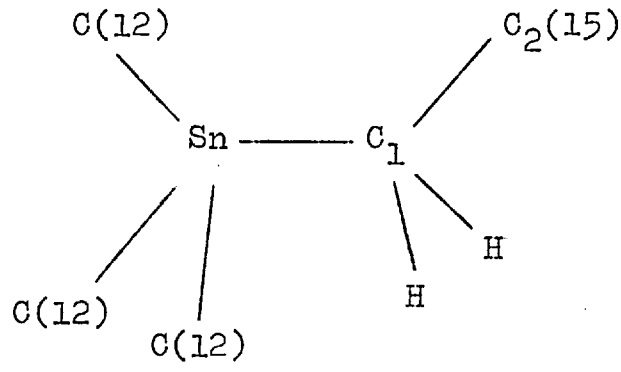


Fig.31:Framework used in the calculation of the Sn-C torsional frequency in $SnEt_4$.

Tetrahedral angles were used throughout and the bond lengths were as follows:

$Sn-C_1 = 2.18$ Å
$C_1-C_2 = 1.54$ Å
$C_1-H = 1.08$ Å

Using the harmonic oscillator approximation with a triple cosine barrier of 650 cals $mole^{-1}$, the torsional frequency was calculated as 33 cm^{-1}.

4.442: Calculation for $Sn(nPr)_4$.

As the torsional frequency about the Sn-C bond was again expected to be below the range of observation, the calculation was not repeated. The torsional frequency about the C_1-C_2 was expected to lie within the observable range, and the calculations were carried out with reference to the framework shown in fig.32 overleaf. The trans form of the n-propyl group was chosen for simplicity; as a consequence of the size of the molecule there is expected to be very little difference between the reduced moments of inertia of the two forms. The reduced moment I_{red} of the ethyl group was calculated by the method of Pitzer for an asymmetric top attached to an

asymmetric frame (89). The value obtained was

$$I_{red} = 21.3 \text{ a.m.u. } \text{Å}^2.$$

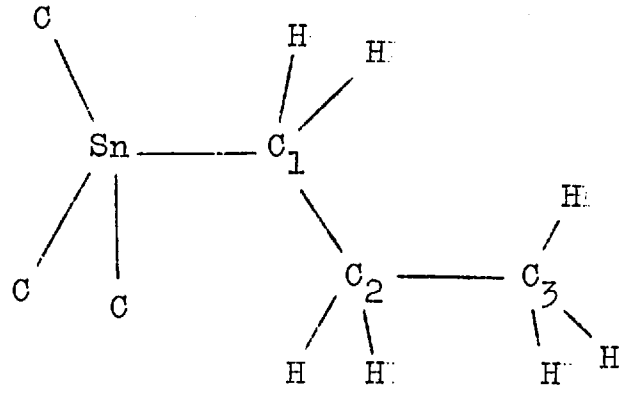


Fig.32: Framework used in the calculation of the C_1-C_2 torsional frequency in $Sn(nPr)_4$. Bond lengths and angles are as in fig.31.

The expression $V_3 = \frac{8}{9}\pi^2 v^2 I_{red}$ based on a harmonic oscillator fitted to a cosine potential function in a section $2\pi/3$ yields a value of $V_3 = 3.8$ kcal mole^{-1} when $v = 97$ cm^{-1}. In view of the uncertainty in the form of the potential function as a consequence of the lack of symmetry - a point discussed by Aston (90), the value of V_3 is not unreasonable.

4.45: Thermodynamic calculations: $SnEt_4$.

As the spectroscopic data allow a complete vibrational assignment to be made for $SnEt_4$, it was thought worthwhile to compute the thermodynamic functions, making the assumption that all configurations of the ethyl groups are equally probable. Calorimetric data, when available, will enable this assumption to be tested.

The calculations are based on the following expressions for the entropy S^o and the usual function for the free energy F^o, viz. $F' = -(F^o - H^o_o)/T$, taken from Taylor and Glasstone, ref.(91).

a).Contribution from translation:

$$S^o_{trans.} = R(\tfrac{5}{2}\ln T - \ln P + \tfrac{3}{2}\ln M + \ln p_s - 1.164)$$

$$F'_{trans.} = R(\tfrac{5}{2}\ln T + \tfrac{3}{2}\ln M - \ln P - 3.664)$$

b).Contribution from overall rotation:

$$S^o_{rot.} = R(\tfrac{3}{2}\ln T + \tfrac{1}{2}\ln ABC - \ln s + 134.687)$$

$$F'_{rot.} = R(\tfrac{3}{2}\ln T + \tfrac{1}{2}\ln ABC - \ln s + 133.186)$$

c).Contribution from free internal rotation:

$$S^o_{free} = R(\tfrac{1}{2}\ln I_{red} + \tfrac{1}{2}\ln T - \ln s' + 45.286)$$

$$F'_{free} = R(\tfrac{1}{2}\ln I_{red} + \tfrac{1}{2}\ln T - \ln s' + 44.786)$$ for each rotor.

T is the absolute temperature, M the molecular weight in a.m.u., P the pressure of the gas in atmospheres, ABC the product of the three principal moments of inertia of the molecule in g^3 cm^6, s the number of indistinguishable configurations produced by rigid overall rotation of the molecule about the principal axes, s' the number of identical configurations produced by 1 rotation of the rotor through 360^o, and p_s the number of spin states.

Contributions from rotation restricted by a cosine potential are tabulated as corrections to the free rotor contribution (91, or 92). Contributions from each normal vibration are tabulated separately as a function of the frequency v.

The results of the calculations are given below:

For Ideal gas at 273.0°K, 1 atm.	S°	$-(F^\circ-E_o^\circ)/T$
	both in cal $deg^{-1}mole^{-1}$	
Translation (M = 235 a.m.u.)	41.8	36.8
Overall rotation (ABC = 9.38 x 10^{-112} $g.^3cm^6$)	30.2	27.3
Less Rln(12) for the 12 indishtinguishable orientations of the central tetrahedral framework.	-4.9	-4.9
Vibrations, cm^{-1}, (degeneracy in brackets) 86(2); 132(3); 272(4); 490(1); 508(3); 680(4); 946(4); 961(4); 1012(4); 1089(4);1146(1);1191(4); 1382(3);1474(8);1427(4); 2827(20).	26.0	11.5
Free internal rotation		
4 Me groups (I_{red}=5.2x10^{-40})	13.9	9.9
4 Et groups (I_{red}=56x10^{-40})	32.1	28.2
Correction for restriction of internal rotation		
4 Me groups (V = 3.0 kcal)m	-5.8	-6.6
4 Et groups (V = 0.65 kcal)	-0.7	-3.8
TOTAL:	132.6	98.4

Since the high frequency vibrations contribute a negligible amount to the functions, the average value of the C-H stretching vibrations, of which there are 20, was used.

4.5: Conclusions.

The spectra can be readily accounted for on the basis of the following assumptions:

(a). The vibrations of the atoms directly attached to the metal atom follow quite closely the rules for tetrahedral symmetry.

(b). There is very little interaction between the vibrations of the alkyl groups.

(c). Substantial proportions of both the trans and gauche forms of the n-propyl group are present in liquid $Sn(nPr)_4$, and probably in the solid state also.

(d). Rotation about the Sn-C and Pb-C bonds is free, or restricted by a barrier of less than about 1 kcal/mole.

(e). Rotation about the C_1-C_2 bond of the propyl group is restricted by a barrier of 3-4 kcal/mole.

(f). No changes in the simple valence force field constants derived from $SnMe_4$ are needed to fit the observed frequencies of $SnEt_4$.

5: THE VIBRATIONAL SPECTRA OF ALKYL TIN CHLORIDES.

5.1: The vibrational spectra of $SnMe_3Cl$, $SnMe_2Cl_2$, $SnMeCl_3$.

5.11: Introduction.

The Raman and near infra-red spectra of the series $(CH_3)_nSnCl_{4-n}$ in the liquid state have been reported by Edgell and Ward (92), who have also given a complete vibrational assignment for these compounds. One of the key features of their results is the coincidence of the Sn-Cl stretching vibrations, and the superposition of the skeletal deformation frequencies. In view of this it was thought worth while to record the far infra-red spectra of this series to see if it were possible to resolve these accidental degeneracies.

During the course of this work Kriegsmann and Pischtchan (93) reported the Raman and near infra-red spectra of the series Me_3SnX (X= H,F,Cl, and Br), which showed that the Sn-halogen stretching frequency is extremely sensitive to environment.

5.12: Experimental.

5.121: Preparation of the compounds.

All three compounds were prepared by heating together equivalent mixtures of pure tin tetramethyl and tin tetrachloride:

$$SnCl_4 + 3SnMe_4 = 4SnMe_3Cl$$

$$SnCl_4 + SnMe_4 = 2SnMe_2Cl_2$$

$$3SnCl_4 + SnMe_4 = 4SnMeCl_3$$

The reactions were carried out in a 'Quickfit' MDH/111/50 flask which incorporates a Vigreux column. ~~For~~

$SnMe_3Cl$: The mixture was refluxed for about 2 hours after which time the vapour temperature had risen to a steady 150°C. The main fraction distilled at 156°C and was collected and dissolved in warm 60/80 petroleum ether. The crystals obtained on cooling in ice were washed in cold pet. ether and filtered off. After recrystallisation, the product melted at 35°C (c.f. 38°C found by Edgell and Ward), but Microanalysis gave a chlorine content of 17.92% (c.f. 17.82 calculated).

$SnMe_2Cl_2$: On mixing the reactants, the dichloride precipitated out as a white solid. After refluxing for 2 hours, the solid distilled over at 191°C. It was not very soluble in pet. ether; since the other halides are extremely soluble, the product was washed thoroughly in pet. ether (40/60). This sample and one which was obtained by crystallisation from pet. ether at -10°C both melted at 108°C (c.f. 107.5-108°C, ref. 94).

$SnMeCl_3$: The mixture was refluxed for 5 hours after which the main fraction distilled over at 176°C. It was crystallised from petroleum ether as described for $SnMe_3Cl$. The most probable impurity is $SnMe_2Cl_2$ which would giva a white precipitate on the addition of ammonia to an aqueous solution. This test was negative, and the compound melted at 47°C (c.f. 45-46°C, ref.94).

5.122: Recording of spectra.

The far infra-red spectra in the range 400-55 cm^{-1} were obtained with the spectrometer described in section 3.1. All three compounds are solids at room temperature,

so the spectra were taken as mulls in 'Nujol' enclosed in polythene bags, as described in section 3.22. Spectra in the range 800-400 cm^{-1} were recorded on a Perkin-Elmer 21 equipped with a KBr prism, also as mulls.

5.13: Results.

The far infra-red spectra are shown in figs.33, 45 and 49 and documented in the appendix. The results, together with those of Edgell and Ward, are given in tables VIII, XI and XIII, together with the assignments.

5.14: Discussion.

5.141: $SnMe_3Cl$.

Since $SnMe_3Cl$ is extremely soluble in 'Nujol', the mulls were in reality concentrated solutions in 'Nujol'. This was confirmed by further work on solvent effects (see later, section 6), which also showed that the only indication of the presence of solid in the "mull" was in the form of a pronounced shoulder on one of the bands (the Sn-Cl stretching frequency at 344cm^{-1}) corresponding to the position of this band in the solid.

(a). Vibrational assignment. The results of Edgell and Ward (92), who have given a detailed assignment of the entire spectrum indicate that, as expected, the vibrations of the CH_3 groups are apparently not coupled - a consequence of the large mass of the central tin atom. It is therefore safe to treat the methyl groups as point masses when considering the skeletal frequencies.

With this assumption, there will be 3x5-6=9 normal vibrations of which three are doubly degenerate E type and three non-degenerate A type. From the spectrum

of $SnCl_4$ (95), the Sn-Cl stretching frequency is expected to lie between 300 and 400 cm^{-1} and must therefore be assigned to the very strong infra-red band at 344 cm^{-1}. Similarly the spectrum of $SnMe_4$ (92) shows that the Sn-C stretching frequencies lie between 500 and 600 cm^{-1} and the two bands at 512 and 542 cm^{-1} are thus assigned to the A and E type vibrations of this mode respectively. The Raman spectrum given by Edgell and Ward indicates that the 512 cm^{-1} band is strongly polarised and must be of the A type.

There remain the A and E type Sn-Me_3 deformation and the E type Me-Sn-Cl bending frequencies to be assigned, From the spectra of $SnMe_4$ and $SnCl_4$ these are expected to lie between 55 and 200 cm^{-1}. There is, in fact, only one fairly sharp band between 55 and 300 cm^{-1}, viz. the band at 148 cm^{-1} which is consequently assigned to all three bending fundamentals. Only one band at 150 cm^{-1} was found by Edgell and Ward in the Raman spectrum, and they ascribe the accidental degeneracy of these vibrations to the piling up of fundamentals resulting from the large mass of the central Sn atom. Valence force calculations (see later) show this to be plausible.

The considerable difference (26 cm^{-1}) between the Sn-Cl stretching frequencies of the liquid and 'Nujol' solution is due to environmental effects and will be discussed in section 6.

There are two bands in the spectral range investigated which are due to hydrocarbon vibrations. These occur at 720(s) and 778(vs) cm^{-1} and are both very broad. Edgell and Ward observed only one very broad and strong band at 790 cm^{-1} in the liquid state which they assigned

TABLE VIII

VIBRATIONAL SPECTRA AND ASSIGNMENTS FOR $SnMe_3Cl$.

DESCRIPTION	FREQUENCIES cm^{-1} IR[a]	R[b]	R[c]	IR[d]
C-H asymm. stretch.	n.i.	2998	3001	3002s
C-H symm. stretch.	n.i.	2921	2923	2925s
$C-H_3$ asymm def.	n.i.	1401	1401	1400s
$C-H_3$ symm. def.	n.i.	1198	1202	1193s
CH_3 rocking	778 vs 720 s	-	790	787vvs
Sn-C stretch. E	542 s	545	548	545s
Sn-C stretch. A	512 m	514	518	514s
Sn-Cl stretch. A	344 vs	315	318	(325vs)
$Sn-Me_3$ def. E $Sn-Me_3$ def. A Me-Sn-Cl bend. E	150 s	145	150	(145s)

NOTES: a, Infra-red, 'Nujol' mull (solution), this work.

b, Raman, Kriegsmann and Pischtchan (93), liquid.

c, Raman, Edgell and Ward (92), liquid.

d, Infra-red, Edgell and Ward (92), liquid. This work below 400 cm^{-1}

n.i., not investigated.

to the Sn-CH_3 rocking mode. In CS_2 solution we found a weak band at 725 cm^{-1} which was also reported by Kriegsmann and Pischtchan (93) (see table XX , section 6). The presence of this band, which cannot be attributed to any combination or difference bands, would thus seem to indicate some degree of coupling between the rocking vibrations of the Me groups since in the absence of such coupling only one band would be expected. As emphasised by Edgell and Ward, however, there are no indications of splitting of the other hydrocarbon fundamentals, and the overall coupling is still negligible. A similar effect was found by Lee Smith (96) in $SiMe_3Cl$ where the frequency difference between the corresponding bands was 110 cm^{-1} compared with about 55 cm^{-1} in $SnMe_3Cl$.

Evidently the CH_3 rocking vibrations in this molecule are much more susceptible to coupling than tha other CH_3 modes. This is to be anticipated if one considers the form that the coupling takes in the two cases. For instance, any coupling arising between the C-H stretching vibrations of different CH_3 groups requires some movement of the heavy central atom. For the CH_3 rocking modes on the other hand, an appreciable degree of coupling can arise simply from the tendency of the whole molecule to react to changes in the angular momentum caused by the rocking of one of the CH_3 groups, since these have a comparatively large moment of inertia at the C atoms. Coupling can thus take place which requires very little movement of the Sn atom. In this sense it can be said that the Sn-CH_3 rocking is a quasi-skeletal vibration, for it is not wholly an internal vibration of the CH_3 group.

(b). Frequency calculations. In order to test the plausibility of the assignment, especially in respect of the low frequency bending modes, valence force calculations using transferred and guessed force constants were carried out for the skeletal frequencies, assuming point masses for the methyl groups. The equations given by Wagner (97, error corrected ref. 98) for the valence force system XYZ_3, point group C_{3v}, excluding interaction constants, were used. These give the coefficients of the two cubic equations for the three A and the three E type frequencies which are obtained from the respective GF matrices.

The force constants $f_{Sn-Me} = 2.25 \times 10^5$ and $d_{Me-Sn-Me} = 0.07 \times 10^5$ dynes cm^{-1} were calculated from $Sn\,Me_4$ (see section 4.43). The Me-Sn-Cl bending constant was taken as 0.08×10^5 dynes cm^{-1} (c.f. $d_{Cl-Sn-Cl} = 0.08 \times 10^5$ dynes cm^{-1} for $SnCl_4$). In $SnCl_4$ the Sn-Cl stretching constant is 2.80 dynes cm^{-1}, but using this value the Sn-Cl stretching frequency was found to be 402 cm^{-1}, which is greatly in excess of the observed values. By guessing much lower values for this constant, a better fit of the observed frequencies is obtained. The results of the calculations are given in table IX, together with the force constants used and the observed frequencies.

By suitably adjusting the force constants a much closer fit with the observed frequencies could probably be obtained, but in view of the considerable environmental effects on at least one fundamental frequency, these would be of little value in the absence of a gas phase spectrum. In any case, since there is some indication of coupling between the methyl groups, a more refined calculation which includes the hydrocarbon modes is called for. The

calculations do show however, that the observed accidental degeneracy of the low frequency bending modes is reasonable.

TABLE IX.

FORCE CONSTANTS $x10^{-5}$ dyn.cm^{-1}				$SnMe_3Cl$	
f_{Sn-Cl}	2.80	1.50	1.92	OBSERVED FREQUENCIES	
f_{Sn-Me}	2.25	2.25	2.20		
$d_{Me-Sn-Me}$	0.07	0.07	0.07	R(92) liquid	This wk. mull
$d_{Me-Sn-Cl}$	0.08	0.08	0.08		
Me-Sn-Me bend. A	149	147	148		
Me-Sn-Me bend. E	-	150	140	150	150
Me-Sn-Cl bend. E	-	149	139		
Sn-Cl stretch. A	402	309	344	318	344
Sn-Me stretch. A	530	515	512	518	512
Sn-Me stretch. E	-	544	557	548	542
DESCRIPTION	CAICULATED FREQS.				

5.142: $SnMeCl_3$.

As was found in the case of $SnMe_3Cl$, due to the extremely high solubility of $SnMeCl_3$ in 'Nujol' the mull was in reality a concentrated solution in'Nujol'.

(a). Vibrational assignment. This compound has the same symmetry as $SnMe_3Cl$ (point group C_{3v}) and will have the same number of skeletal frequencies. The vibrational spectrum is given in table XI, together with assignments and Edgell and Ward's data for the liquid state. The partially resolved band at 725 cm^{-1} is probably due to 'Nujol' which has a weak band there: there is no comparable band in CS_2 solution, nor could it be due to a splitting of the CH_3 rocking mode (as was found in $SnMe_3Cl$) since there is only one methyl group present.

Only one Sn-C stretching vibration is expected. However, three bands, at 565, 542 and 521 cm^{-1} were found in the 'nujol' solution. Edgell and Ward also found bands at 562, 548, and 525 cm^{-1} in the liquid and ascribed these to the PQR structure of the Sn-C stretching fundamental centred at 548 cm^{-1}. In view of the environmental effects on the Sn-Cl bands (section 6), it is extremely unlikely that the molecule is free to rotate perpendicular to the symmetry axis which is required for the appearance of rotational wings for this mode (99). It would seem then, that the 562 and 525 cm^{-1} bands are due to the presence of $SnMe_2Cl_2$ as impurity, since this compound has strong bands at 563 and 524 cm^{-1}. Due to the relative intensities of the Sn-C vibrations in these two compounds (comparatively weak in $SnMeCl_3$), the impurity reveals its presence here but not in the region of the Sn-Cl vibrations. The high frequency bands are in any case almost coincident.

TABLE XI

VIBRATIONAL SPECTRA AND ASSIGNMENTS FOR $SnMeCl_3$.

DESCRIPTION	SYMM[a]	Frequencies cm^{-1} IR[b]	R[c]	IR[d]
C-H asymm. stretch.		n.i.	3024	3033s
C-H symm. stretch.		n.i.	2932	2940s
CH_3 asymm. def.		n.i.	-	1402s
CH_3 symm. def.		n.i.	1200	1200s
CH_3 rocking		781vs	-	800vvs
		(565m)		(562m)
Sn-Me stretch.	A	542s	550	548s
		(521m)		(525m)
Sn-Cl stretch.	E	384vs	363	n.i.
Sn-Cl stretch.	A	366s shoulder		n.i.
Me-Sn-Cl bending	E	152w	142	n.i.
$SnCl_3$ def.	E	132s		n.i.
$SnCl_3$ def.	A	123m	112	n.i.

NOTES: a, symmetry of skeletals, point group C_{3v}

b, Infra-red, 'NUJOL' mull (=solution), this work

c, Raman, liquid, Edgell and Ward (92).

d, Infra-red, liquid, Edgell and Ward,(92).

n.i., not investigated.

The presence of small quantities of $SnMe_2Cl_2$ was later confirmed by the chemical test mentioned previously. $SnMeCl_3$ is the least stable compound of the series, and appears to deteriorate with time, but it is not easy to understand how the dichloride can be formed.

An A and an E type Sn-Cl stretching frequency are expected, but only a single strong band at 384 with a pronounced shoulder on the low frequency side was found. In the Raman spectrum of the liquid, Edgell and Ward found a single band at 363 cm^{-1} which they assigned to both modes. The difference of 20 cm^{-1} between 'Nujol' solution and the liquid again indicates considerable environmental effects on the Sn-Cl bond.

Three deformation modes are expected: an A and an E type $SnCl_3$ deformation, and an E type Cl-Sn-Me bending. In the Raman spectrum of the liquid, Edgell and Ward found two bands, at 142 and 112 cm^{-1} ; they assigned the lower band to the Cl-Sn-Me bending mode and the higher to the two $SnCl_3$ deformations. In the far infra-red spectrum of the mull three bands were found, at 152w, 132s and 123m cm^{-1}. The 152 cm^{-1} band is assigned to the Cl-Sn-Me bending and the other two to the $SnCl_3$ deformations. Frequency calculations (table XII) show this to be plausible but predict a frequency of 110 cm^{-1} for the A and 105 cm^{-1} for the E type deformations. Usually it is found that the E type XY_3 deformation is more intense and higher in frequency than the A type, suggesting that the 132 and 123 cm^{-1} bands be assigned to the E and A type $SnCl_3$ deformation vibrations respectively. That the corresponding values of the calculated frequencies are the other way round, with a splitting of 5 cm^{-1}, does not invalidate the above assignment; it indicates rather that the force con-

TABLE XII

THE SKELETAL VIBRATIONS OF $SnMeCl_3$

(CALCULATED AND OBSERVED)

DESCRIPTION	C_{3v} SYMM.	R(92) liquid	IR(92) liquid	CALCD.
Sn-Me stretching	A	550 cm^{-1}	542 cm^{-1}	544 cm^{-1}
Sn-Cl stretching	E	363	384	440
Sn-Cl stretching	A		366 sh.	380
$SnCl_3$ deformation	E	142	132	105
$SnCl_3$ deformation	A	112	123	110
Me-Sn-Cl bending	E	142	152	142

Force constants: $f_{Sn-Me} = 2.24 \times 10^5$ dynes cm^{-1}

$f_{Sn-Cl} = 2.80 \times 10^5$ " "

$d_{MeSnCl} = 0.08 \times 10^5$ " "

$d_{ClSnCl} = 0.08 \times 10^5$ " "

stants chosen are inadequate, so that the calculations show only that the two frequencies are likely to be found close together.

There remains the further possibility that the weak 152 cm^{-1} band is the difference band 542-384=158, as there is a corresponding sum band at 542+384=926 cm^{-1}(w), which was found in CS_2 solution. This being so, the Me-Sn-Cl bending mode must also be assigned to the 132 cm^{-1} band. However, since this sum band is weak, the difference band would be expected to be so weak (by approx. 1/8) as to be almost unobservable.

(b) Frequency calculations. A calculation based on the formulae referred to in the case of $SnMe_3Cl$ was carried out, using force constants transferred from $SnMe_4$ and $SnCl_4$ and a guessed constant. The results are shown in table XII, together with the observed frequencies. The calculations show that the Sn-C stretching constant transferred from $SnMe_4$ is almost unchanged in $SnMeCl_3$ (as was also found for $SnMe_3Cl$), but that the Sn-Cl constant transferred from $SnCl_4$ is too high. By taking a value of about 2.5 x 10^5 dynes cm^{-1} for this constant, a better fit with the observed Sn-Cl stretching frequencies at least would be expected: the Sn-C stretching frequency is not very sensitive to changes in the Sn-Cl constant.

5.143: $SnMe_2Cl_2$.

As distinct from the other two compounds of this series, $SnMe_2Cl_2$ is relatively insoluble in 'Nujol', and consequently the spectrum of the mull can be regarded as being due to the solid. Spectra of solutions (section 6) confirm this and show that the 358 cm^{-1}(w) band is due

the dissolved species (see figs. 45 and 46).

(a) Vibrational assignment. The hydrocarbon modes are expected to be little changed from those of the other two compounds. The rocking mode at 797 cm^{-1} again shows a distinct broad shoulder at about 720 cm^{-1}; whether this is due entirely to 'Nujol' or partly to a splitting of the rocking mode is impossible to say as there is no data available for CS_2 solution. However some degree of splitting is to be expected from the comparison with $SnMe_3Cl$. The spectra and assignments are given in table XIII.

For an analysis of the skeletal vibrations, the methyl groups can again be treated as point masses. On this basis the molecule belongs to the point group C_{2v}, and its nine fundamentals are distributed over the various species as follows: $4A_1 + A_2 + 2B_1 + 2B_2$. Of these the twisting vibration of the Cl's against the Me's is the only infra-red inactive A_2 fundamental.

The two strong infra-red bands at 567 and 518 cm^{-1} are assigned to the asymmetric (B_2) and symmetric (A_1) $SnMe_2$ fundamentals repectively. That the higher frequency band is due to the asymmetric vibration is also confirmed ~~confirmed~~ by the frequency calculations which follow. A similar pair of bands near 350 cm^{-1} is to be expected for the two $SnCl_2$ stretching vibrations. These were found at 309vs(A_1) and 332(vs)(B_1) cm^{-1}. A third band, at 358 cm^{-1} is due to the dissolved species.

The bending vibrations fall into two distinct species of which the symmetric A_1 type give rise to the $SnCl_2$ and $SnMe_2$ deformation frequencies, and the three asymmetric B type which are essentially rocking vibrations of the $SnCl_2$ and $SnMe_2$ groups against the rest of the molecule (Cl-Sn-Me bendings). Of the three bands found in

TABLE XIII

VIBRATIONAL SPECTRA AND ASSIGNMENTS FOR $SnMe_2Cl_2$.

DESCRIPTION	SYMM.[a]	Frequencies cm^{-1} IR[b]	R[c]	IR[d]
C-H asymm. stretch.		n.i.	3010	3009s
C-H symm. stretch.		n.i.	2928	2926s
CH_3 asymm. def.		n.i.	-	1402s
CH_3 symm. def.		n.i.	1211	1201s
CH_3 rocking		797vvs (720s)	-	792vvs
$SnMe_2$ asymm. str.	B_2	567s	566	563s
$SnMe_2$ symm. str.	A_1	515s	521	524s
$SnCl_2$ asymm. str.	B_1	332vs	344	n.i.
$SnCl_2$ symm. str.	A_1	309vs		n.i.
$SnMe_2$ bending	A_1	158m		n.i.
Cl-Sn-Me bend.	B_1	146s	135	n.i.
	B_2			
$SnCl_2$ bending	A_1	129m		n.i.

NOTES: a, symmetry of skeletals, point group C_{2v}.

b, Infra-red, 'NUJOL' mull (= solid), this work

c, Raman, liquid, Edgell and Ward (92).

d, Infra-red, liquid, Edgell and Ward (92).

n.i., not investigated.

the region where these are expected to lie, the medium strength band at 158 cm^{-1}, is assigned to the $SnMe_2$ deformation and the lowest, 129 cm^{-1} band to the $SnCl_2$ rocking (Me-Sn-Cl bending, B_2), since these vibrations would be expected to give rise to the highest and lowest frequencies respectively. Frequency calculations confirm this and serve as a guide for the assignment of the remaining bending modes. These indicate (Table XIV) that the central, 146 cm^{-1} band is to be assigned to the B_1 type Cl-Sn-Me bending, and that the $SnCl_2$ bending must be assigned also to the 129 cm^{-1} band.

(b) Frequency calculations. Wagner (100) has given a valence force field treatment for a general pentatomic X_2YZ_2 molecule belonging to the point group C_{2v} which includes one interaction constant to take into account the interactions between the X and Z atoms. This was neglected in the calculations as it is likely to be small in any case and there was no way of estimating its magnitude. He gives equations for the 16 elements for the A_1 block of the general GF matrix, and also expressions for the coefficients of the quadratic characteristic equations of the two B_1 and B_2 blocks. These formulae are too lengthy to be given here.

Since the Sn-Cl stretching constant taken from $SnCl_4$ was again expected to be too large, an estimate of its probable value was obtained by substituting two of the observed frequencies into the quadratic equation for the B_1 frequencies and solving it for the force constants. This yielded two sets of positive constants of which one set was obviously too large. The other set gave 1.60×10^5 dynes cm^{-1} for the Sn-Cl stretching constant and this was the value used in the subsequent calculations. The other force constants were identical with those used in calcu-

TABLE XIV

THE SKELETAL VIBRATIONS OF $SnMe_2Cl_2$
(CALCULATED AND OBSERVED).

Description	C_{2v} Symm.	R(92) liquid	IR (mull)	Calcd.
$SnMe_2$ asymm. stretch.	B_2	566 cm^{-1}	567 cm^{-1}	552 cm^{-1}
$SnMe_2$ symm. stretch.	A_1	521	515	529
$SnCl_2$ asymm. stretch.	B_1	344	332	338
$SnCl_2$ symm. stretch.	A_1		309	302
$SnMe_2$ bending	A_1	135	158	137
Cl-Sn-Me bending	B_2		129	109
Cl-Sn-Me bending	B_1		146	131
Cl-Sn-Me bend.(twist.)	A_2		in-active	not calcd.
$SnCl_2$ bending	A_1		129	124

Force constants: $f_{Sn-Me} = 2.25 \times 10^5$ dynes cm^{-1}

$f_{Sn-Cl} = 1.60 \times 10^5$ " "

$d_{MeSnMe} = 0.07 \times 10^5$ " "

$d_{MeSnCl} = 0.08 \times 10^5$ " "

$d_{ClSnCl} = 0.08 \times 10^5$ " "

lating the frequencies of the other methyl tin chlorides; These are given in table XIV, together with the calculated and observed skeletal frequencies.

It can be seen from the table that the Sn-Cl stretching frequencies are reproduced very well by the force constant used. Since, however, the gas phase frequencies would be nearer to those of the solution (389 and 352 cm^{-1} in benzene, see later), a force constant of about 2.1-2.2 would be a more realistic one for this molecule.

5.15: Conclusins: Intercomparison of the methyl tin chlorides.

The striking differences between the far infra-red spectra of the mulls in 'Nujol' and Edgell and Ward's Raman data for the liquids indicate that considerable associative effects between the molecules are present in varying degrees in the liquid and the solid states.

As was expected, the accidental degeneracies of the vibrations below 400 cm^{-1} were partially resolved in nearly all cases.

The valence force field calculations show that above the environmental effects there is distinguishable a distinct trend in the force constants. The Sn-Cl stretching constant falls through the series $SnCl_4$, $SnMeCl_3$, $SnMe_2Cl_2$, $SnMe_3Cl$, while the Sn-Me stretching constant remains unchanged. The sequence follows the increasing electron release by the methyl groups, facilitating the ionisation of the Sn-Cl bond. A parallel decrease in the Cl-Sn-Cl bending force constant would be expected, but is not apparent from the calculations made.

5.2: The Vibrational spectra of $SnEt_3Cl$ and $Sn(n\text{-}Pr)_3Cl$.

5.21: Introduction.

As was the case with the tetra alkyl compounds, the corresponding monochlorides are expected to have a large number of bands in the far infra-red region, and together with near infra-red spectra a complete vibrational assignment should be possible. Neither Raman nor near infra-red spectra of these compounds are known to have been reported.

5.22: Experimental.

Both compounds were obtained from Pure Chemicals Ltd. The sample of $SnEt_3Cl$ used was a small middle cut from the distillation of a very large sample (b.p. 94°C at 13mm Hg) and is probably 99 °/o pure. The $Sn(nPr)_3Cl$ was used without further purification.

All spectra were taken in the liquid state, at room temperature. The far infra-red spectra, from 55 - 400 cm^{-1}, were recorded with the spectrometer and methods already described, and the spectra from 400 - 3500 cm^{-1} were recorded with a Grubb-Parsons "Spectromaster" grating spectrometer.

5.23: Results.

The far infra-red spectra are shown in figs. 52, 56, and the results, together with those of similar compounds taken from the literature are given in tables XV and XVI.

5.24: Discussion.

5.241: $SnEt_3Cl$.

As was to be expected, the high frequency spectrum of this compound is very similar to that of $SnEt_4$ which is therefore used as a basis for the assignment. An organotin compound having three ethyl groups whose infra-red spectrum has been reported (75) is $SnEt_3Me$ and this is therefore included in table XV together with the spectra of $SnMe_3Cl$ and EtI. The assignments of the high frequencies for the ethyl compounds are based largely on Sheppard's assignment of the ethyl iodide frequencies (81), with the added assumption that there is very little interaction between the purely internal vibrations of the ethyl groups.

On this basis a very satisfactory assignment of nearly all the hydrocarbon modes is obtained. In the case of $SnEt_4$ (section 4) and $SnEt_3Me$ the two very strong bands at 680, 667 cm^{-1} and 670, 663 cm^{-1} are assigned to the CH_2 rocking mode. This would seem to indicate that for this mode at least the interaction between the ethyl groups is sufficient to split the CH_2 rocking frequency which is not internal to the CH_2 group. In the case of $SnEt_3Cl$, however, there is only one very strong and broad band at 671 cm^{-1} which could easily mask a 7 cm^{-1} splitting as observed in $SnEt_3Me$.

The fact that the CH_2 rocking frequencies are split would lead one to expect a corresponding coupling between the CH_2 wagging and the CH_2 twisting modes, since these are also not internal to the CH_2 group. The strong band at 1235 cm^{-1} in $SnEt_3Cl$ has a counterpart in $SnEt_3Me$ (at 1234 cm^{-1}) but not in $SnEt_4$ or EtI, and the only plausible assignment of this band would be to the CH_2

TABLE XV: Infrared spectra[a] of $SnEt_3Cl$ and related compounds

DESCRIPTION	(a) Et_3SnCl	(b) $SnEt_4$	(c) Me_3SnCl	(d) Et_3SnMe	(e) EtI
C-H stretch.	2916vs	2842vs	3002s	2856vs	
	2817s	2813vs	2925s	2801vs	
	2732m			2715ms	
CH_3 asym.def.	1449s	1474vs	1400s	1470vs	1440s
CH_3 sym.def.	1379s	1382vs	1193s	1379vs	1372
CH_3 rock. —	1075w	(1089s,R)	-		1049
\	962s	946vs	-	957vs	960
$Sn-CH_3$ rock.	-	-	790vvs	728vs	-
C-C stretch.	962s	961vs	-	957vs	955
CH_2 bending	1418s	1427vs	-	1426vs	1440
CH_2 wagging —	1190s	1191vs	-	1189vs	1210
\	1235s		-	1234vs	-
CH_2 twisting	1010vs	1012vs	-	1011vs	985
CH_2 rocking —	671vvs	680vs	-	670vs	740
\		667vs	-	663vs	-
Sn-C a.s.str.	518vs	508s	548vs	508s	-
Sn-C sy. str.	489s		518s		-
Sn-Cl str.	318vs	-	318vs(R) 325vs(IR)	-	-
Sn-C-C bend.	275m	272s	-	n.i.	-
$Sn-C_3$ a.s.d.	129s	(132m)	150s	n.i.	-
SnC_3 s.d.	110m		150s	n.i.	-
Cl-Sn-C bend.	125s	-	150s	n.i.	-

NOTES: (a), IR, liquid, this work.
(b), IR, liquid, (75), this work below 700 cm^{-1}
(c), IR,R, liquid (74).
(d), IR, liquid, (75).
(e), IR, liquid, (81).

n.i. = not investigated.

wagging mode to which were already assigned the bands at 1190 cm^{-1} in $SnEt_3Cl$ and 1189 cm^{-1} in $SnEt_3Me$. That no corresponding splitting of this mode is observed in $SnEt_4$ seems more likely to result from the decrease in intensity arising from symmetry, rather than the absence of coupling. The CH_2 twisting mode shows no such clear indication of splitting; either the coupling is not as great in this case, or the split counterpart coincides with another band.

Two CH_3 rocking frequencies are expected: an in-plane (Sn-C-C) and an out of plane vibration. The former occurs at 960 cm^{-1} in EtI and has a counterpart at 946 cm^{-1} in $SnEt_4$. In the case of $SnEt_3Cl$ and $SnEt_3Me$, there is only one strong band, at 962 and 957 cm^{-1} respectively, to which must also be assigned the C-C stretching frequency (955 and 961 cm^{-1} in EtI and $SnEt_4$). Hence both the C-C stretching and out of plane CH_3 rocking modes are assigned to the single band at 962 in $SnEt_3Cl$ and at 957 cm^{-1} in $SnEt_3Me$.

The in-plane CH_3 rocking occurs at 1049 cm^{-1} in EtI, but the only available band in $SnEt_3Cl$ is the weak band at 1075 cm^{-1} which has a counterpart at 1089 Cm^{-1} in the Raman spectrum of $SnEt_4$.

Turning now to the skeletal frequencies, by comparison with $SnEt_4$ the bands at 962 and 275 cm^{-1} are assigned to the C-C stretching and Sn-C-C bending modes respectively. The remaining skeletal vibrations involve essentially motions adjacent to the central tin atom where the local symmetry is C_{3v}. Therefore two Sn-C stretching frequencies are expected - a symmetric (A) and an asymmetric (E) band. In $SnMe_3Cl$ these occur at 548 and 518 cm^{-1} respectively, and consequently the two bands at

518(vs) and 489(s) cm^{-1} in $SnEt_3Cl$ are assigned to these modes. Similarly the very strong band at 318 cm^{-1} is assigned to the Sn-Cl stretching mode.

Again on the basis of C_{3v} symmetry at the tin atom, an A and an E type $SnMe_3^c$ deformation and an E type Me^c-Sn-Cl bending are expected, below about 150 cm^{-1}. Three bands were in fact observed in this region. In $SnEt_4$ the F type deformation occurs at 132 cm^{-1}; thus it is probable that the strong band at 129 cm^{-1} in $SnEt_3Cl$ is the corresponding asymmetric (E type) $SnMe_3^c$ deformation. The A type $SnMe_3^c$ deformation is expected to be less intense in the infra-red, as is usually found, and to lie at a lower frequency. Hence the medium strength band at 110 cm^{-1} is assigned to this mode. This leaves the strong band at 125 cm^{-1} to be assigned to the Me^c-Sn-Cl bending mode.

5.242: $Sn(n\text{-}Pr)_3Cl$.

It has been shown (section 4) that the entire infra-red spectrum of $Sn(nPr)_4$ can be satisfactorily assigned on the assumption that the n-propyl group is present in both the trans and gauche forms. Therefore it is to be expected that the spectrum of $Sn(nPr)_3Cl$ can be assigned on the same basis.

In the spectrum of $Sn(nPr)_4$ there are 17 bands between 1500 and 650 cm^{-1}, but only 13 in the corresponding monochloride, though this number is still more than can be assigned without the assumption of the presence of trans and gauche forms. However, in this case it is the far infra-red spectrum which suggests that this assumption can still be made with some degree of confidence.

TABLE XVI: Infrared spectra of $Sn(nPr)_3Cl$ and related compounds

DESCRIPTION	(a) $Sn(nPr)_3Cl$	(b) $Sn(nPr)_4$	(c) nPrI
C-H str.	2963vs cm^{-1} 2931vs 2916s 2874vs	2880vs cm^{-1} 2800vs 2690w	cm^{-1}
CH_3 a.s.d.	1460vs	1455vs	1457
CH_3 s.d.	1418m 1379s	1405s 1365s	1378
CH_3 rock.	1046vs	1055vs	1093m 1077m
CH_3 rock.	995s	985s	892s 875s
C-C str.	1020m	1018s	1019m 1011m
CH_2 bend.	1460vs	1443vs	1429
CH_2 wag.	1282m 1333s	(1325vs 1318s) (1190m 1270s)	(1324 1340) (1187vs 1274vs)
CH_2 twist.	1160m 1188w	1150m 1170m	1130m 1195vs
CH_2 rock.	(709s 667s) (797m)	(685s 655s) (785s 715m)	827s 816s 715m 763s
Sn-C str. E asymm.	601s 554m	590s 500s	593s 503s
Sn-C str. A symm.	554m 518m		(I-C str.)
Sn-Cl str.	336vs	-	-
C-C-C b.	298m 390vs	294vs 390s	288 390
Sn-C-C b.	219w 277w	225m 294vs	203 260 (I-C-C bend.)
$Sn-C_3$ a.s.d.	152s	129s	-
$Sn-C_3$ s.d.	131vs		
Cl-Sn-C b.	127vs		
C-C torsion	101m	97s	n.i.

NOTES: (a), IR, liquid, this work.
(b), IR, liquid, this work.
(c), IR&R, liquid, (79).

The first column under any one compound refers to the trans and the second to the gauche form of the n-propyl group.

Table XVI shows the infra-red spectra of $Sn(nPr)_3Cl$ $Sn(nPr)_4$ and nPrI (Sheppard, ref.79) together with the assignments, By comparison with nPrI, the four bands at 219(w), 277(w), 298(m) and 390(vs) cm^{-1} can be assigned as follows: The 219 and 277 cm^{-1} bands to the trans and gauche forms of the Sn-C-C bending vibration respectively, and the 298 and 390 bands to the corresponding C-C-C bending vibrations. The medium strength band at 101 cm^{-1} is clearly the counterpart of the 97 cm^{-1} band of $Sn(nPr)_4$ which was assigned to the $SnCH_2$-Et torsional vibration.

The remaining hydrocarbon modes can now be assigned on the basis of the trans and gauche forms of the n-propyl group, as shown in the table. For the CH_2 wagging mode there are only two bands (c.f. four in $Sn(nPr)_4$) in the expected region. These are assigned one each to the trans and gauche forms. Similarly there is only one band, at 1379 cm^{-1}, which can be assigned to the symmetric CH_3 deformation mode, but in this case only one band was also found in nPrI (at 1378 cm^{-1}). For the CH_2 rocking mode two pairs of bands are expected from the comparison with $Sn(nPr)_4$ and nPrI - one pair each for the $C_{(1)}H_2$ and $C_{(2)}H_2$ groups, but only three were found. Possibly the "missing" bands are either too weak (the counterparts of these bands in $Sn(nPr)_4$ are in fact weaker than the others) or are obscured by the presence of other bands, but to this extent the assignment must be regarded as tentative.

On the basis of C_{3v} symmetry at the tin atom, both the Sn-C stretching vibrations are infra-red active. Furthermore, as a result of the presence of both gauche and trans forms of the n-propyl groups, these should each split into two widely spaced bands. There were found, however, only three bands which could be assigned to these

vibrations, viz. the bands at 601(s), 554(m) and 518(m) cm^{-1}. If, by comparison with $Sn(nPr)_4$, the 601 and 518 bands are assigned respectively to the trans and gauche forms of the asymmetric Sn-Me^c stretching mode, that leaves the band at 554 cm^{-1} to be assigned to the trans form of the Sn-Me^c symmetric stretching. The gauche counterpart of this band is then either absent, or more likely coincident with the band at 518 cm^{-1}.

In the region of the low frequency bending vibrations there were found three bands - at 127, 131 and 152 cm^{-1} - which are to be assigned to the three bending modes at the tin atom. There is no indication of two forms in these vibrations and the assignment given in the table is suggested on comparison with $SnEt^t_3Cl$. This involves an increase of about 20 cm^{-1} for both forms of the Sn-Me^c_3 deformation frequencies on going from the ethyl to the propyl compound, due, perhaps, to an increased mutual repulsion between the propyl groups.

5.25: Conclusions.

It was previously thought that no appreciable coupling between the ethyl groups took place (section 4), but a satisfactory assignment of the spectrum of $SnEt_3Cl$ can only be made with the assumption that both the CH_2 rocking and wagging modes are split. In other respects the spectrum is similar to that of $SnEt_4$ and $SnMe_3Cl$.

As distinct from $SnEt_3Cl$, the high frequency spectrum of $Sn(nPr)_3Cl$ contains a smaller number of bands than the corresponding tetra-alkyl, and can be assigned on the assumption of the presence of both forms of the nPr group. That no splitting of the CH_2 rocking and wagging modes have been invoked does not necessarily indicate an absence of coupling; these modes are in any case split as a result of the presence of two CH_2 groups on the propyl chain, and the resulting complexity of the spectrum prevented any splitting being distinguished.

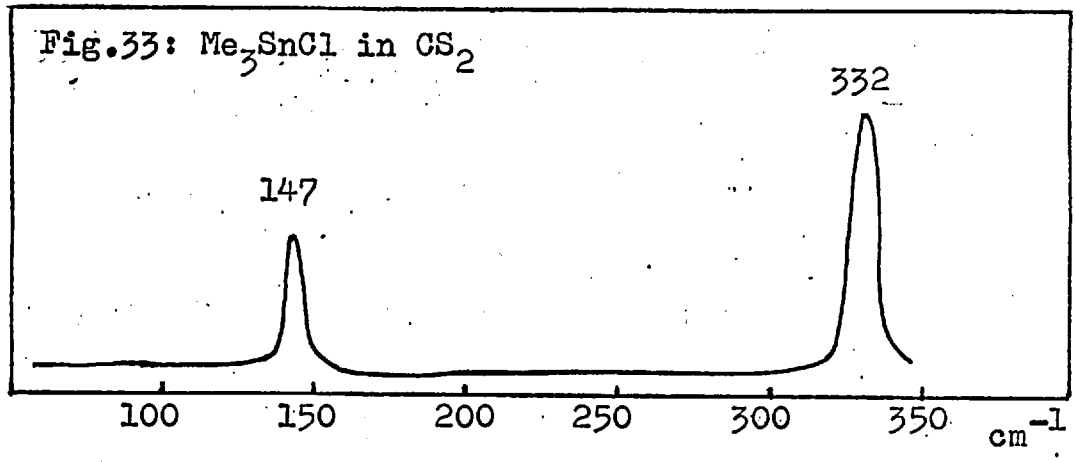


Fig.33: Me_3SnCl in CS_2

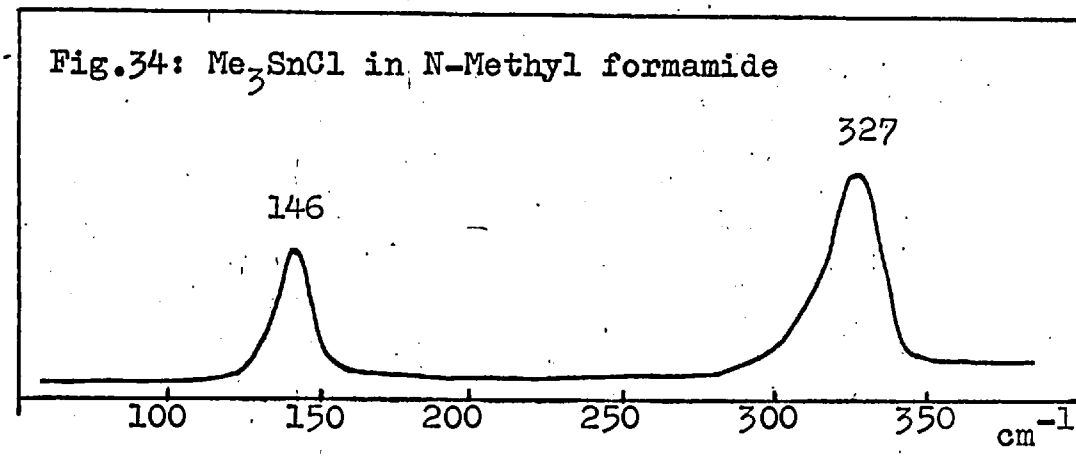


Fig.34: Me_3SnCl in N-Methyl formamide

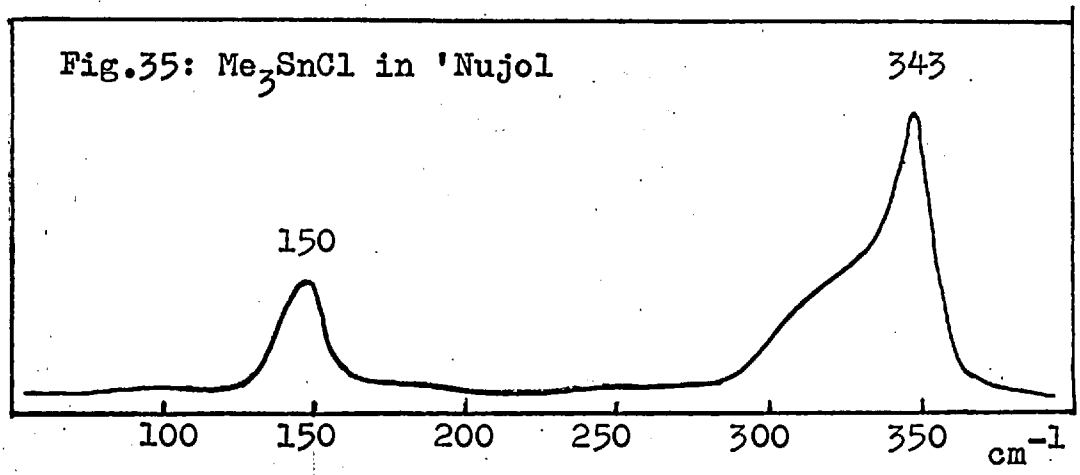
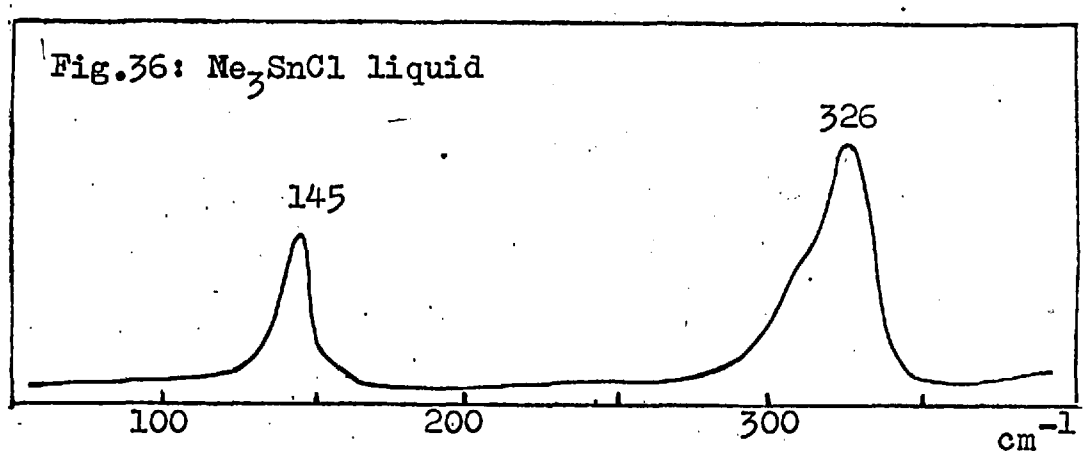
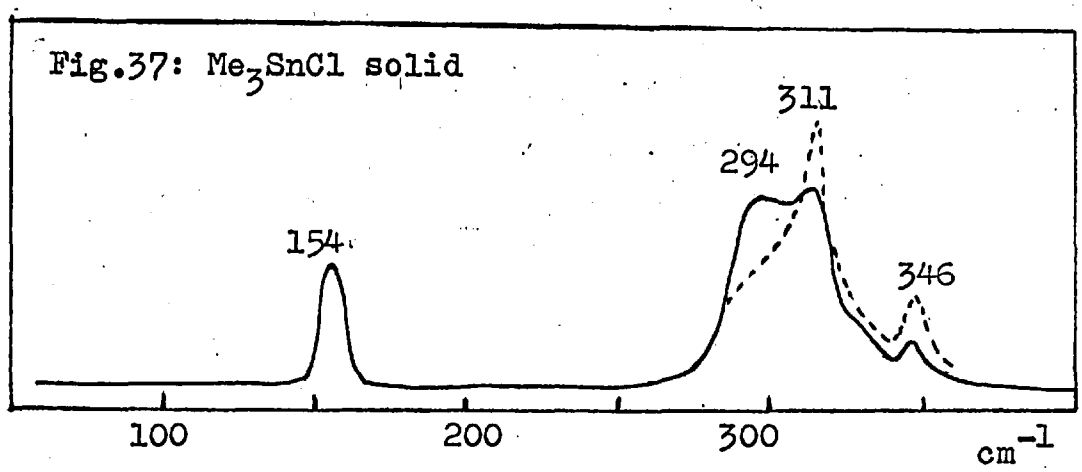
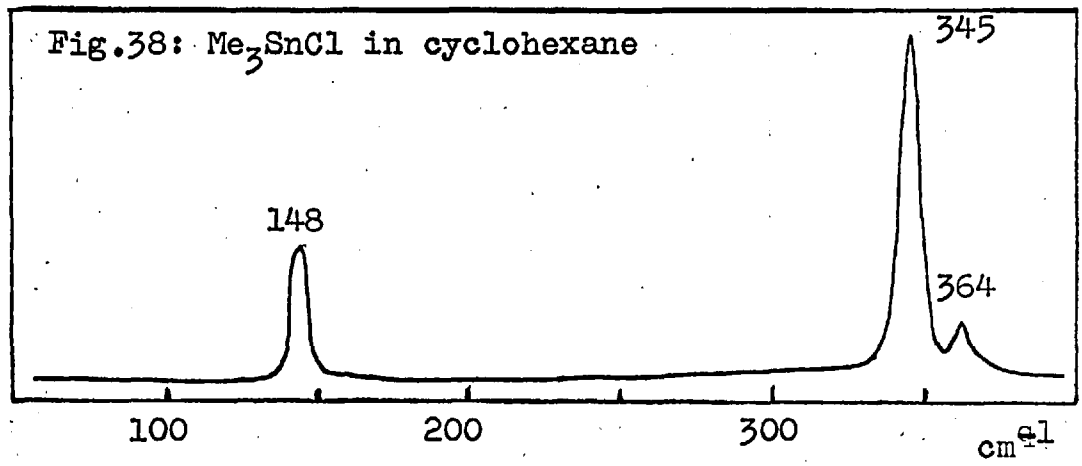


Fig.35: Me_3SnCl in 'Nujol


Fig.36: Me_3SnCl liquid
326
145
100
200
300
cm-1


Fig.37: Me_3SnCl solid
311
294
154
346
100
200
300
cm-1


Fig.38: Me_3SnCl in cyclohexane
345
148
364
100
200
300
cm-1

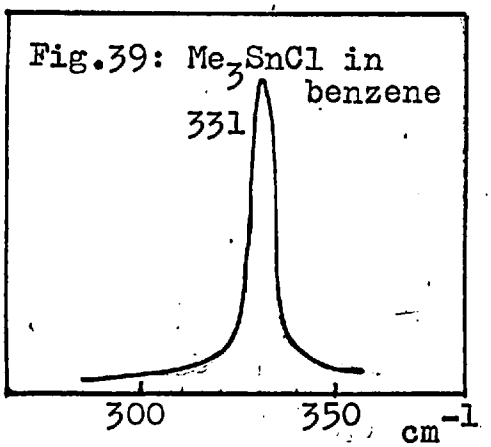


Fig.39: Me_3SnCl in benzene

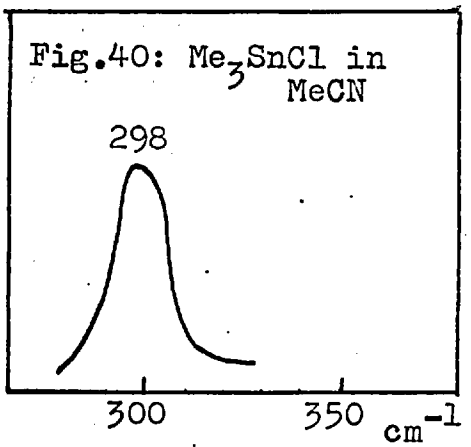


Fig.40: Me_3SnCl in MeCN

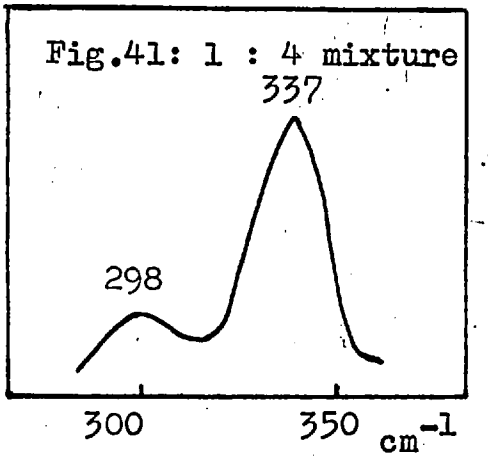


Fig.41: 1 : 4 mixture

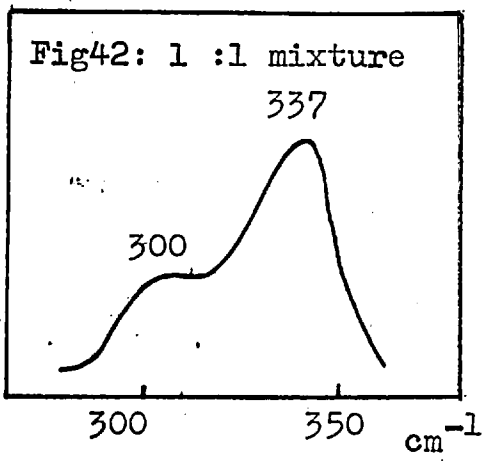


Fig42: 1 :1 mixture

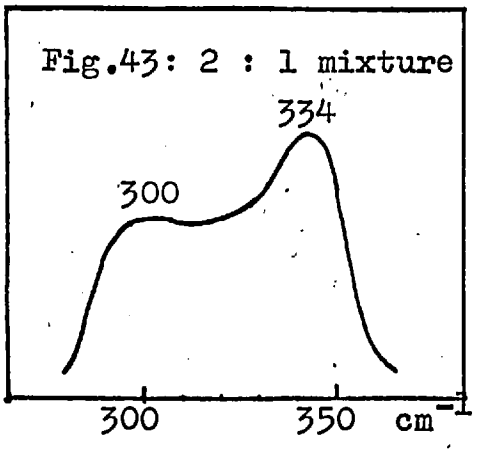


Fig.43: 2 : 1 mixture

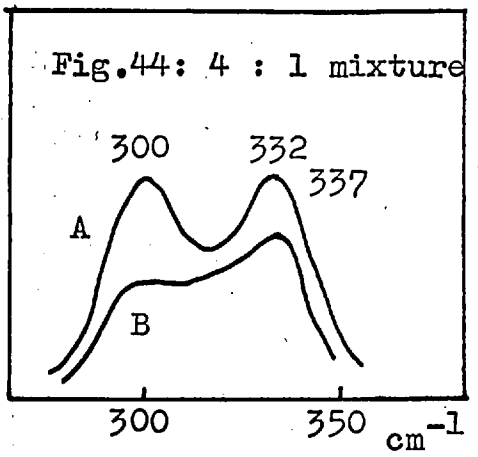


Fig.44: 4 : 1 mixture

In figs. 41-4, the ratio given refers to the composition of mixtures of MeCN and benzene, by volume.

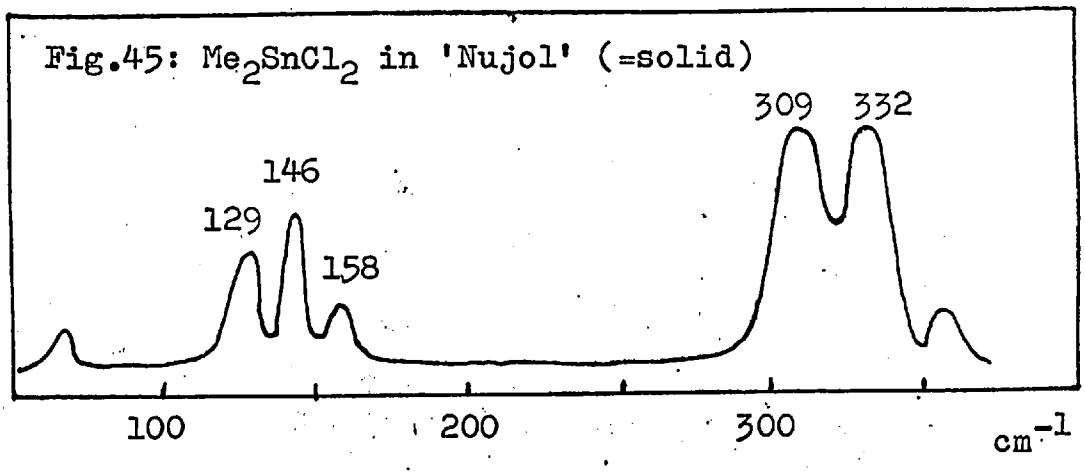


Fig.45: Me_2SnCl_2 in 'Nujol' (=solid)

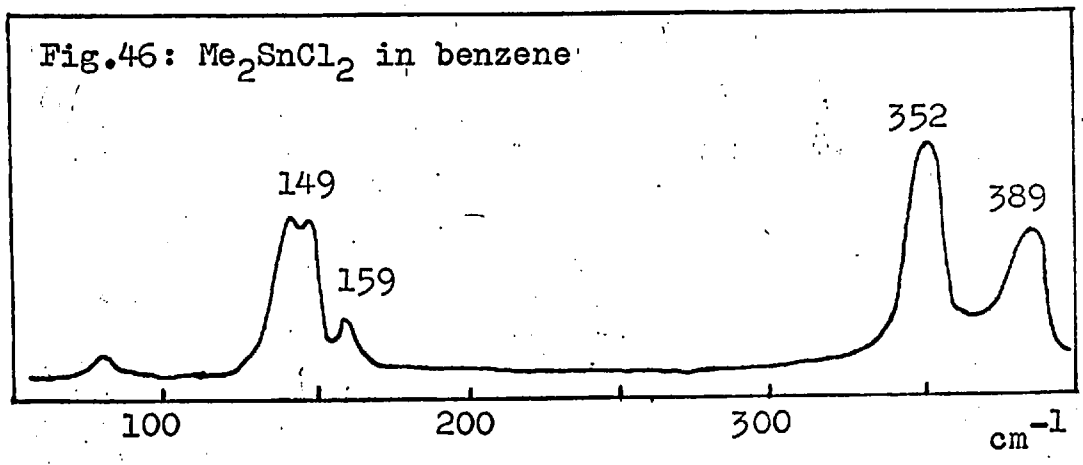


Fig.46: Me_2SnCl_2 in benzene

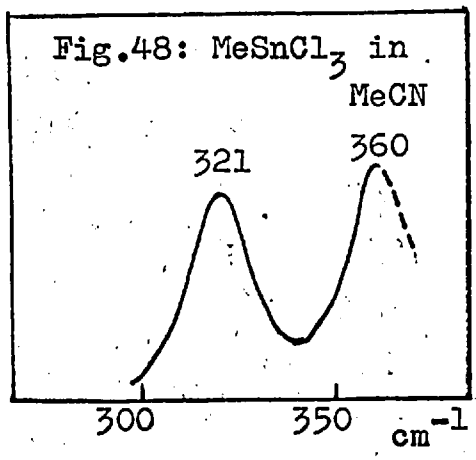


Fig.48: $MeSnCl_3$ in MeCN

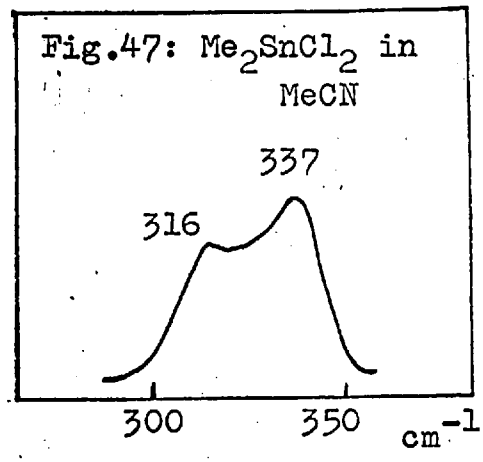


Fig.47: Me_2SnCl_2 in MeCN

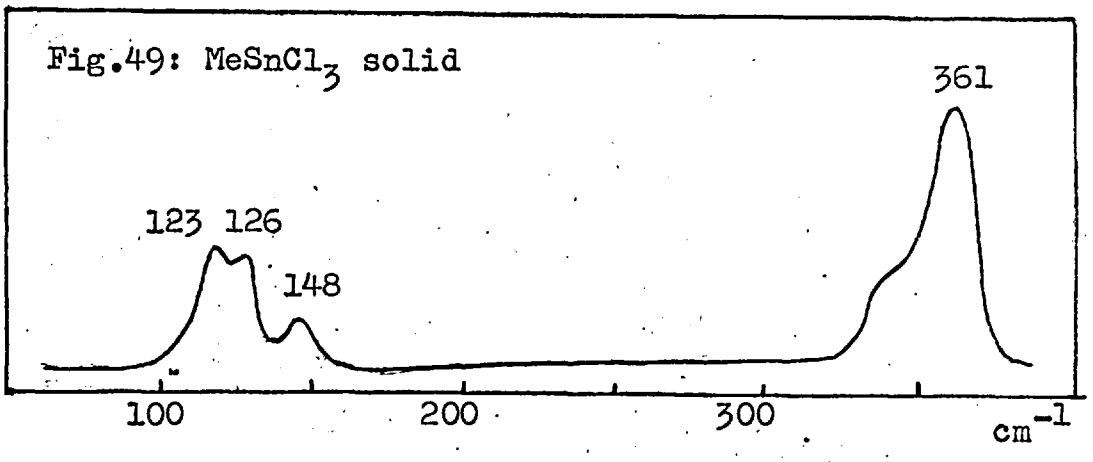


Fig.49: $MeSnCl_3$ solid

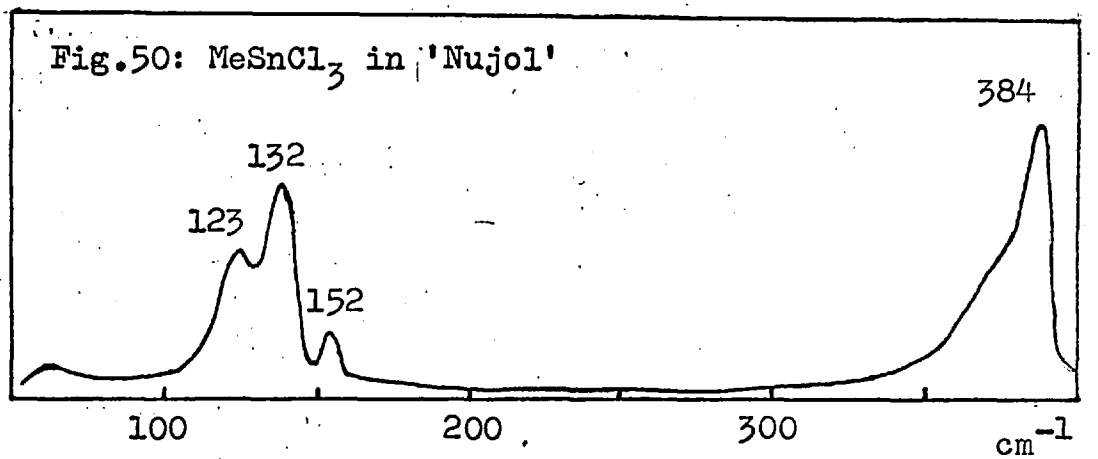


Fig.50: $MeSnCl_3$ in 'Nujol'

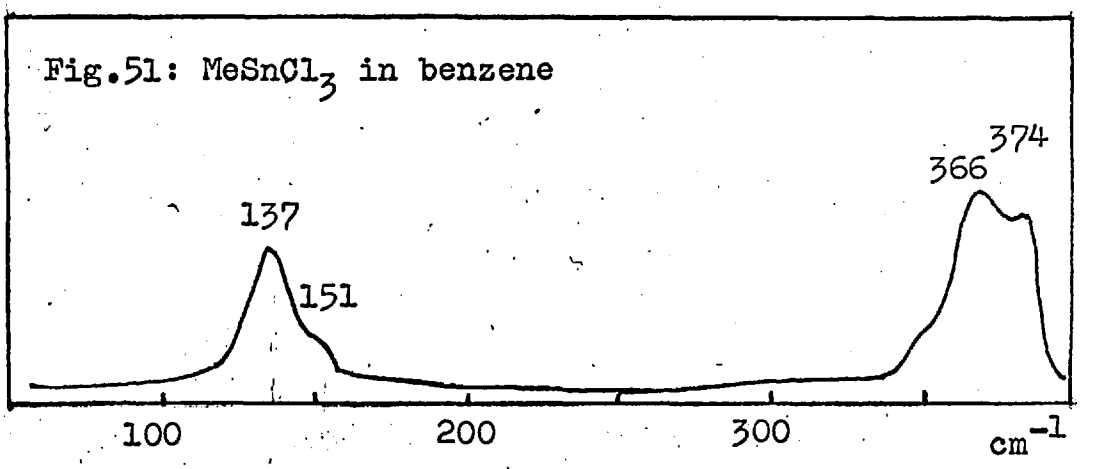
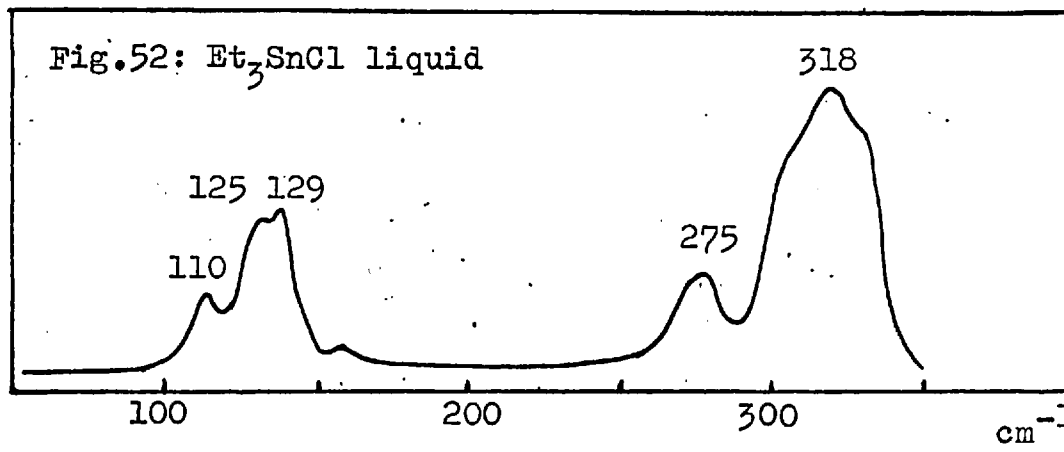
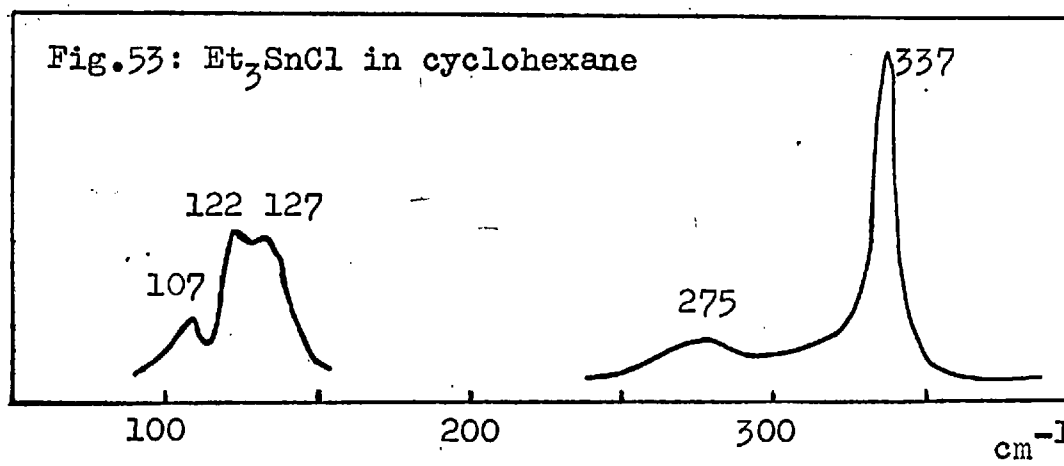
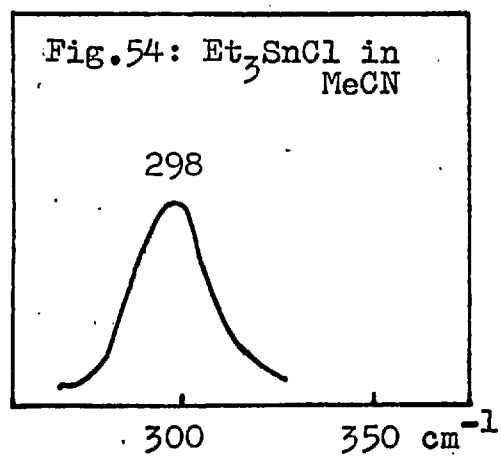
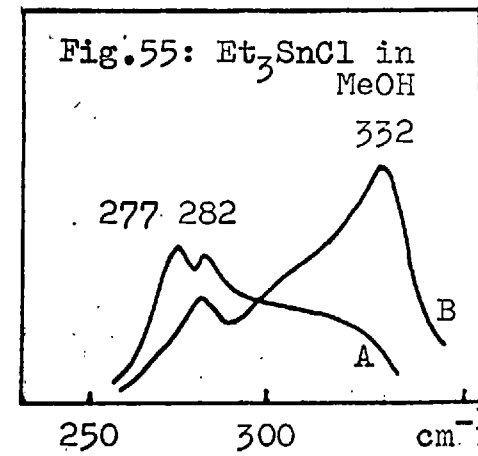


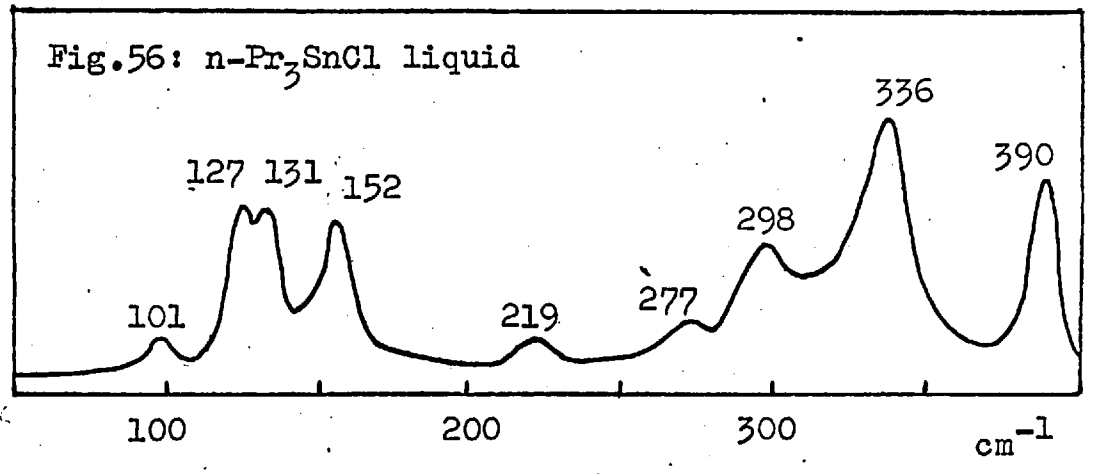
Fig.51: $MeSnCl_3$ in benzene

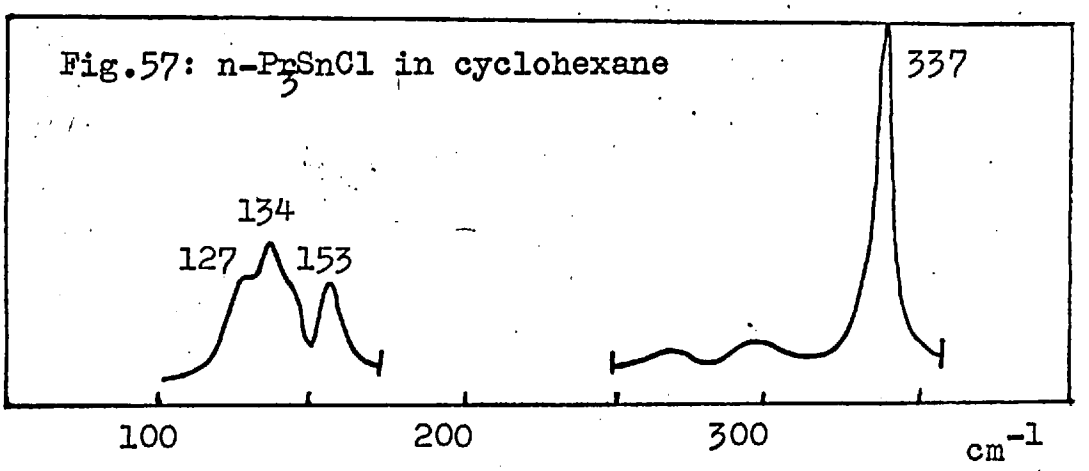

Fig.52: Et_3SnCl liquid
318
125 129
275
110
100
200
300
cm-1

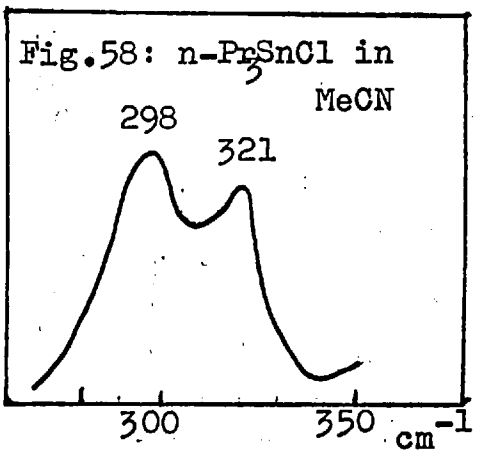

Fig.53: Et_3SnCl in cyclohexane
337
122 127
107
275
100
200
300
cm-1


Fig.54: Et_3SnCl in MeCN
298
300
350 cm-1


Fig.55: Et_3SnCl in MeOH
332
277 282
B
A
250
300
cm-1


Fig.56: n-Pr3SnCl liquid
336
390
127 131
152
298
101
219
277
100
200
300
cm-1


Fig.57: n-Pr3SnCl in cyclohexane
337
134
127
153
100
200
300
cm-1


Fig.58: n-Pr3SnCl in
MeCN
298
321
300
350
cm-1

6: ENVIRONMENTAL EFFECTS ON THE FAR INFRA-RED SPECTRA OF ALKYL TIN CHLORIDES.

6.1: Introduction.

General solvent effects on vibrational spectra have long been studied in the near infra-red but no general theoretical treatment of the results has proved entirely satisfactory. The expressions derived by Kirkwood (101) and Bauer and Magat (102) linking the fractional frequency shift with the dielectric constant or refractive index of the solvent is adequate in only a few cases, as is its extension by Buckingham (103). These theories fail because the solvent-solute interactions, giving rise to frequency shifts are extremely specific, depending upon the polarities and configurations of both molecules. As emphasised by Hallam (104), one of the major factors giving rise to the solvent shift is dipole association between solute and solvent.

Since the Sn-Cl bond is extremely polar in character, it is to be expected that the methyl tin chlorides at least would exhibit solvent effects in the far infra-red. The work of Kriegsmann and Pischtschan (93), and the work described in the previous section have shown that some solvent effects do in fact take place, and also that there are considerable differences in the Sn-Cl stretching frequencies in the liquid and solid states. For these reasons it was decided to study the far infra-red spectra of the alkyl tin chlorides dissolved in a number of different solvents.

6.2: Experimental.

The far infra-red spectra were recorded in the manner already described. The solutions were enclosed in polythene bags, but with volatile solvents some degree of evaporation occurred during the runs and care had to be taken to ensure that the solute did not crystallise out. For this reason it has not been possible to give more than a rough indication of the concentrations of the solutions. Unless otherwise stated, these were approximately of the order of 30 °/o or more. All the solvents excluding acetomitrile and methanol showed no more than broad continuous absorption over the spectral ranges investigated.

The far infra-red spectrum of liquid $SnMe_3Cl$ was obtained by filling the dewar finger of the sample cell with hot (65-70°C) water. The polythene bag containing a film of the sample was clamped to the 'finger' in the usual manner and there was sufficient thermal contact to ensure that the sample did not solidify during the recording. A small immersion heater was used to control the temperature of the water. The melting point of $SnMeCl_3$ is about 12° higher and it was not possible to obtain the spectrum of liquid $SnMeCl_3$ in this way.

The spectra of the solid state of both compounds were recorded by allowing the liquid films to cool and solidify. For reasons already discussed, the 'Nujol' mull spectrum of $SnMe_2Cl_2$ can be regarded as being equivalent to that of the solid.

Near infra-red spectra, where given, were recorded with a Grubb-Parsons "Spectromaster" grating spectrometer.

6.3: Results.

The far infra-red spectra are shown in figs. 33 to 58 and fully documented in the appendix. Further references to these, and to tables of frequencies are made in the discussion.

6.4: Discussion.

6.41: $SnMe_3Cl$.

This compound has only one sensitive Sn-Cl stretching fundamental which lies conveniently in the NaF reststrahlen region. Tables XVII and XIX give the frequencies observed in the liquid, solid and mull (= solution in 'Nujol'), and as solutions in benzene, cyclohexane, carbon disulphide, N-methyl formamide, acetonitrile, water and mixtures of benzene and acetonitrile. A solution in methanol showed no bands above 300 cm^{-1}, but at frequencies below this, absorption due to the Me-OH torsional vibration becomes appreciable and it was not possible to decide whether the Sn-Cl stretching band was present or not.

The results fall naturally into four categories as follows:

6.411: The dissociation of $SnMe_3Cl$.

Kriegsmann and Pischtschan (93) have shown that trimethyl tin fluoride forms an ionic lattice in the solid state, which indicates that the Me_3Sn-F bond is ionic in character. They also showed that $SnMe_3Cl$ is probably ionised in aqueous solution, insofar as no trace of the Sn-Cl stretching frequency could be found. If this were due to a simple ionisation process arising from the high dielectric constant of water (=80), the compound should

also be completely dissociated in a solvent having a higher dielectric constant than water. N-methyl formamide has one of the highest dielectric constants known (≒182 at 25°C) but the spectrum of $SnMe_3Cl$ in this solvent shows a strong, broad absorption at 327 cm^{-1} which is clearly due to the Sn-Cl stretching vibration. One concludes that the dissociative action of water on this compound is not due to its high dielectric constant but rather to specific solvation effects which help to stabilise the cation:

$$SnMe_3Cl + nH_2O = SnMe_3 \cdot (H_2O)_n^+ + Cl^-$$

This interpretation is supported by the results of Rochow and Seyferth (105) who found that in the case of $SnMe_2Cl_2$ in aqueous solution, electrolytic dissociation takes place:

$$SnMe_2Cl_2 + nH_2O = Me_2Sn \cdot (H_2O)_n^{++} + 2Cl^-$$

but that solutions in benzene, cyclohexane and other hydrocarbon solvents were non-conducting.

Similarly conductance measurements of $SnMe_2Cl_2$ and $SnMe_3Cl$ in N,N-dimethyl formamide by Thomas and Rochow (106) showed only residual conductivities which were attributed to the presence of small quantities of water as impurity.

The possibility that in aqueous solutions the corresponding hydroxide is formed has been discounted by Kriegsmann on the grounds that the pH of the solution was insufficiently acidic.

Methanol and ethanol would be expected to exhibit similar solvating properties to water. The far infra-red spectrum of $SnMe_3Cl$ in methanol was not conclusive, but conductivity measurements on this substance in ethanol, by Kraus and Callis (107), yielded a value of 30.8 for the equivalent

conductivity at infinite dilution, suggesting that some ions are in fact present.

6.412: General solvent effects in $SnMe_3Cl$.

If the spectrum of the solution in cyclohexane is taken as the nearest approximation to the gas phase frequencies, then the fractional frequency shift $\Delta\nu/\nu$ can be calculated for each solvent. These range from 3×10^{-3} in 'Nujol' to 52×10^{-3} in N-methyl formamide and 140×10^{-3} in acetonitrile. (table XVII). The latter is clearly at variance with the trend of the rest of the series, and according to the table given by Hallam (104) to illustrate solvent patterns for solute dipoles, acetonitrile would be expected to give a frequency lowering less than that due to N-methyl formamide. Moreover, the values of $\Delta\nu/\nu$ obtained with the other solvents are of the same order of magnitude as those found for the stretching frequencies of other highly polar bonds occurring in the near infra-red region (104). It would thus seem probable that the shifts in the other aprotic solvents are caused by the normal dipole-dipole associations in which there is usually found a progressive lowering in frequency accompanied by a corresponding broadening of the band as the solvent-solute interaction increases. (c.f. for example the behaviour of the N-H stretching frequency of pyrrole dissolved in various solvents, ref.108). The behaviour of the Sn-Cl stretching frequency in $SnMe_3Cl$ follows this general pattern except in acetonitrile solution, where it seems probable that a more specific interaction or complexing occurs (see later).

TABLE XVII

SOLVENT EFFECTS ON THE Sn-Cl STRETCHING BAND IN $SnMe_3Cl$

STATE	FREQUENCY	$\frac{\Delta\nu}{\nu} \times 10^2$	DIEL. CONST.
Solution in cyclohexane	345 cm^{-1}	0	2
Solution in 'Nujol'	344	0.3	2
Solution in CS_2	332	3.8	2.6
Solution in benzene	331	4.0	2.3
Solution in N-Me formamide	327	5.2	182(25°c)
Liquid	325	5.8	-
Solid { Glass	311	9.6	-
Solid { Crystal	294	15	-
Solution in acetonitrile	298	14	37(25°c)
Solution in water	absent	-	80

6.413: Frequency shifts in liquid and solid $SnMe_3Cl$.

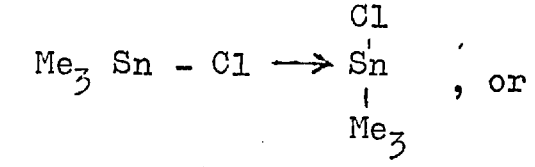
These frequency shifts are similarly indicative of some form of association between the molecules. The Sn-Cl stretching frequencies of the solid, liquid and solution in cyclohexane, together with the Raman data of Edgell and Ward (92) and Kriegsmann and Pischtschan (93), are shown in table XVIII.

TABLE XVIII

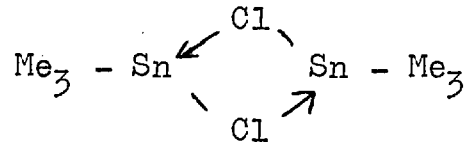
FREQUENCY SHIFTS IN SOLID AND LIQUID $SnMe_3Cl$.

STATE	IR soln.	IR (92) liq.	R (92) liq.	IR solid	R(93) solid
"free"	345	-	-	346	
glass/liquid	-	325	318	311	
crystal	-	-	-	294	288

Kriegsmann and Pischtschan have suggested that these shifts are due to chlorine bridging:



, or



This being so, it is not unreasonable to expect that the degree or strength of the bridging is dependent on the state of the substance, being stronger in the solid than in the liquid. The far infra-red spectrum of solid $SnMe_3Cl$

is shown in fig.37 , showing that the Sn-Cl stretching region has rather an unusual shape, with three distinct peaks. The dotted curve shows the band shape observed with a different sample. These samples were prepared by cooling a film of the liquid contained in polythene bags, and had a transparent, glassy appearance at times. Therefore it is presumed that the different band contours observed for the two samples are due to the presence of differing proportions of glassy and genuinely crystalline solid, giving rise to Sn-Cl stretching frequencies corresponding to the different degrees of bridging in each. The band at 346 cm^{-1} would then correspond to a free, unbridged Sn-Cl stretching.

If the bridging is at all analogous to hydrogen bonding, there might be expected a slight rise in the bending frequencies involving the bridged chlorine atoms. These are given in table XIX together with the data of other workers where available. Due to the uncertainties in the positions of the band centres ($\pm$ 1-2 cm^{-1}), the only clear indication of a frequency increase was, in fact, observed in the solid.

If the frequency shifts were caused by some kind of interaction with the methyl groups, then there would be expected corresponding shifts in the $SnMe_3$ stretching as well as in the hydrocarbon frequencies. Table XX gives the high frequency spectra of the liquid, solid and solution in CS_2, together with data for the solution in acetonitrile. From the comparison it can be seen that the differences are comparatively slight.

TABLE XIX

SOLVENT EFFECTS ON THE BENDING FREQUENCIES

$SnMe_3Cl$

STATE	IR	R(93)
Solution in cyclohexane	148 cm^{-1}	-
Solution in 'Nujol'	151	-
Solution in CS_2	147	146
Soln. in N-methyl formamide	146	-
Liquid	145	145 (Edgell, 150)
Solid	154	-
Solution in MeCN	not observable.	-
Solution in water		152

TABLE XX

SOLVENT EFFECTS ON THE HIGH FREQUENCY FUNDAMENTALS

DESCRIPTION	IR[a] Liquid	R[b] Solid	IR[c] CS_2	IR[d] MeCN
C-H a.s.str.	3002s	2994	2997m	-
C-H s.str.	2925s	2914	2920m	-
CH_3 a.s.d.	1400s	weak	1400m	1405m
CH_3 s.d.	1193s	1197	1192m	1191m
CH_3 rock.	787vvs broad	weak	785vs 725m	784vvs sharp.
Sn-Me a.s.str.	545s	546	543vs	547vs
Sn-Me s. str.	514s	513	514m	514s

NOTES: a, Edgell & Ward, (92)
b, Kriegsmann & Pischtschan, (93).
c, " " (93), solution
d, This work, solution.

6.414: The association of $SnMe_3Cl$ with MeCN.

In order to determine whether the considerable shift of the Sn-Cl stretching frequency in MeCN solution is due in fact to a specific association or complexing between the solvent and solute, the far infra-red spectra of $SnMe_3Cl$ dissolved in mixtures of MeCN and benzene were recorded. The results are shown in figs.39-44 . The solution in the 1;2 mixture (by volume) contained approximately 50 °/o of $SnMe_3Cl$ which was progressively diluted by additions of MeCN to obtain the 1:1, 2:1 and 4:1 proportions. The curve A of fig.44 was obtained on the addition of more $SnMe_3Cl$ to the 4:1 solvent.

These results show that there are two distinct species present in the mixed solution and that the addition of more MeCN to the mixture causes the intensity of the lower frequency band, which corresponds to the band observed in pure MeCN solution, to increase. Slight variations in the position of the higher frequency band were observed and the band itself was about 5 cm^{-1} higher in frequency than was found in pure benzene solution. This could be due to a concentration effect; when the concentration of the solution was increased to obtain curve A, the band shifted from 337 down to 332 cm^{-1}, the value in pure benzene.

There remains the question of the nature of the interaction between $SnMe_3Cl$ and MeCN. As it would seem probable that the association involves the CN group, there would be expected some changes in the CN stretching frequency on going from the free nitrile to the solution. In pure MeCN, in addition to the CN stretching band at 2253 cm^{-1}, there is a combination band at 2295 cm^{-1}, and their intensities are roughly in the ratio 10:9. In a very highly

concentrated solution of $SnMe_3Cl$ in MeCN (a few drops of MeCN added to the solid) , these two bands were observed at 2261 and 2295 cm^{-1} with their intensities in the ratio 2:1. There occurs then a positive shift of 8 cm^{-1} and a change in the relative intensities (assuming that the intensity of the combination band - CC str. + CH_3 sym. def. - remains unchanged).

Terenin et al (109) and Brune and Zeil (110) have studied the spectra of addition complexes formed between metal halides and nitriles. In some cases solid complexes could be isolated from mixtures of MeCN and $SnCl_4$ in which increases of 40-65 cm^{-1} in the CN stretching frequency were observed. Brune and Zeil interprete this as being due to co-ordination of the CN group with the tin atom, while the frequency increase may be attributed to the fact that the 'lone pair' of electrons on the N, which have an anti-bonding effect on the CN bond, are donated to the Sn, resulting in an increase in the strength of this bond in the complex.

It would seem probable, then, that a similar mechanism operates in the association between $SnMe_3Cl$ and MeCN , with the difference that whereas in the stable $SnCl_4$ complex the co-ordination is predominantly covalent in the sense that the orbital configuration around the Sn closely approaches d_2sp_3 hybridisation, in the $SnMe_3Cl$ the basic sp_3 hybridisation of the Sn is perturbed only slightly. Thus the highly covalent Sn-C bonds remain undisturbed, as is shown by the near-invariance of the Sn-C stretching frequencies (see table XX), but the highly polar Sn-Cl bond is strongly influenced by the lone pair from the CN group, leading to the observed decrease in the corresponding stretching frequency. Unfortunately due to the absorption

of MeCN around 140 cm^{-1}, it was not possible to observe the bending frequencies of $SnMe_3Cl$ in this solvent.

Table XX gives the higher frequencies of the MeCN solution. It was found that the methyl rocking mode gave a comparatively sharp band in MeCn, but the 725 cm^{-1} band observed in CS_2 solution had disappeared. This band had been ascribed to a splitting of the rocking mode, so the spectrum seems to indicate that in MeCn solution there is no apparent coupling between the Me groups.

6.42: $SnEt_3Cl$ and $Sn(nPr)_3Cl$.

The spectra of both compounds were recorded in cyclohexane and MeCN (NaF region only). These are shown in figs.53,54,57,58. Table XXI gives the frequencies in cyclohexane together with the values for the pure liquids. The mixtures consisted of approximately 1 part of the tin compound to 3 parts of cyclohexane, but had to be greatly diluted to obtain optimum absorption for the very sharp Sn-Cl bands.

TABLE XXI

$SnEt_3Cl$	
LIQUID	C'HEX.
-	-
318vs	337vvs
-	-
275m	275w
-	-
129s	127s
110m	107m
125s	122s
-	-

$Sn(nPr)_3Cl$	
LIQUID	C'HEX.
390vs	n.i.
336vs	337vvs
298m	298w
277w	277w
219w	n.i.
152s	153s
131vs	134vs
127vs	127s
101m	n.i.

It can be seen that there must also exist in liquid $SnEt_3Cl$ some degree of chlorine bridging to give rise to the observed frequency lowering of 19 cm^{-1}. In $Sn(nPr)_3Cl$ however, there is very little difference between the spectra in cyclohexane solution and the pure liquid. Presumably the bridging effect is hindered by the presence of long n-propyl groups. In both cases the solvent has the effect of sharpening considerably the Sn-Cl stretching bands.

Turning now to the spectra in MeCN (figs.54,58), there is in both compounds a pronounced band at 298 cm^{-1} which is evidently the Sn-Cl stretching mode lowered in frequency through the interactions already described for $SnMe_3Cl$. The almost equally pronounced band at 321 in $Sn(nPr)_3Cl$ + MeCN would then be due to a residual uncomplexed species. This band is absent in a mixture of $SnEt_3Cl$ and MeCN, indicating that probably all the $SnEt_3Cl$ is complexed. It would seem that again the long n-propyl groups are hindering the formation of the complex; one would then expect that in $Sn(nBu)_3Cl$ for example, only very little complexing takes place.

The spectra shown in figs.55 are of mixtures of $SnEt_3Cl$ and methanol in the ratios 1:3 (curve A) and 15:3 (curve B), by volume. Again due to the absorption of MeOH itself near 280 cm^{-1}, it is difficult to draw any definite conclusions from spectrum A, but curve B, where there is a large excess of $SnEt_3Cl$, would seem to indicate that the chlorine bridging in liquid $SnEt_3Cl$ is disrupted by the addition of small amounts of solvent, since 332 cm^{-1} band is only 5 cm^{-1} lower than the frequency in cyclohexane. If the fact that MeOH has a fairly large dielectric constant (= 33) is significant, then one could conclude that the bridging is predominantly electrostatic or ionic in character.

6.43: $SnMe_2Cl_2$ and $SnMeCl_3$.

The far infra-red spectra of these compounds in benzene solution, in the solid state and in acetonitrile are shown in figs.45-51, pp 118-9, and are given in tables XXII and XXIII together with the Raman data of Edgell and Ward for the liquid state (92).

The presence of two Sn-Cl stretching frequencies complicates the interpretation of environmental effects in these compounds, but in general the causative mechanisms would not be expected to differ from those for $SnMe_3Cl$. The spectra do in fact show considerable differences between these frequencies on going from benzene solution to liquid to solid. In $SnMeCl_3$ the shift from benzene to solid is only about 20 cm^{-1}, and the average liquid frequency only a little higher than in the solid.

In $SnMe_2Cl_2$ however, the corresponding shift is 57 and 43 for the asymmetric and symmetric modes respectively, while the liquid value lies more nearly in between the solid and solution values. One concludes that the bridging is stronger in the dichloride, possibly because the symmetry of this molecule favours the formation of an extensive intermolecular network of bridges. This would explain the fact that the melting point of this compound is about 50°C higher than those of the other members of the series and that it is reatively insoluble in hydrocarbon solvents but extremely soluble in highly polar solvents.

It is also possible that the presence of the Me groups actually favours the bridging process in that they allow the two molecules to approach to a distance where bridging becomes possible. In $SnCl_4$ on the other hand,

TABLE XXII: SOLVENT EFFECTS, $SnMeCl_3$

R(92) Liquid	IR Solid	IR Benzene soln.	IR MeCN soln.
363	361vs 343m,shl.	384vs 368vs,shl.	360vs ? 321m
142	148m 126s	151m,shld	
112	123s	137s	n.i.

TABLE XXIII: SOLVENT EFFECTS, $SnMe_2Cl_2$

R(92) Liquid	IR Solid (mull)	IR Benzene soln.	IR MeCN soln.
344	332vs 309vs	389s 352 vs	337s 316s
135	158m 146s 129s	159m 148s	n.i.

the mutual repulsion of the electonegative Cl atoms of different molecules acts as a barrier to bridging. This results in $SnCl_4$ being a liquid boiling near 100°C while the others are solids at room temperature.

By analogy with $SnMe_3Cl$, there would be expected a similar type of association or complexing between these compounds and MeCN. The frequency shift in the Sn-Cl stretching frequencies is of the same order and a similar slight increase of 5-8 cm^{-1} was observed in the CN stretching frequencies for highly concentrated solutions.

6.5: Conclusions.

The absence of a band corresponding to the Sn-Cl stretching frequency in water solution confirms a similar observation in the Raman spectrum by Kriegsmann (93) and indicates that $SnMe_3Cl$ is ionised in water. That this is due to the solvating power of water and not to its dielectric constant is shown by the spectrum of the solution in N-Me formamide.

The considerable differences between the spectra of the solid , liquid and solutions are attributed to chlorine bridging between the molecules.

In acetonitrile solution a distinct complex is formed between solvent and solute molecules, probably as a result of incipient co-ordination of the CN group with the Sn.

The Sn-Cl band in $SnMe_3Cl$ and probably in the other compounds too is highly sensitive to solvent effects which follow the pattern found in the near infra-red for dipole-dipole systems.

APPENDIX

In the following tables the experimental data obtained with the far infra-red spectrometer are listed for each compound investigated.

The first column gives the reference number of each chart or 'run', and the second the frequency range covered.

The third column indicates the filters used. Only the restsstrahlen reflectors used are given since in all cases the other filters consisted of the KBr chopper and one sheet of 500 gauge black polythene.

In the fourth column are given the bands observed, if any, and the last column is reserved for comments.

The abbreviations used in the tables are as follows: BG denotes background, i.e. one used for the calculation of the intensity ratios which might, in fact be either a thick , medium, or thin sample. If no bands are observed, the column is left blank.

S denotes small or thin sample
M denotes medium sample
L denotes large or thick sample.

In many cases the resulting ratio plot was confusing, due mostly to interference effects which prevented any definite conclusions being drawn as to the presence or otherwise of a band. Similarly, in many cases the thickness of sample used was either too thick or too small for the bands to show up clearly: the runs were then repeated under different conditions.

TETRAETHYL TIN, $SnEt_4$.

Run no.	Recorded ν range cm^{-1}	R'strahlen filters	Bands observed cm^{-1}	Comments
132	520-200	1 LiF	BG	
133	"	"	506(2nd order)	Room temp.
134	"	"	500 "	frozen, app.
			520 "	100°K.
91	380-230	1 NaF	273 s	
92	"	"	BG	
226	"	2 NaF	BG	
227	"	"	BG S	
228	"	"	L	Poor run
232	"	"	273	L
233	"	"	BG	
77	300-170	1 NaCl		water present
80	"	"		" "
89	"	"		L, poor run
90	"	"	BG	
135	"	"	275 s	L
136	"	"	BG	
93	230-150	1 KCl	BG	200 1 grat.
94	"	"		L "
97	200-130	"	BG	80 1 grat,
98	"	"	135, 126 m	L "
74	190-90	1 KBr		L, water present
75	"	"	BG	
78	"	"		M, confused
79	"	"		L, "
83	"	"		S, too small
95	"	"		L, interf.
96	"	"	BG	

TETRAETHYL TIN (continued).

Run no.	Recorded ν range cm^{-1}	R'strahlen filters.	Bands observed cm^{-1}	Comments
229	190-90	1KBr	BG	
230	"	"	126 m	S
231	"	"	127 m	L
236	150-55	CsI+KRS-5	86 vw	L
237	"	"	BG	S
242	150-60	2 KRS-5	BG	S
243		"	86 w	L
244		"	86 w	L

TETRAETHYL LEAD, $PbEt_4$

Run no.	Recorded ν range cm^{-1}	R'strahlen filters	Bands observed cm^{-1}	Comments
160	520-200	1 LiF	BG	
161	"	"	450(2nd order)	L; 100°K
171	"	"	474 "	L, too thick
172	"	"	440(2nd order) 470 "	L, room temp.
156	350-220	1 $CaCO_3$	BG	
157	"	"		L, poor run
162	300-170	1 NaCl		L, too thick
163	"	"	BG	
170	"	"	245 vs, 220 m	M, 100° K some interf.

TETRAETHYL LEAD (continued)

Run no.	Recorded v range cm^{-1}	R'strahlen filters	Bands observed cm^{-1}	Comments
265	300-170	1 NaCl	240 vs	L
266	"	"	240 vs, broad	M
267	"	"	BG	S
154	200-130	1 KCl		M, 80 grat. confused
155	"	"	BG	S, 80 grat.
158	"	"		M, 200 gr.
159	"	"	BG	"
153	170-90	1KBr	122 w	M
164	"	"	122 m	L
165	"	"	BG	
167	"	"		M confused
168	"	"	BG	
169	"	"		M, interference
229	"	"	BG	
230	"	"		S
231	"	"		L
268	"	"	121 m	S
269	"	"		M, interf.
273	"	"	120 s	L
274	"	"		S
153	150-60	2 CsI		S not good
166		"		L "
183	150-55	CsI+KRS-5	BG	
184	"	"	86 w	M
185	"	"	86 m	L

TETRA n-PROPYL TIN, $Sn(nPr)_4$

Run no.	Recorded v range cm^{-1}	R'strahlen filters	Bands observed cm^{-1}	Comments
121	520-200	1 LiF	BG	
122	"	"	504s, 390vs (2nd order) 294 vs	M
131	"	"	294 s	M
132	"	"	BG	
124	350-220	1 $CaCO_3$	294 s	M
125	"	"	BG	
285	380-230	2NaF	BG	S
288	"	"	294 vs	M
123	300-170	1 NaCl	294s, 224m	M
126	"	"	BG	
286	"	"		S, too small
287	"	"	294s, 225m	L
127	230-150	1 KCl	BG	200 gr.
128	"	"		M, interf.
332	200-130	"	BG	80 gr.
333	"	"		poor run
334	230-150	"	225 m	L
335	"	"	BG	S
148	170-90	1 KBr		M, confused
151	"	"	BG	
280	"	"	128 m	M
281	"	"	128 m	L
284	"	"		M not plotted
282	150-55	CsI+KRS-5	127s, 97s	L
283	"	"	BG	S

TRIMETHYL TIN MONOCHLORIDE, $SnMe_3Cl$, in 'Nujol'.

Run no.	Recorded v range cm^{-1}	R'strahlen filters	Bands observed cm^{-1}	Comments
388	380-230	2 NaF	BG	S
389	"	"		L, too thick
392	"	"	343vs, 316m shldr	L
505	"	"	BG	
506	"	"	344vs	50°C
507	"	"	344vs	rm.temp.
386	300-170	1 NaCl	BG	S
391	300-170	1 NaCl		L
387	230-150	1 KCl	BG	S, 200 grat.
390	"	"	153 s	L "
405	200-130	"	151 s	L, 80 grat.
406		"	BG	S "
403	170-90	1 KBr	BG	S
404	"	"	149 s	
399	159-55	CsI+KRS-5		L
400	"	"	BG	S
401	"	"		L
402	"	"		M

TRIMETHYL TIN MONOCHLORIDE, liquid, at 60°C

Run no.	Recorded v range cm^{-1}	R'strahlen filters	Bands observed $c\ m^{-1}$	Comments
504	380-230	2 NaF	BG	
503	"	"	331s, 316s	L, solid present
509	"	"		L, confused
594	"	"	326vs	L, good run
619	"	"	326 s	M
620	"	"	BG	S
582	170-90	1 KBr	BG	S
583	"		145s sharp	L
584	"			M

TRIMETHYL TIN MONOCHLORIDE, solid, at room temp.

588	380-230	2 NaF	BG	S
589	"	"	346w,311s,294s	L
590	"	"	346m,311vs,294m (shldr)	L, difft. sample
585	170-90	1 KBr		M, too small
586	"	"	BG	S
587	"	"	154 s, sharp	L

TRIMETHYL TIN MONOCHLORIDE, solution in benzene (approx 30 %)

591	380-230	2 NaF	331 vvs	L
592	"	"	331 vvs	M
593	"	"	BG	S

TRIMETHYL TIN MONOCHLORIDE, solution in N-methyl formamide,(app. 30 °/o).

Run no.	Recorded v range cm^{-1}	R'strahlen filters	Bands observed cm^{-1}	Comments
788	380-230	2NaF		NMF, S
789	"	"		NMF, L
792	"	"		NMF, v.L
790	"	"	327 vs	L
791	"	"	BG	S
781	170-90	1 KBr		NMF, S
782	"	"		NMF, L
787	"	"		NMF, v.L
783	"	"		too thick
784	"	"	146 s	M
785	"	"	146 s	M, v conc soln
786	"	"	BG	S

TRIMETHYL TIN MONOCHLORIDE, solution in acetonitrile (conc., 30°/o +)

793	380-230	2 NaF		MeCN,S
794	"	"		L, too thick
796	"	"	298vs,311s	M, solid present
796	"	"	BG	S
797a	"	"		MeCN, L
797b	"	"		dild. soln. L
797c	"	"	298 vs	" M

TRIMETHYL TIN MONOCHLORIDE, solutions in acetonitrile and benzene mixtures.

Run no.	Recorded v range cm^{-1}	R'strahlen filters	Bands observed cm^{-1}	Comments
	a) MeCN:Benzene = 1 : 2 by vol.			
838	380-230	2 NaF		M, poor run
839	"	"	344vs,298w	M
840	"	"	BG	S
841	"	"		M, evapor^{d}
842	"	"	337vs,300 m	M
843	"	"	340vs,298m	S
844	"	"	BG	benzene
	b) MeCN:Benzene = 1 : 1 by vol.			
845	380-230	2 NaF	337vs,300m shldr	L
846	"	"	344vs, 300m "	S
	c) MeCN:Benzene = 2 : 1 by vol.			
847	380-230	2 NaF		too thick
848	"	"	344vs,300s	M
849	"	"	BG	S
	d) MeCN:Benzene = 4 : 1 by vol.			
850	380-230	2 NaF	337vs,301s	M
851	"	"	332vs,300vs	L,more cpd.added
852	"	"	BG	S

TRIMETHYL TIN MONOCHLORIDE, solution in cyclohexane.

Run no.	Recorded ν range cm^{-1}	R'strahlen filters	Bands observed cm^{-1}	Comments
857	380-230	2 NaF		C_6H_{12},L
858	"	"	BG	" ,S
853	"	"		L, too conc.
854	"	"		too thick
855	"	"	345vvs,364m	soln diluted
856	"	"	345vvs,364m	diluted more
951	160-90	1 KBr		C_6H_{12},L
952	"	"	BG	S
953	"	"	148s, sharp	M

TRIMETHYL TIN MONOCHLORIDE, solution in carbon disulphide.

956	380-230	2 NaF		CS_2,S
957	"	"	332 vvs	L
958	"	"	332 vvs	M
954	150-90	1KBR	BG	CS_2, S
955	"	"	147 s, sharp	M
		"		

TRIMETHYL TIN MONOCHLORIDE, solution in methanol (approx. 30-40°/o)

826	380-230	2 NaF	277s,327m	MeOH, L
827	"	"	277s,327m	S
828	"	"		MeOH, S
832	"	"	257,277,327	L.MeOH absorbs
834	160-90	1 KBr	BG	S inconclusive
835	"	"		L "
836	"	"		M "
837	"	"		v.L "

TRIMETHYL TIN MONOCHLORIDE, solution in water, (approx. 40% o)

Run no.	Recorded v range cm^{-1}	R'strahlen filters	Bands observed	Comments
814	380-230	2 NaF		L, too thick
815	"	"		H_2O,S
816	"	"		" L
817	"	"	BG	S
818	"	"	none	M,
819	"	"	none	L
820	"	"	none	L
810	160-90	1 KBr		H_2O, L
811	"	"		L
812	"	"	no	L
813	"	"	bands	L
821	"	"	observed	L
822	"	"		M
823	"	"	BG	S
824	"	"		L,conc HCl soln

DIMETHYL TIN DICHLORIDE, mull with 'Nujol',
(mainly solid)

Run no.	Recorded v range cm^{-1}	R'strahlen filters	Bands observed cm^{-1}	Comments
409	380-230	2 NaF	BG	S
410	"	"	307vs,332vs,358w	M
411	"	"	307vs,332vs	L
439	"	"	BG	S
440	"	"	310vs,332vs,358m	L
412	300-170	1 NaCl	BG	S
413	"	"		L
414	"	"		M
416	230-150	1 KCl	158s	L, 200 grat.
417	"	"	BG	S, "
407	200-130	"	BG	S, 80 grat.
408	"	"	132s,146s,158m	L "
418	160-90	1 KBr	BG	S
419	"	"	129s,146s	L.
640	"	"		M, too thin
641	"	"	BG	S
642	"	"	129s,146s,158w	L
420	150-55	CsI+KRS-5	BG	S
421	"	"	63?, 129s	L 2nd order?
422	"	"	BG	S
423	"	"	63?	L "
638	100-55	2 KRS-5	BG	S
639	"	"	64m	L

DIMETHYL TIN DICHLORIDE, solution in benzene (approx. 15 %o)

Run no.	Recorded v range cm^{-1}	R'strahlen filters	Bands observed cm^{-1}	Comments
628	380-230	2 NaF	310s,329s	M, solid
629	"	"	BG	S
630	"	"	350vs,389s	M, interf.
631	"	"	320s,383s	M, solid present
632	"	"	BG	S
633	"	"	352vs,389s	M, good run
645	200-130	1 Kcl	BG	S, 80 grat.
646	"	"	148s,159w	L "
647	"	"	148s ..	M "
634	160-90	1 KBr	BG	S, interf.
635	"	"		M interf.
641	"	"	BG	S
644	"	"	147s,157s	M
636	100-55	2 KRS-5	BG	S
637	"	"	73m	L 2nd order?

DIMETHYL TIN DICHLORIDE, solution in acetonitrile (approx. 30%o)

798	380-230	2 NaF	BG	S, MeCN
799	"	"	BG	S
800	"	"	316s,337s	M
801	"	"		L, MeCN

METHYL TIN TRICHLORIDE , in 'Nujol'.

Run no.	Recorded ν range cm^{-1}	R'strahlen filters	Bands observed cm^{-1}	Comments
441	520-200	1 LiF	BG	S
442	"	"		L, too thick
443	"	"	384vs (2nd order)	M
434	380-230	2 NaF	BG	S
435	"	"		L
436	"	"		M
437	300-170	1 NaCl	BG	S
438	"	"		L
432	200-130	1 KCl	BG	S, 80 grat.
433	"	"	133s, 153m	L "

METHYL TIN TRICHLORIDE, solid.

659	520-200	1 LiF	BG	S
660	"	"	360s	L
657	380-230	2 NaF	BG	S
658	"	"	361vs, 343m shldr	M
653	160-90	1 KBr	BG	S
654	"	"	123s, 126s, 148m	L
651	100-55	2 KRS-5	BG	S
652	"	"		M, too thin
655	"	"		L
656	"	"		L

METHYL TIN TRICHLORIDE, solution in benzene, (approx. 30 °/o)

Run no.	Recorded ν range cm^{-1}	R'strahlen filters	Bands observed cm^{-1}	Comments
666	520-230	1 LiF	BG	S
667	"	"	368vs,384vs	L
662	160-90	1 KBr	BG	S
663	"	"		L, confused
671	"	"	BG	S
672	"	"	137s, 151m shldr	L
664	100-55	2 KRS-5	BG	S
665	"	"		L
669	"	"	BG	S
670	"	"		L

METHYL TIN TRICHLORIDE, solution in acetonitrile. (approx. 30 °/o)

802	380-230	2 NaF	BG	S
803	"	"		L, too thick
804	"	"	321s, 367vs app.	M

TRIETHYL TIN MONOCHLORIDE, solution in methanol (approx. 1 ; 3)

868	380-230	2 NaF	BG	S
869	"	"	277,282..MeOH	L
870	"	"		M, confused
871	"	"	282m,332vs	L, mixt. 15:3

TRIETHYL TIN MONOCHLORIDE, liquid.

Run no.	Recorded v range cm^{-1}	R'strahlen filters	Bands observed cm^{-1}	Comments
369	380-230	2 NaF	334,318,302 vs	L PQR?
370	"	"	328,318 vs	M
371	"	"	BG	S
372	300-170	1 NaCl	BG	S
375	"	"	275s	M
376	"	"	273s	L
373	230-150	1 KCL	BG	S,200 grat.
374	"	"		M "
377	"	"		L "
379	200-130	"	BG	S, 80 grat.
380	"	"		L " poor
383	"	"		M " "
378	160-90	1 KBr	BG	S
381	"	"	127-131s	L
382	"	"	127s	M
807	"	"	127s	M, confused
808	""	"	110,125,129,165.	L
809	""	"		S
384	100-55	CsI+KRS-5	BG	S interference
385	"	"		L "
805	"	2 KRS-5	BG	
806	"	"		L "

TRIETHYL TIN MONOCHLORIDE, solution in cyclohexane, (approx. 1 : 3)

Run no.	Recorded ν range cm^{-1}	R'strahlen filters	Bands observed cm^{-1}	Comments
862	380-230	2 NaF		S too absorbing
863	"	"		M "
864	"	"		L 1: 3 too thick
865	"	"	337vvs,275m	M "
866	"	"	337 vvs, sharp	S diluted
867	"	"	337 vvs "	S "
959	150-90	1 KBr	BG	S, C_6H_{12}
960	"	"		M, not drawn
961	"	"	107m,125s	M
962	"	"	BG	S
963	"	"	107m,123/127s	M
964	"	"		L, too thick
965	"	"	107m,122/127s	L
966	"	"	BG	

TRIETHYL MONOCHLORIDE, solution in acetonitrile (approx. 1 : 3)

859	380-230	2 NaF	BG	S
860	"	"	298s broad	M
861	"	"	298s broad	L

TRI n-PROPYL TIN MONOCHLORIDE, liquid.

Run no.	Recorded ν range cm^{-1}	R'strahlen filters	Bands observed cm^{-1}	Comments
688	380-230	2 NaF	BG	S
689	"	"	277w,298m,336vs	L
690	"	"	302m,336vs,277w	M
685	300-170	1 NaCl	BG	S
686	"	"	219m	L,
687	"	"		M, too thin
683	520-250	1 LiF	BG	S
684	"	"	390vs(2nd order)	L
681	200-130	1 KCl	159m	L, 80 grating
682	"	"	BG	S "
970	"	2 KCl	BG	S "
974	"	"	156m	L "
677	160-90	1 KBr	BG	S
678	"	"		M, poor run
680	"	"	127s,131s	L
			153m	
673	100-55	2 KRS-5	BG	S
674	"	"	101m	L
			336(3rd order)	
			127s	
			153m	

TRI n-PROPYL TIN MONOCHLORIDE, solution in cyclohexane (approx 1 : 3)

Run no.	Recorded v range cm^{-1}	R'strahlen filters	Bands observed cm^{-1}	Comments
872	380-230	2 NaF		L, too thick
873	"	"	269w,300m,337vvs	M
874	"	"	BG	S
967	160-90	1 KBr		M, confusing
968	"	"	BG	S
969	"	"	134s,153s	L
971	200-130	2 KCl	BG	S
972	"	"	153m	M
973	"	"	153m	L

TRI n-PROPYL TIN MONOCHLORIDE, solution in acetonitrile (approx. 1 : 3)

875	380-230	2 NaF	BG	S
876	"	"	298vs,321vs	M
877	"	"		L,too thick

REFERENCES

(1). Herschel, Sir W.: Phil. Trans. Roy. Soc. 1800, 90, 284 and 437.

(2). Nobili, (see Infrared Physics, 1961, 1, 105)

(3). Melloni, M.: Ann. Phys. 1835, 35, 385, 530.

(4). Herschel, Sir J.: Phil. Trans. Roy. Soc. 1840, 130, 1.

(5). Langley, S.P.: Proc. Amer. Acad. Arts & Sci. 1881, 16, 342.

(6). Bjerrum, N.: Verh. d. D. Phys. Ges. 1916, 16, 737.

(9). Rubens and Nichols: Wied. Ann. 1897, 60, 418;
Phys. Rev. 1897, 4, 314;
Phys. Rev. 1897, 5, 98, 152.

(9a). Nichols, E.F.: Ann. Phys. (4), 1897, 60, 401.

(10). Rubens and Hollnagel: Phil. Mag.(6), 1910, 19, 761.

(11). Strong: Phys. Rev. 1931, 38, 1818.

(12). O'Loane: J.Chem.Phys. 1953, 21, 669.

(13). Rubens and Aschkinass: Wied. Ann. 1899, 67, 459.

(14). Rubens and Wood: Phil. Mag.(6), 1911, 21, 249.

(15). Rubens and von Bayer: Berl.Ber. 1911, 339,666;
Phil.Mag.(6), 1911.

(16). Koch: Ann. Physik 1938, 33, 335.

(17). Dahlke: Z. f. Physik, 1939, 114, 205, 672;
Z. f. Physik, 1940, 115, 1.

(18). Nichols and Tear: Astrophys. J., 1925, 61, 17.

(19). Glagolewa and Arkadiew: Nature, 1924, 113, 640.

(20). Weber: Archiv. Sci. Phys. et Mat.(3), 1887, 18, 347.

(21). Crookes: Phil. Trans.(II), 1876, 166, 325;
Nichols: Phys. Rev. 1897, 4, 297.

(22). d'Arsonval: Soc. Franc. de Phys. 1886, pp 30, 87.
Boys: Proc. Roy. Soc. 1887, 42, 189.

(23). Witt: Physik. Z. 1920, 21, 374.

(24). Rubens: Berl. Ber. 1921, 8.

(25). Czerny: Z. f. Physik, 1925, 34, 227.

(26). Barnes: Phys. Rev. 1932, 39, 562.

(27). Barnes: Rev. Sci. Instr. 1934, 5, 237;
Phys. Rev. 1935, 47, 658.

(28). Badger and Cartwright: Phys. Rev. 1929, 33, 692.

(29). Cartwright: J.Opt.Soc.Amer. 1931, 21, 785.

(30). Wood: Phil. Mag. 1910, 20, 770.

(31). Randall: Rev.Sci.Instr. 1932, 3, 196.

(32). Randall, Ginsburg, Dennison and Weber: Phys. Rev. 1937, 52, 160.

(33). Randall and Firestone: Rev.Sci.Instr. 1938, 9, 404.

(34). Wright and Randall: Phys. Rev. 1933, 44, 391.

(35). Barnes, Benedict and Lewis: Phys. Rev. 1934, 45, 347.

(36). Fuson, Randall and Dennison: Phys. Rev. 1939, 56, 982.

(37). Golay: Rev.Sci.Instr. 1947, 18, 347, 357.

(38). "New Scientist", 1962, p.

(39). (see ref. 42)

(40). Rössler: Z. f. Physik, 1954, 139, 56.

(41). Conn and Avery: "INFRARED METHODS", Academic Press,1960.

(42). Yaroslawski: Uspekhi Fiz. Nauk, 1957, 62, 159.

(43). Schwarz: Research(london), 1952, 5, 407.

(44). Bird: (see ref. 42)

(45). 'Unicam' Golay SP 60 Manual.

(46). Bloor, Dean, Jones, Martin, Mawer and Perry, Proc. Roy. Soc. 1961, A260, 510.

(47). Wilkinson, Inglis and Smart, "Spectroscopy", Institute of Petroleum, London, 1962; pp.157-80

(48). Martin: Contemporary Physics, 1962/3, 4, 139, 187.

(49). Hadni: Rev. d'Optique, 1954, 33, 576.

(50). Oetjen, Haynie, Ward, Hansler, Schauwecker and Bell: J.Opt.Soc.Amer. 1952, 42, 559.

(51). Czerny: Z. f. Physik, 1923, 16, 321.

(52). Strong: J.Opt.Soc.Amer. 1939, 29, 520.

(53). Lord and McCubbin: J.Opt.Soc.Amer. 1957, 47, 689.

(54). White: J.Opt.Soc.Amer. 1947, 37, 713.

(55). Strong: J.Opt.Soc.Amer. 1949, 39, 320.

(56). Pfund: J.Opt.Soc.Amer. 1927, 17, 337.

(57). Maar: Z.f. Physik, 1939, 113, 415.

(58). Hopf: Z.f. Physik, 1940, 116, 310.

(59). Meier: Ann. Physik, 1953, 12, 26.

(60). McCubbin and Sinton: J.Opt.Soc.Amer. 1952, 42, 113.

(61). Yaroslawski, Zheludow, Stanevich: Optika i Spekt. 1956, 1, 507.

(62). Bohn, Freeman, Gwinn, Hollenberg and Pitzer: J. Chem. Phys. 1953, 21, 719.

(63). Czerny and Turner: Z. f. Physik 1930, 61, 792

(64). Genzel and Eckhardt: Z. f. Physik 1954, 139, 578

(65). Yoshinaga, Fujita, Minami, Mitsuishi, Oetjen and Yamada: J.Opt.Soc.Amer., 1958, 48, 315

(66). Murzin and Demshina: Opt. i Spekt. 1962, 13 ,826

(67). Ebert: Wied. Ann., 1889, 38, 489

(68). Fastie: J.Opt.Soc.A mer., 1952, 42, 647

(69). Robinson: J.Opt.Soc.Amer., 1959, 49, 966

(70). Benesch and Strong: J.Opt.Soc.Amer., 1951, 41, 252

(71). Carey: Carey Instruments, Technical Brochure.

(72). Greenler: J.Opt.Soc.Amer., 1956, 46, 433

(73). Lippincott and Tobin: J.Amer.Chem.Soc.,1953, 75, 4141

(74). Edgell and Ward: J.Amer.Chem.Soc., 1955, 77, 6486

(75). Dillard and Lawson: J.Opt.Soc.Amer., 1960, 50, 1271

(76). Duncan and Murray: J.Chem.Phys., 1934, 2, 636

(77). Jackson, J.A., Jr., Dissertation Abs., 1956, 16, 357

(78). Butcher and Cahill: Report of 1961 Spectroscopy Conf., Columbus, Ohio.

(79). Brown and Sheppard: Trans.Far.Soc., 1954, 50,1164

(80). Herzberg, "Infra-red and Raman Spectra", p.315, van Nostrand, 1945.

(81). Sheppard: J.Chem.Phys., 1949, 17, 79

(82). King and Crawford: J.Mol.Spect., 1960, 5, 421

(83). Herzberg, ref.80, p.182

(84). Pitzer: J.Chem.Phys., 1944: 12, 310

(85). Rosenthal: Phys. Rev., 1936, 49, 535

(86). Freeman and Ross: Spectrochim. Acta, 1960, 16, 1393

(87). Urey and Bradley: Phys.Rev., 1932, 38, 1696

(88). Pitzer and Gwinn: J.Chem.Phys., 1942, 10, 428

(89). Pitzer, J.Chem.Phys., 1946, 14, 239

(90). Aston et al.: J.Chem.Phys., 1946, 14, 67

(91). Taylor and Glasstone, "Textbook of Physical Chemistry", van Nostrand.

(92). Edgell and Ward: J.Mol.Spect., 1962, 8, 343

(93). Kriegsmann and Pischtchan: Z. f, anorg. u. allg. Chem., 1961, 308, 212

(94). Ingham et al., Chem.Revs., 1960, 60, 459

(95). Herzberg, ref.80, p. 167

(96). Lee Smith: J.Chem.Phys., 1953, 21, 1997

(97). Wagner: Z. Physik. Chem. B, 1938, 40, 36

(98). Wagner: Z. Physik. Chem. B, 1939, 45, 355

(99). Sheppard, "Spectroscopy", ref.47, p.181

(100). Wagner: Z. Physik. Chem. B, 1939, 45, 69

(101). Kirkwood: J.Chem.Phys., 1937, 5, 14

(102). Bauer and Magat: J. Phys. Radium, 1938, 9, 319

(103). Buckingham: Trans. Far. Soc., 1960, 56, 753

(104). Hallam: "Spectroscopy", ref.47, p.245

(105). Rochow and Seyferth: J.Amer.Chem.Soc.,1953, 75, 2877

(106). Thomas and Rochow: J.Amer.Chem.Soc., 1957, 79, 1843

(107). Kraus and Callis: J.Amer.Chem.Soc., 1923, 45, 2624

(108). Price, Sherman and Wilkinson: Ptoc.Roy.Soc.,1960,A255,5.

(109). Terenin et al.: Z.Elektrochem. 1958, 62, 180

(110). Brune and Zeil: Z.Naturforschung 1961, 16a, 1251